UNIVERSITÀ DEGLI STUDI DI PADOVA

DIPARTIMENTO DI INGEGNERIA INDUSTRIALE

CORSO DI LAUREA MAGISTRALE IN INGEGNERIA CHIMICA E DEI PROCESSI INDUSTRIALI

ADDITIVE MANUFACTURING AND INJECTION MOLDING FOR RAPID PROTOTYPING OF MESO-SCALE DEVICES FOR BIOMEDICAL STUDIES

Relatore: Prof.ssa Elisa Cimetta

Correlatore: Ing. Sara Micheli

Laureando: LUCA PASSALACQUA

ANNO ACCADEMICO 2019 – 2020

Abstract

Nowadays many research activities have been focused on the study and production of integrated microfluidic devices on a mass-production scale with relatively low costs. This is especially important for applications where disposable devices are used for biomedical analysis. In this context, Additive Manufacturing (AM) is a very advantageous technology for the production of inserts for the injection molding of thermoplastic microfluidic devices.

In this study, a microfluidic chip was made by Injection Molding using the 3D mold technique for the fabrication of micro-structured inserts. For the design of the chip, a configuration was chosen that would allow to carry out different biological studies with more than one cell species.

The first part of the study concerned the production of the inserts via Additive Manufacturing; in particular, three different molds were made with angles at 0, 45, and 90° with respect to the axis of the 3D printing machine. Subsequently, to evaluate the actual reproduction of the 3D printed inserts compared to the computer-aided design (CAD) model, each of the molds was subjected to metrological characterization in order to identify the best insert for injection molding.

At the same time, a study was carried out regarding the choice of the thermoplastic material to be used in the injection molding process. Based on criteria concerning the final biological application and the feasibility of the injection mold, the choice fell on polystyrene (PS).

The validation of the production process consisted on fabricating 500 polystyrene prints to both evaluate the durability of the insert and analyze the molded pieces to verify the correct replication of all features and identify potential problems due to wear of the insert.

Subsequently, biocompatibility tests of the polystyrene chips were carried out using specific cellular species; cell behavior was analyzed under the microscope with the use of suitable cellular markers at several timepoints.

Finally, a Polyethylene terephthalate (PET) lid was produced to adapt the chip to specific biological studies at controlled oxygen partial pressures.

Riassunto

Oggigiorno molte attività di ricerca stanno studiando la produzione di massa di dispositivi microfluidici con costi relativamente bassi. Ciò è particolarmente importante per le applicazioni in cui vengono utilizzati dispositivi monouso per l'analisi biomedica. In questo contesto, l'*Additive Manufacturing* (Produzione Additiva) è una tecnologia molto vantaggiosa per la produzione di inserti per lo stampaggio a iniezione di dispositivi microfluidici termoplastici.
In questo studio, un chip microfluidico è stato realizzato mediante stampaggio ad iniezione utilizzando la tecnica della stampa 3D per la fabbricazione di inserti micro-strutturati. Per la progettazione del chip è stata scelta una configurazione che consentisse di effettuare diversi studi biologici con più di una specie cellulare.
La prima parte dello studio svolto ha riguardato la produzione degli inserti tramite *Additive Manufacturing*: in particolare sono stati realizzati tre stampi differenti con angoli a 0, 45 e 90° rispetto all'asse della macchina da stampa 3D. Successivamente, per valutare l'effettiva riproduzione degli inserti stampati in 3D rispetto al modello CAD (progettazione assistita dall'elaboratore), ciascuno degli stampi è stato sottoposto a caratterizzazione metrologica al profilometro al fine di identificare il miglior inserto per il successivo stampaggio ad iniezione.
Contemporaneamente, è stato svolto uno studio sulla scelta del materiale termoplastico da utilizzare nel processo di stampaggio ad iniezione. In base a criteri riguardanti gli studi biologici da effettuare e la fattibilità dello stampaggio ad iniezione, la scelta è ricaduta sul polistirene (PS).
La validazione del processo produttivo è consistita nell'effettuare 500 stampe in polistirene per valutare sia la durabilità dell'inserto che le caratteristiche dei pezzi stampati per verificarne la corretta replica ed evidenziare eventuali problemi di funzionalità dovuti all'usura dell'inserto.
Successivamente sono stati effettuati alcuni test di biocompatibilità dei chip in PS con specifiche linee cellulari; il comportamento cellulare è stato analizzato al microscopio in più giorni successivi con l'utilizzo di opportuni marcatori cellulari.
Infine, sul dispositivo microfluidico è stata realizzata una copertura superiore in polietilene tereftalato (PET) per effettuare specifici studi biologici a pressioni parziali di ossigeno controllate.

Index

Introduction

The term microfluidics does not only mean the science that studies the behavior of fluids inside microchannels, but also the technology of manufacturing microminiaturized devices through which these fluid flows are confined[1]. Additionally, microfluidic devices offer several advantages over conventional sized systems. Microfluidics allows the analysis and use of lower volume of samples, chemicals and reagents reducing the global costs of the experiments. Many operations can be executed at the same time thanks to their compact size, also shortening the time of the experiment. For this purpose, microfluidics uses chips, devices capable of scaling single or multiple laboratory functions down to chip-format. The size of these chips varies from micrometers, millimeters, to a few square centimeters.

Given the great success of these microfluidic devices in recent years, research activities aim at simultaneously satisfying two goals: on the one hand, the possibility of obtaining a product with good customization, and on the other, the attempt to create standardized and economically sustainable production processes. The technology that allows creating a meeting point between the two needs is Injection Molding (IM).

Generally speaking, Injection Molding is the gold standard for device manufacturing and enables high-throughput manufacturing of devices (in volumes of hundreds of thousands to millions) at low per-device costs, while maintaining tight tolerances and high reproducibility[2]. Furthermore, this technique enables device production in polymeric materials; their characteristics and their manufacturing processes make them more than adequate for current needs[3]. However, traditional high-volume Injection Molding approaches utilize complex molds fabricated using high quality steel with high precision milling. The tooling of these molds is usually expensive and induces significant lead times of up to 12 weeks; in general, the high mold cost is typically out of budget for academic research projects, which seldom require millions of devices.

In recent years, Additive Manufacturing (AM), also known as three-dimensional (3D) printing, has proved to be an excellent alternative to traditional techniques for producing the inserts required for Injection Molding in terms of costs and processing times[4].

In this thesis, the main advantages offered in using Additive Manufacturing in the production of inserts for Injection Molding were analyzed. In particular, AM has shown that it can satisfy two fundamental aspects regarding microfluidic chips: rapid prototyping of devices and the high level of customization. In fact, AM allows both to physically create tools for Injection Molding molds in relatively short times compared to other technologies and to obtain very complex geometries with a high specification.

Regarding the work done in this thesis, it is structured as follows.

In Chapter 1 Microfluidics is introduced, the importance it is having more and more in the In Chapter 1 Microfluidics is introduced, highlighting among others its increasing importance in the biomedical field as a potential alternative to animal experimentation. The microfluidic devices, the materials and the technologies that allow their realization will then be discussed, with their respective advantages and disadvantages. At the end of the chapter, the purpose of the thesis will be introduced.

Chapter 2 is entirely dedicated to Injection Molding, the growth that has been experiencing lately in the field of Microfluidics. Its operating mechanism will be discussed, analyzing the components that make up the injection machine and its functions. Subsequently, the inserts for the mold, the methods and materials with which they can be made will be described, highlighting the importance of Additive Manufacturing in this field.

In Chapter 3, the various steps that led first to the design and then to the actual realization of the PS chips are discussed; subsequently, the biological validation of the microdevices carried out in the laboratory is described.

In Chapter 4, the results of all the steps performed in this thesis will be analyzed and discussed, in particular those of metrological characterization and cellular experiments carried out in the BIAMET laboratory.

In a final section, conclusions are drawn on the work done in this thesis, on the results obtained and on the possible future developments of microfluidic devices in plastic material.

Chapter 1

State of the art

In this first chapter, the concept of microfluidics and the importance it has assumed in recent years in the field of scientific research is highlighted. In particular, we will focus on microfluidic devices, the techniques that are used for their realization and the materials used. Finally, the purpose of the thesis will be explained.

1.1 Microfluidics and microfluidic devices

Since the 1990s, attempts have been made to implement a process of miniaturization in the field of biological and chemical analysis. Biological microfluidics is an emerging multidisciplinary science that intersects the fields of biotechnology, biochemistry, chemistry, nanotechnology and physics to create devices that control the cell culture microenvironment[1]. In fact, what has made microfluidics, and in particular microfluidic devices, a state of the art science is the ability to perform complete analyses in a single chip and at dimensions well correlated with cell size so it let manipulations of small amount of product easily than traditional methods. Following the guidelines of microelectronics and, more specifically, of MEMS (MicroElectroMechanical Systems), a miniaturized system designed, assembled and used to produced electronic modifications to the microscale, a microfluidic chip is a pattern of microchannels, molded or engraved[5]. This microchannel network embedded in the microfluidic chip is connected to the macroenvironment by different sized holes carved through the chip. It is then through these pathways that fluids are injected and ejected from the microfluidic chip. More appropriately, the term Lab-on-Chip (LOC, Figure 1.1) is introduced in microfluidics jargon, which is a device measuring from a few millimeters to a few square centimeters capable of scaling one or more laboratory functions up to chip format[6]. In general, LOCs may provide advantages, very specifically for their applications. Typical advantages are[7]:

- low fluid volume consumption, due to the low internal chip volumes, which is advantageous e.g. environmental pollution (less waste), lower costs of expensive reagents, and less use of sample fluid for diagnostics;
- faster analysis and chip control speed and higher efficiency thanks to short mixing times (short diffusion distances), fast heating (short distances, high wall surface/fluid volume ratio, small thermal capacities);

- better control of the process thanks to a faster response of the system (eg thermal control for exothermic chemical reactions);
- compactness of the systems, due to the great integration of functionality and small volumes;
- lower manufacturing costs, allowing for cheap disposable chips manufactured in mass production.

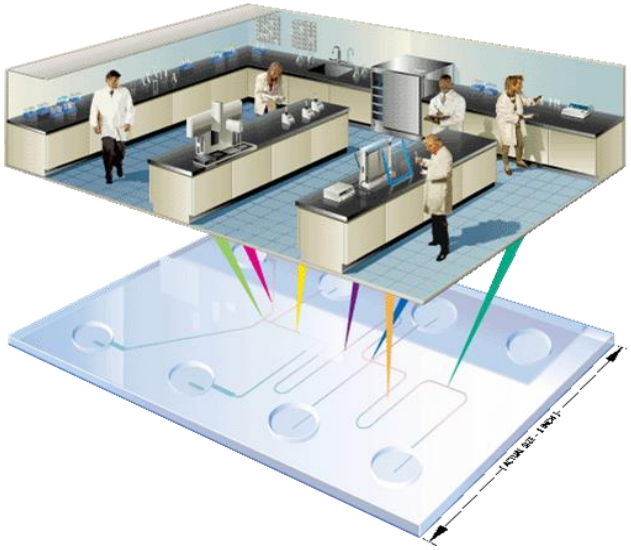

Figure 1.1. A graphic representation of how the work of a large laboratory could be carried out by a "Lab on Chip", a sort of mini laboratory enclosed in a few centimeters; adapted from[7].

Obviously, when a fluid is analyzed on a microscopic scale, its behavior turns out to be very different from a fluid studied on a macroscopic scale[8]. First of all, due to the minuscule characteristic lengths of microfluidic channels, microfluidic flow is generally laminar[9]. Turbulent flow is chaotic, whereas laminar flow allows precise calculation of mass transport as a function of time. The convective flow profile for laminar flow is straightforward to calculate from parameters such as channel geometry, pressure drop, and fluid properties[9]. Due to the translation invariance of laminar flow, fluid streamlines remain constant over time, and mixing of microfluidic streams occurs primarily by diffusion. In fact, the dominant transport mechanism at the microscopic level is that of diffusion, which is usually neglected otherwise. Figure 1.2 shows the difference between the two flow regimes[10].

Figure 1.2. Difference between laminar (left) and turbulent (right) flow[10].

Another very important factor, which makes the surface effects prevail over the volumetric ones, is the area-volume ratio, generally very high; therefore, the viscous and tensile forces will prevail over those of inertia. It is important to underline that the term microfluidics is not so much aimed at the concept of operating with very small devices, but rather at the fact that the microscale determines a very different behavior of the fluid compared to that which occurs on a macroscopic scale. However, making devices smaller and smaller but capable of carrying out the same large-scale task has become the most important challenge of recent years for microfluidics, and in particular for the micro-engineering it relies on.
The main problem is that each microfluidic device is conceived and designed to perform a specific task and it is very complicated to find a single chip that can satisfy every type of requirement. Furthermore, the features that differentiate each chip from the other make it difficult to standardize the entire production system, with the consequent problem of obtaining a process that is not very advantageous from an economic point of view.
Another important aspect is the type of material with which to make the microfluidic chip, which will also affect the choice of the production process with which it will be made. However, at the same time, this is why engineers are becoming more active in lab-on-a-chip research, offering a multitude of different fabrication possibilities ranging from material selection and design to fabrication methods and processing parameters.

1.2 Materials and manufacturing methods

As already mentioned in the previous paragraph, the choice of the material for the microdevice is dictated by chemical and biological considerations, that is which technical characteristics (optical transparency, permeability to gas exchanges, biocompatibility) the chip must have to perform a specific task. Obviously, this choice affects the manufacturing technique of the microfluidic device compatible with the selected material, to reduce production costs and times. As for the material (Figure 1.3[11]), many times its choice was linked to the scientific progress underway in that period; in other words, over the years there has been a clear transition from the use of glass as the main material in biomedical studies to a more marked use of polymeric materials. This follows the engineering process implemented by research activities in the last years. Overall, the materials from which the chips are made evolve trying to meet the two main trends in microfluidics technology: powerful microscale research platforms and low-cost portable analyses[12].

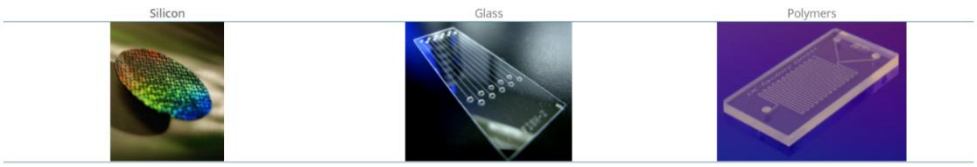

Figure 1.3. Three types of materials are commonly used to create microfluidic chips; adapted from[11].

The first materials used for microfluidic applications were silicone and glass, but soon as time went by and scientific progress advanced, new materials such as polymers and even paper were used[13].
In the following paragraphs, some materials used in the microfluidics field are discussed with the respective advantages and disadvantages of their use, and some of the important techniques used for their production.

1.2.1 Silicon

The first material used for microfluidics was silicon although it was quickly replaced by glass and then by polymers[14]. Fabrication of silicon (as well as glass) devices uses either subtractive methods (e.g., wet or dry etching) or additive methods, such as metal or chemical vapor deposition, to create structures. Silicon was first selected due to its resistance to organic solvents, ease in metal depositing and high thermal conductivity. However, this material is not easy to handle due to its hardness which doesn't make it easy to create active microfluidic components such as valves and pumps. Moreover, it is transparent to infrared but not visible light, making typical fluorescence detection or fluid imaging challenging for embedded structures. This issue can be solved by having a transparent material (polymer or glass) bound to silicon in a hybrid system.

1.2.2 Glass

Given the long tradition of glass processing in chemical and biomedical laboratories, it is not surprising that the most used material for microfluidic chips over the years has been glass. It is an amorphous material and its advantage is to have excellent optical properties, being transparent, excellent resistance to chemical reagents and is electrically insulating[14]. Generally, different types of glass are used in microfluidics, such as soda-lime, quartz and borosilicate. The most widely used is borosilicate (Figure 1.4), thanks to its optical characteristics (transparent from about 350 nm to 700 nm) and its physical properties (resistant to most chemicals), while soda-lime glass gives autofluorescence problems and quartz is difficult to work due to the high annealing temperatures (approximately 1000 °C).

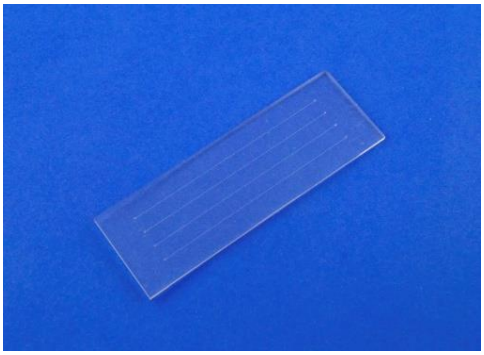

Figure 1.4. Example of glass (borosilicate) microfluidic chip.

Typically, two techniques are used for the production of microfluidic devices in glass: photolithography and etching, wet or dry. Although they are two fairly established techniques, they are not suitable for mass production which makes glass a rather niche material for microfluidics. In fact, from an engineering point of view, we prefer to look at other materials such as polymers and other techniques such as injection molding, which are more predisposed to mass production. However, in some cases it may be economically more advantageous to build small quantities of glass devices, rather than having to design and build molds suitable for the processing techniques of polymeric materials.

1.2.3 Polymers

Polymers are organic-based, long-chain materials that have gained significant traction in microfluidics in the last years. The wide range of polymers offers great flexibility in choosing suitable materials with specific properties[14]. Compared to silicone and glass, polymers have the advantage of being inexpensive and easily accessible, making them the best materials for rapid prototyping and mass production, becoming the most widely used for the construction of microfluidic chips today. Based on their physical properties, polymers can be classified into elastomers, thermoplastics, and thermosets, with the first two being widely used today as materials for microfluidic devices. Figure 1.5 shows an example of a polymeric microfluidic chip.

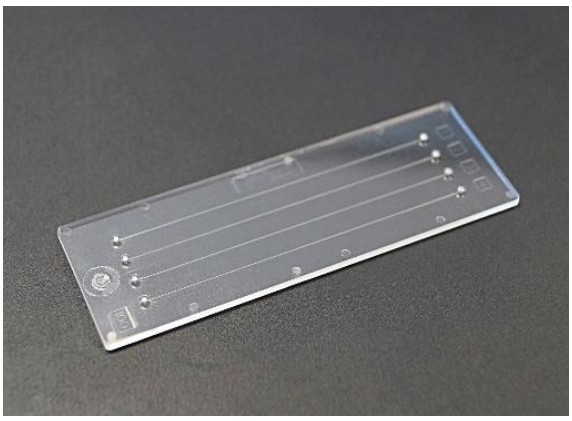

Figure 1.5. Example of polymeric microfluidic chip.

Elastomers are made up of normally entangled cross-linked polymer chains; they can stretch or compress when an external force is exerted and then return to their original shape when that force stops. In this class of polymers, we find the most widely used polymeric material in the field of microfluidics: polydimethylsiloxane (PDMS). Thermoplastic polymers are fusible and soluble polymers, they can be crystalline or amorphous based on their glass transition temperature (T_g)[15]. Thermosetting polymers, on the other hand, cross-link, so they are non-fusible and insoluble, and can also be rigid or flexible. In general, thermoplastic polymers are

more easily workable and easier to produce, and for this reason they find greater use in the field of microfluidics.

1.2.4 Polydimethylsiloxane (PDMS)

PDMS deserves a separate paragraph since it has been the main material used in biomedical laboratories, especially in the academic community, for many years and one of the polymers that lend itself very well to mass production techniques. In fact, PDMS (Figure 1.6) is preferred many times over other materials because it exhibits numerous advantages, such as its elasticity, low toxicity, optical transparency, chemical inertness, low cost and rich permeability to gases, which can be advantageous for oxygen and carbon dioxide transport in cell studies[16].

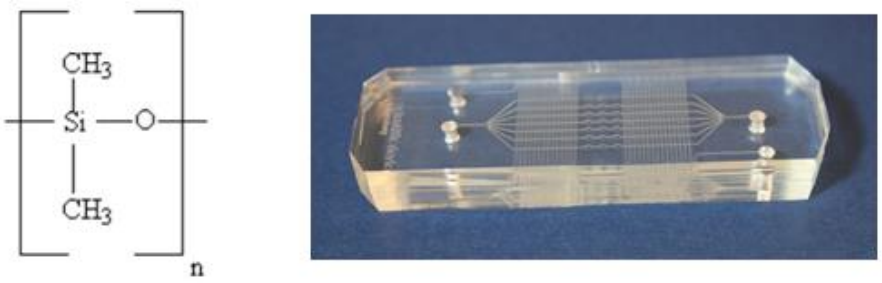

Figure 1.6. Chemical structure of Poly(dimethylsiloxane) and an example of a PDMS micro platform.

However, an increasing number of scientific reports have begun to raise awareness on the potential negative effects associated with culturing and studying cells in PDMS microdevices[17]. For example, PDMS is limited by material aging and poor chemical compatibility with many organic solvents. Furthermore, PDMS absorbs small molecules on its surface and water vapor that can occur unintentionally during the experiment. Also, PDMS chips are not appropriate for high-pressure operations, as this can change the geometry of the microchannels.

1.2.5 Thermoplastic polymers

As already mentioned above, thermoplastic polymers are widely used in the microfluidics field thanks to their easy workability and ease of production, as they are meltable and soluble. The fact of being crystalline or amorphous at room temperature depends on their glass transition temperature (T_g); above T_g the polymeric chains have a certain mobility and can flow[18]. This temperature regulates the phase transition of the second order and marks the boundary between the glassy and the rubbery amorphous states, the latter being a very rigid liquid characterized by high viscosity. The glass transition is not a thermodynamic transition, but a kinetic one, which does not correspond to any change in the arrangement of the atoms or molecules in space, as occurs in the transition from a crystalline solid to a liquid state.

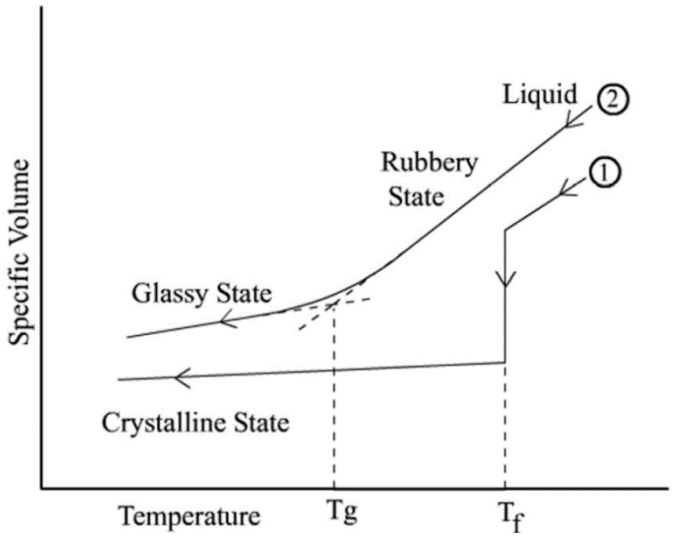

Figure 1.7. Difference in behavior between an amorphous and a crystalline polymer.

Typical plastic materials for microchips are polymethyl methacrylate (PMMA), polycarbonate (PC), polystyrene (PS), polyethylene terephthalate (PET) and polyvinyl chloride (PVC). In general, they show a slightly better solvent compatibility than PDMS, fair resistance to alcohols, but are incompatible with most other organic solvents such as ketones and hydrocarbons. From an engineering point of view, given their relative low cost, they lend themselves well to being stored and used in the form of granules for injection molding, which makes them very attractive for rapid prototyping[19].

1.2.6 Manufacturing techniques for microfluidic devices

Some methods for manufacturing microfluidic devices are now described, including etching, photolithography, soft lithography, and hot embossing, with respective advantages and disadvantages of each method[20]. As regards injection molding, since it represents the technology used in this work, it will be discussed widely in the next chapter.

- Photolithography: it is a process that transfers shapes from a photomask to the surface of a silicon wafer using light. The modern process that is used today requires many steps and several different tools and chemicals[21]. First of all, it is important that the silicon wafer is treated chemically with hydrogen peroxide to remove any contaminations that may be present; humidity can also be a problem for the process, and must therefore also be removed[21]. After cleaning, silicon dioxide, which serves as a barrier layer, is deposited on the surface of the wafer; in this step "adhesion promoter" in liquid or gaseous form is also added to favor the adhesion of the photoresist on the wafer surface. At this point the wafer is covered with photoresist by spin coating; the photoresist can be liquid (wet) or a solid sheet (dry film) and is dispersed onto the wafer in such a way as to quickly create a thick uniform layer[15]. Before exposing the system to light, all

solvents must be removed from the photoresist coating by evaporating, thanks to moderate heat; this phase is called soft baking. The next step, the crucial one, is aligning the mask with the wafer so that the individual areas of the photoresist are selectively exposed to optical or UV light. A mask, which looks like the chip, is a square glass plate with holes or transparencies that allow light to shine through in a defined pattern[21]. However, a distinction should be made between negative photoresist and positive photoresist: in the case of the positive photoresist, exposure to UV rays changes the chemical structure of the photoresist to make it more soluble in the developer; conversely, UV exposure of the negative resistance causes its polymerization and makes it more difficult to remove. One of the last steps of the photolithographic process is development: with a positive photoresist, the substrate is immersed in a developing solution that will disintegrate the areas of the photoresist that have been exposed to light, while, if it were negative, the developing solution dissolves only the unexposed parts of the photoresist. At this point, the master is complete and ready for use, and the photopolymer layer remains part of it. However, the most superficial layer of the substrate can be removed in the areas which are not protected by the photoresist through a liquid ("wet") or plasma ("dry") chemical agent; this process is called etching, which can be wet or dry. Once the photoresist is no longer needed, it must be removed from the substrate. This last step usually requires a liquid called "resist stripper", which chemically changes the resist so that it no longer adheres to the substrate. Figure 1.8 provides a graphic illustration of the steps of the Photolithography process[22].

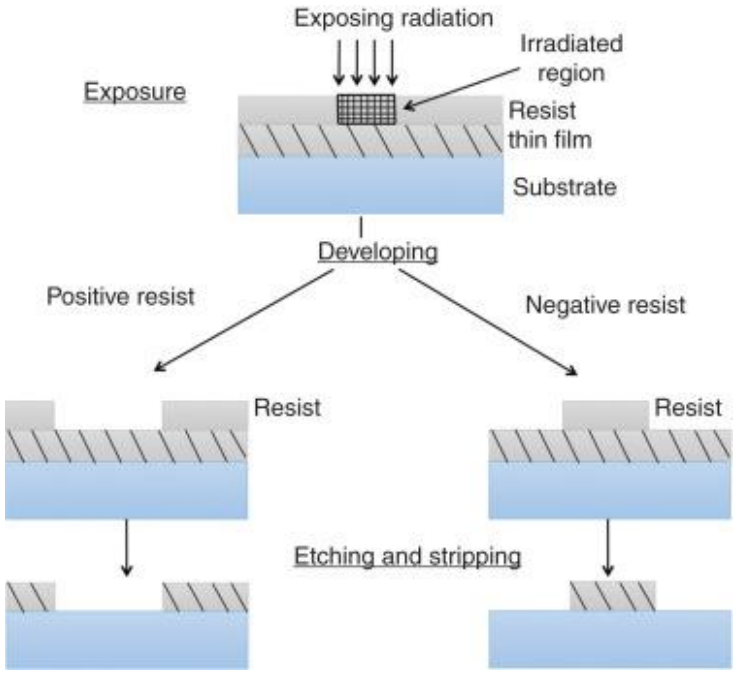

Figure 1.8. Graphic description of the photolithography process; adapted from[22].

- Soft lithography: it can be viewed as a complementary extension of photolithography, but unlike it, soft lithography can process a wide range of elastomeric materials, i.e. mechanically soft materials, most notably PDMS; this is why the term "soft" is used[23]. The basic process consists of building elastomeric microchannels, while the rest of the process depends on which subcategory we are considering; in fact, there are 4 different main sub-categories (Figure 1.9) which are Replica molding, Microcontact printing, Capillary molding and Microtransfer molding[24].

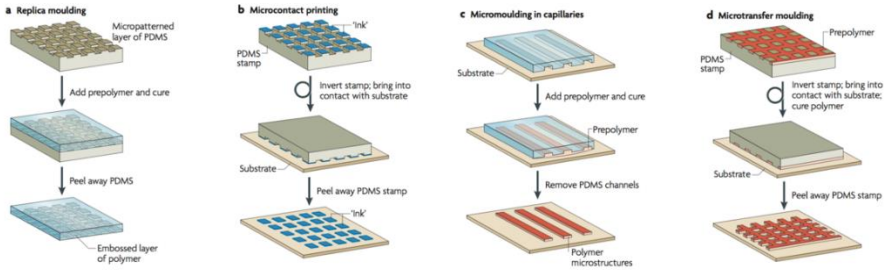

Figure 1.9. Schematic illustration of the four subcategories of the soft lithography process; adapted from[24].

In Replica molding, a micropatterned layer of PDMS is used as a soft mold into which a polymer is poured. Subsequently, the polymerization of the polymer takes place, at the end of which it is separated from the mold in PDMS, which can be reused many times; in fact, this technique can be repeated multiple times and allows to pattern a wide range of materials[25].

Microcontact printing is a technique that uses an elastomeric stamp with relief on its surface to generate patterned self-assembled monolayer onto the substrate surface. The PDMS layer is first dipped in a molecular "ink" and only it is transferred to the substrate. Various inks, including small biomolecules, proteins or suspension of cells can be used.

Capillary molding, also called micro-molding in capillaries, is a second technique where a patterned PDMS is used as a mold. A PDMS stamp is first put into contact on a substrate, the relief pattern facing towards the substrate. Polymer liquid is applied to the ends of the channels and as the name suggests, capillary forces allow the liquid to fill the mold patterns in PDMS. The material is then cured in the shape of the PDMS mold, either by UV, heat or chemically by using a curing agent and once the curing process is complete, the PDMS master is gently removed, leaving the solid microstructures patterned on the substrate surface.

In Micro-transfer molding, the patterned surface of a PDMS layer is filled with a liquid polymer, such as polyurethane (PU) or thermally curable epoxy. After removing excess liquid from the master, the polymeric liquid is then inverted and brought into contact with a solid substrate before being cured. After the curing of the polymer, the PDMS

layer is cautiously peeled away, leaving a solid structure on the surface of the substrate. As the Replica molding process, the same PDMS layer can be refilled many times. Therefore, Soft lithography, whatever the sub-category, using PDMS offers numerous benefits, including fast, low-cost processing and reusability of masters. In addition to the benefits of the fabrication process, PDMS itself is suitable for a variety of biological and cellular applications, due to the high gas permeability of PDMS. At the same time, in some applications where the gas permeability of the PDMS is not suitable for carrying out oxygen-sensitive polymerization reactions in the channel, this advantage could be undesirable. Another great advantage of this manufacturing technique, always linked to elastomeric polymers, is that they can be easily bonded to each other or on plastic or glass substrates by conformal contact.

- Hot embossing: it is a promising process for fabricating high precision and quality features at a micro/nanoscale using thermoplastic polymers[26]. It consists of the stamping of patterns into a polymer substrate by increasing the temperature above the glass transition point (T_g) of the polymer. Generally, hot embossing (Figure 1.10) is carried out in four basic steps: heating, embossing, cooling and demolding[26].

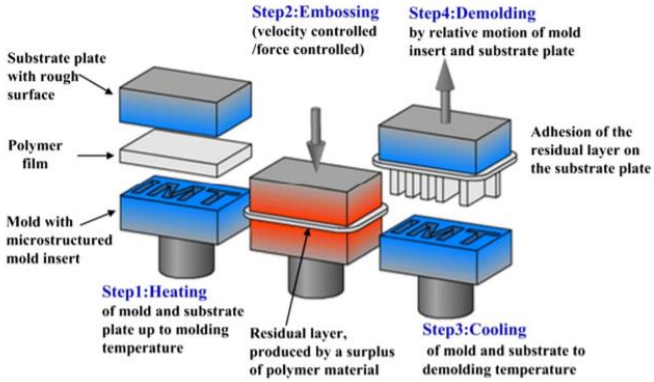

Figure 1.10. Schematic illustration of the hot embossing process; adapted from[26].

Firstly, mold and polymeric stamp, after being conceived, are heated above the glass transition temperature of the stamp to make it deformable; all take place inside a hydraulic press. However, embossing can be achieved without heat as well, by applying extended pressure; it then will be called the room-temperature imprinting method. Next, the master mold is pressed into a polymer substrate with a precisely controlled force to emboss the plastic against the stamp, and the pattern of the mold replicates on the substrate. Finally, when the predetermined embossing time is spent, the system cooled down below the glass-transition temperature of the polymer which sets the pattern. At this temperature, deembossing occurs when the master mold is separated from the substrate. Hot embossing is fairly straightforward, as well as a fast and inexpensive

technique but it requires specific press equipment and a patterned stamp. Moreover, fabrication of the embossing stamp can be a time-consuming process, and thus not ideal for routine microfluidic designs, such as for laboratory testing.

1.3 Injection molding as an alternative technology

With the exception of hot embossing, a technology that concerns only thermoplastic polymers, the other techniques for the production of microfluidic devices are based mainly on the processing of PDMS and, to a lesser extent, of glass. With the search for a possibility of mass production for microfluidic devices that took place in the last 20 years, the introduction of injection molding in the field of microfluidics made it possible to overcome some disadvantageous aspects that characterized the platforms used up to that moment. The characteristics of the polymers have in fact made it possible to overcome the big problem of biomedical and clinical applications, namely the creation of a low-cost, disposable microfluidic device, to be used as a point-of-care test. PDMS-based processes suffer from the fact that many of their steps are purely manual; consequently, in addition to making the manufacturing methods of the device not very robust, the average cost of every single chip is, in fact, higher than for injection molding.

1.4 Aim of the thesis

The purpose of this thesis was to exploit Additive Manufacturing, in particular PolyJet technology used by Stratasys' Objet printers, to produce injection molding plastic molds for the realization of a microfluidic chip starting from its CAD design. The replicability of the CAD model by the inserts has been tested using this additive technology, which allows printing plastic inserts in times ranging from 1 to 4 hours. In particular, their durability will be characterized after 500 prints, as well as the microfluidic platform obtained by injection molding. The realization of the insert and subsequent molding of the microfluidic device, as well as the analysis and characterization of the inserts, before and after molding, and of the final chips were performed at the TE.SI. laboratory in Rovigo. The second part of the thesis took place at the BIAMET laboratory in Padua and concerned the study of the biocompatibility of the thermoplastic microdevices with some preliminary biological tests. This thesis, therefore, aims to validate the manufacturing process of microfluidic devices using techniques that allow obtaining inserts at low cost and in fairly rapid time, while maintaining a high level of customization.

Chapter 2

Injection molding and Additive Manufacturing in microfluidics

This chapter introduces Injection molding, its operating mechanism and its use in the field of microfluidics, considering advantages and disadvantages. In addition, Additive Manufacturing will be introduced as a technique for producing the inserts needed for injection molding; it will be compared with other techniques for mold production highlighting its useful role in rapid prototyping.

2.1 Significance of injection molding for LOC devices

Microfluidic injection molding or, micro injection molding, was first developed around the 1990s due to the fact that it uses a wide range of available thermoplastics to generate high throughput, cost-efficient, and precise microfluidic devices[27]. It also has the advantage of reducing cycle time compared to other technologies: it is highly automated and guarantees the possibility to obtain complex pieces with good accuracy and precision. Therefore, it represents by far the most widespread polymer manufacturing process in the macro world, but it is not yet as successful in the field of microfluidics at the laboratory stage. The main reason has to be ascribed to the high initial cost of the mold and the need for extreme precision to ensure correct replication of the features. Recently, efforts have focused on the development of additive manufacturing technologies to guarantee greater cost-effectiveness in the production of molds.

2.2 Injection molding process

Injection molding is an industrial production process in which a plastic material is melted (plasticized) and injected at high pressure inside a closed mold, which is opened after the solidification of the product[27]. More specifically, the polymer in the form of granules is fed through a hopper, heated and forced by means of a screw or piston through an appropriately heated cylinder. After heating and melting (or softening), the molten polymer (with a melt temperature of the order of 200 – 350 °C depending on the polymer) is injected under high pressures (typically between 600 and 1000 bar) and at a specific rate into the mold cavity where

the material is allowed to solidify. The mold is then opened, and the piece extracted. For a good replication of the microstructure, it is important to obtain a good filling of the mold and to prevent the formation of air pockets. Figure 2.1 shows an injection molding machine[28].

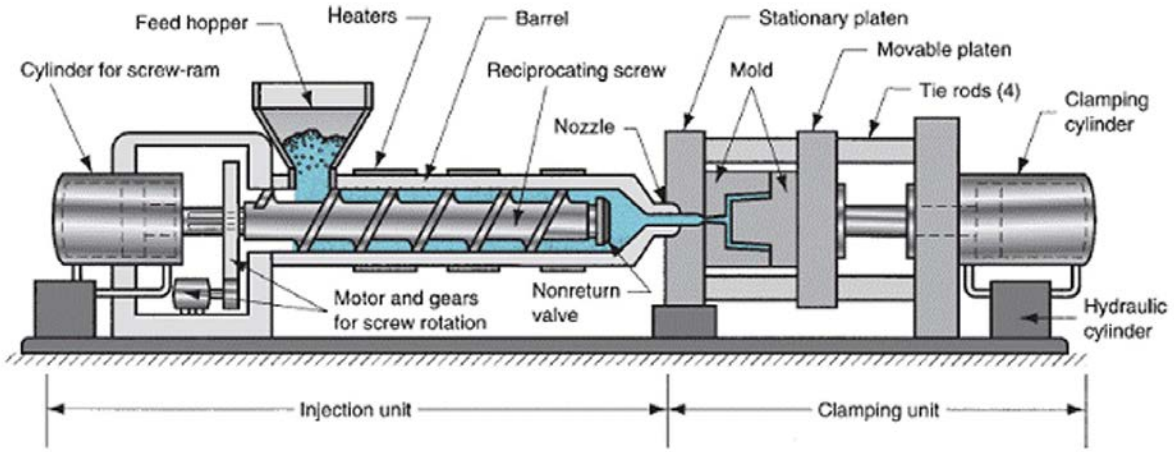

Figure 2.1. Cross-sectional diagram of an injection molding machine; adapted from[28].

To control the process, various variables can be modified such as the process conditions (T mold/melt), the rheological properties (viscosity, melt flow rate) and the thermal, physical and mechanical properties of the polymer (specific heat, density, Young's modulus).

2.2.1 Operating cycle

Injection molding mainly consists of five stages: closing of the mold, injection (or filling), holding, cooling and extraction[29]. Figure 2.2 shows a block diagram that describes the phases of injection molding.

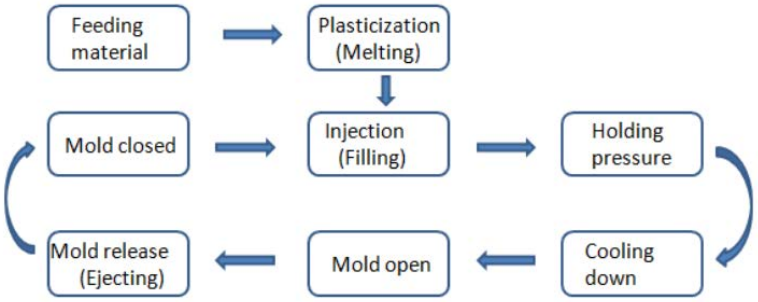

Figure 2.2. The detail of the process; adapted from[29].

Therefore, first of all it is important that the closing of the mold takes place as quickly as possible and that the moving platen of the press closes in such a way that the clamping unit exerts sufficient energy to clamp the two halves of the mold, fixed platen and movable platen. At this point, the material passes from the hopper into the cylinder. The screw rotates pushing the solid material forward and the cylinder is kept, at least in the area near the mold, at a temperature higher than the melting temperature of the polymer. The latter, once melted,

accumulates in the injection chamber and, when the volume of material accumulated has become sufficient for filling the mold, it is pushed through a nozzle into the cavity of the mold itself by a forward translation exerted by the screw. The amount of molten material that accumulates in the cylinder head (final part of the screw) is called the metering amount and must be more or less equal, unless the polymer is compacted, to the volume of the mold cavity. Therefore, the injection phase is also called the filling phase because, once the metering level has been reached, the molten polymer is pushed into the cavity through suitable channels, of which often the first (called sprue) has a cylindrical geometry with the increasing section along the flow direction. Actually, before entering the cavity, the molten runs along a short section of a considerably lower section called the "gate". Once the cavity is filled, the maintenance phase begins, during which the polymer is kept under high pressure in order to force other material into the cavity to increase the density, and therefore compensate for the shrinkage of the product. This is connected with the decrease in temperature and with solidification, which occurs both in the same holding phase and in the cooling phase. Since the gate is the smallest section of the passage of the material, here the solidification occurs before the actual mold, and this starts the cooling phase. In reality, the molten polymer begins to cool as soon as it comes into contact with the cold walls of the mold and therefore already in the injection and holding phases. In fact, after the gate is closed, the polymer can no longer enter the cavity, whatever the pressure exerted in the injection chamber. During the cooling phase, the piece solidifies reaching the temperature of the mold and the pressure decreases more rapidly and its final value in the cavity at the opening of the mold (residual pressure P_r) is determined by the mass of polymer present at the moment of closing the gate. After cooling, the mold is opened and the piece is extracted using automatic extractors.

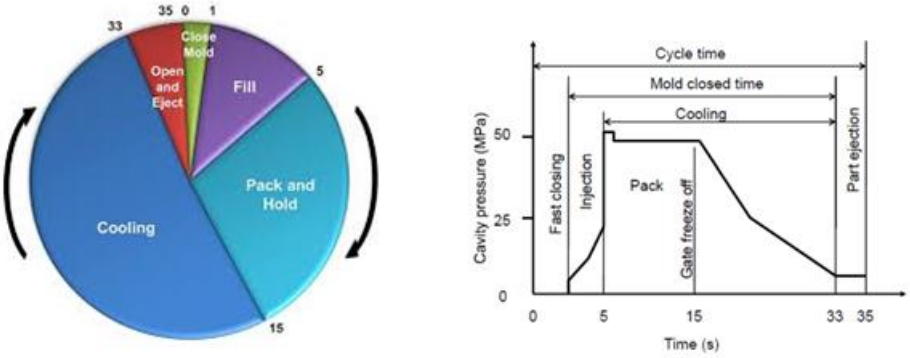

Figure 2.3. Cycle time and Pressure history in Injection molding; adapted from[30].

From Figure 2.3 it can be understood that most of the time spent in a molding cycle is occupied by the cooling phase[30]; the melt cannot be cooled too quickly because the polymer chains would tend to freeze on the surface, while the core of the mold cools in a variable time depending on the size of the mold itself. As for the pressure in the cavity, it begins to grow the instant the melt reaches the pressure sensor positioned in the cavity. Once the mold has been filled, the

pressure rapidly changes level as the maintenance phase begins. Subsequently, the pressure undergoes gradual variations connected with the progressive cooling of the polymer.

2.2.2 Pressure and other parameters in the injection process

It is clear that the machine must be supplied with hydraulic pressure to overcome the resistance that the nozzle, injection channels and mold cavity oppose to the flow of material[30]. In addition to this, there is another specific, or process, pressure that is applied directly to the plastic by the piston and is required by the screw to push the molten polymer into the mold cavity and to manage solidification. In particular, there are two process pressures (as reported in Figure 2.4): injection pressure and holding pressure. The first is the pressure necessary to push the molten polymer into the mold and depends on the rheological properties of the material, while the holding pressure is the pressure, constant and slightly lower than the injection pressure, which is applied to compensate for the shrinkage and has a strong influence on the density of printed materials, on the presence of defects or residual stresses. Therefore, one of the fundamental parameters of injection molding is the switch-over position (switch-over pressure), that is the ram position where the filling (injection) stage switches to the post-filling (holding) stage. In other words, the first phase is in flow control and the screw advances looking only at the injection velocity, not caring about the pressure, after which it passes into pressure control, that is the maintenance one.

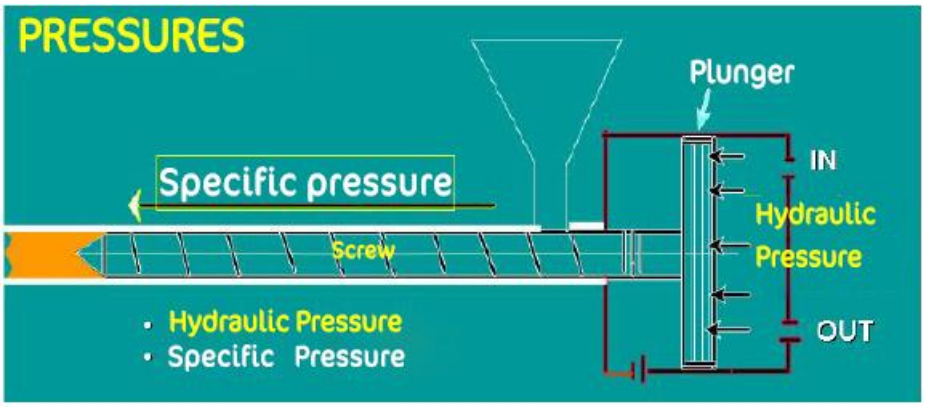

Figure 2.4. Pressures in Injection molding.

However, there are many types of materials that can be used in the injection molding process, so the process parameters are dictated by the type of material you intend to use. Each material has, for example, its own melting and degradation temperatures and requires a different set of processing parameters in the injection molding process, including injection temperature, injection pressure, mold temperature, cooling temperature and time. of cycle. For example, an optimal temperature must be found for the mold, as this together with the thermal characteristics of the polymer determines the cooling time. In fact, with low mold temperatures, faster cycles are obtained, however penalizing quality; in this case, in addition to a poor surface appearance, high molecular orientations and internal stresses are found with a consequent reduction in

mechanical properties. On the contrary, the slow cooling facilitates the formation of crystals also towards the surfaces of the piece, thus increasing the mechanical characteristics and dimensional stability. This inevitably leads to longer molding cycles and higher production costs.

2.3 Clamping unit: the mold

The clamping unit has the task of keeping the mold closed for the duration of the phase that goes from injection to cooling and is part of the closing unit where the mold of the piece to be made is mounted. It provides the necessary movements to close, lock and open the mold. The latter represents the heart of injection molding and consists of two parts: a movable plate and a fixed plate. These, in addition to the feeding channels, the conditioning system and the extractors, are prepared to house the inserts that will shape the finished product.

2.3.1 Hot & Cold Runners for Injection Molding

The term "hot runner" process (Figure 2.5), often referred to as no sprue, refers to the system of parts used in injection molding that are physically heated in such a way that the transfer of the polymer from the plasticizing cylinder to the cavity always occurs while maintaining the molten polymer. This type of system, which allows keeping the material in the guides always melted up to the gate, consists of two plates heated by a manifold system inside one-half of the mold. As the mold cools, the gate solidifies but the material contained in the guides is kept warm.

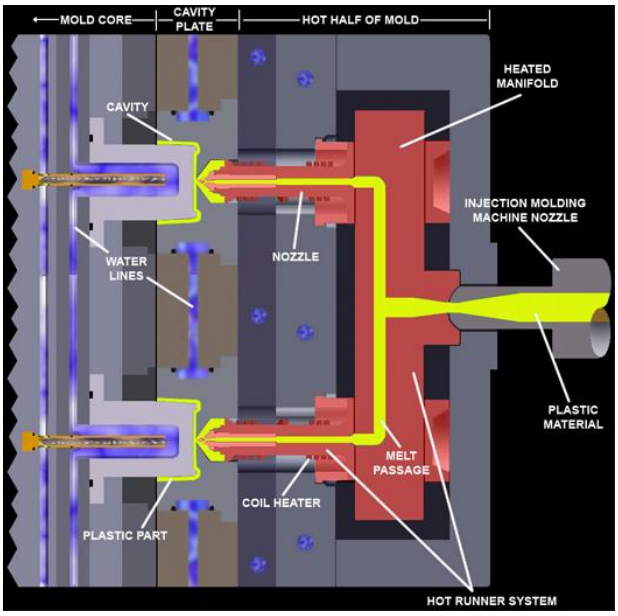

Figure 2.5. Scheme of a hot runner process; adapted from[31].

This system represents an innovation for injection molding compared to the past since historically the cold runner process was the most common among injection molding machines. In fact, although hot runners are not required for injection molding processes, they can be useful in ensuring a higher quality part; furthermore, since a large amount of waste is produced during the molding process for each cycle due to the sprue and runners, hot runners can be useful for reducing plastic waste during high volume shooting[31]. In contrast, the cold runner system simply consists of an unheated physical channel that is used to direct molten plastic into a mold cavity after it has left the nozzle. Hence, since the cold channels are not heated, the channel needs to be larger and therefore more plastic needs to be fired during each cycle. However, although hot runner technology is designed to maximize manufacturing productivity by reducing cycle time, it has the drawback of costing more for part fabrication and system maintenance than a cold runner setup. Figure 2.6 shows the clear difference between a piece produced by a cold runner process (with the presence of the sprue) and one made with a hot runner process.

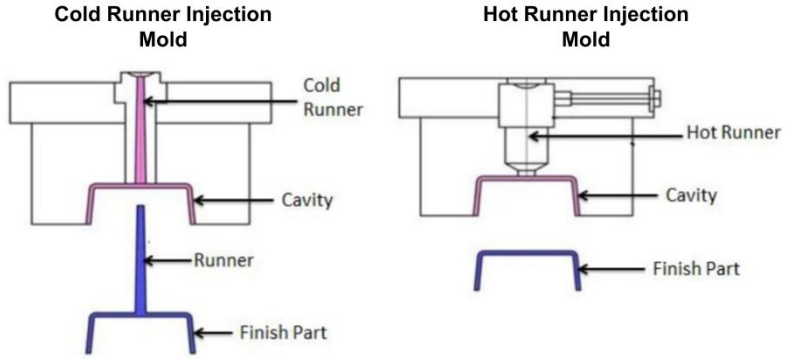

Figure 2.6. Difference between cold and hot runner.

2.4 The inserts

Injection molding is a technique that requires a tool to transfer the microstructures to the polymer material; a key issue is therefore the manufacturing of the insert[32]. This is usually a pre-formed piece, often made of metal, which is loaded into a mold where it is then over-molded with a thermoplastic resin to create a final component. Thus, the metal mold is fabricated prior to the molten material by providing a configuration with an opening into which the insert will be plugged. In this way, the insert and aperture are characterized by dimensions such that the insert is forcibly retained in the aperture. The inserts contain the cavities and the features of the pieces to be molded and must possess certain characteristics: a sufficiently smooth surface not to oppose resistance to the injection flow, good resistance to high injection pressures and during

the extraction phase of the device, dimensional stability during the molding cycle and wear resistance. Depending on the piece to be molded and the polymeric material used, there are different technologies used to make the inserts; in particular, there is the first distinction between subtractive and additive techniques.

2.4.1 The subtractive techniques

Subtractive manufacturing is any process in which parts are produced by removing material from a solid block to produce the desired shape through cutting, boring, drilling and grinding and are generally the most used technologies for making inserts. These processes are performed manually or, more commonly, with the aid of a computerized numerical control (CNC)[33]. In general, these are ideal for applications that require tight tolerances and geometries that are difficult to model, cast or manufacture with other traditional manufacturing methods, but have the disadvantage of being very slow and expensive techniques. The two main techniques are Micro-milling and Electrical discharge machining (EDM).

2.4.1.1 Micro-milling

It can be useful in microfluidics applications for two main functions: processing of the mold used in subsequent manufacturing steps (for example, injection molds or hot embossing) or processing of microchannels and features directly in the final part[34]. Micro-milling operates using rotary cutters to remove material by advancing a cutter into a solid block until the final piece is reached using the instructions provided by the CAM software (at least for modern cutters), which refers to a 3D model of the piece[35]. Micro-milling has numerous advantages due to its ability to produce complex, high-precision geometries with micro-features in a wide range of materials, as long as they do not have high hardness (up to about 60 HRC); however, it is not possible to create geometries with an aspect ratio (height-to-diameter ratio of the tool) greater than 3[35]. Figure 2.7 shows the basic components of a CNC milling machine, from the CAD model to the finished product.

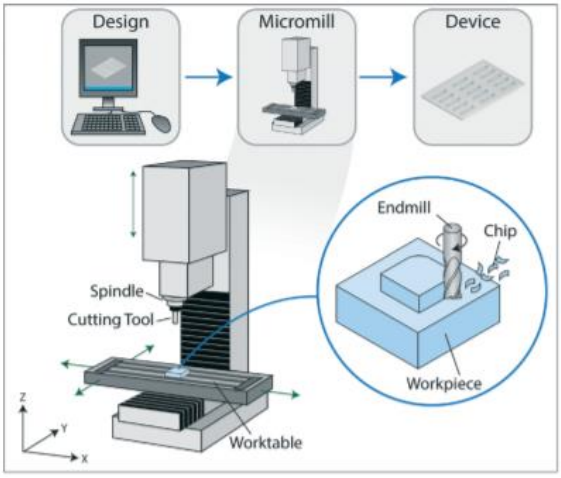

Figure 2.7. A schematic of micro-milling technique; adapted from[35].

2.4.1.2 Electrical discharge machining (EDM)

It is another subtractive manufacturing process and it is based on a series of discrete electrical discharges occurring between two electrodes, the tool and the workpiece, separated by dielectric fluid[36]. During the discharge, the electrical energy is transformed into thermal energy, which generates a plasma channel between the cathode and the anode and significantly raises the temperature in a well localized area. This mechanism starts the melting of the materials on the surface of each electrode and the subsequent removal of material from the piece. The key role in this process is performed by the dielectric fluid, which acts as a cutting medium to improve surface roughness, corrosion resistance and wear resistance; it also has the task of dispersing the heat produced by the process and of transporting and removing the material at the end of the process[36]. This technology allows to obtain a good surface finish and, unlike micro-milling, is able to work with very hard materials. However, reproducing sharp edges on the workpiece is difficult due to electrode wear, which in the long run can also have detrimental effects on the geometry of the workpiece. Figure 2.8 shows the mechanism of operation of the EDM process[37].

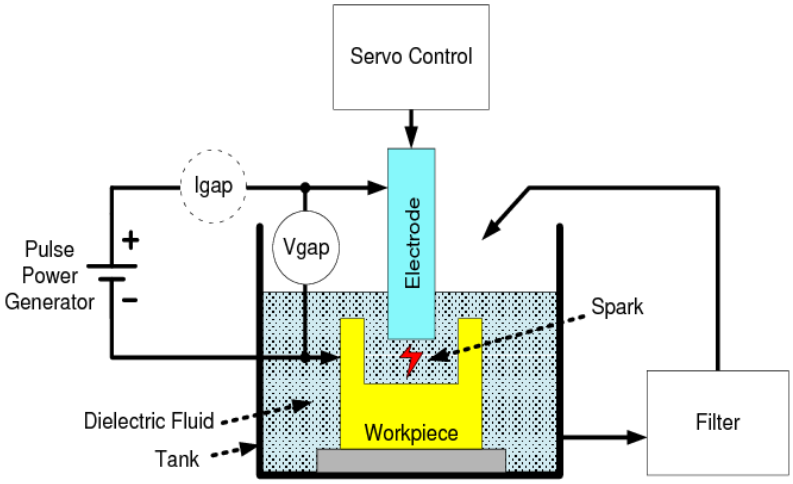

Figure 2.8. Scheme of an Electric discharge process (EDM); adapted from[37].

2.4.2 The additive techniques

Unlike the process of removing material from a larger part, additive processes build objects by adding material layer by layer, each subsequent layer being bonded to the previous layer until the part is completed. Just like subtractive CNC tools, additive techniques create parts in plastics or metals for rapid prototyping directly from CAD models, offer excellent accuracy and surface finish, but are quite expensive. These techniques mainly use metals to make mold inserts. In particular, there are two techniques belonging to this group that is worth listing: the LIGA process and Electroforming.

2.4.2.1 LIGA process

It is a German acronym for Lithographie, Galvanoformung, Abformung (Lithography, Electroplating, and Molding) and combines X-ray lithography with electroplating enabling the fabrication of high aspect ratio microscale structures and excellent accuracy of the lateral surface[38]. The process consists of several steps; first, a substrate with a conductive surface is coated with a thick photoresist. The radiation phase follows, involving the exposure of a thick resist layer to a high-energy X-ray beam coming from a synchrotron[38]. Exposure is followed by the removal of the non-cross-linked photoresist with the use of a developer, followed by the electrodeposition of a metal. After photoresist removal, metal structure formed may be used as a metallic mold insert for injection molding. Figure 2.9 outlines the various steps that characterize the LIGA process[39].

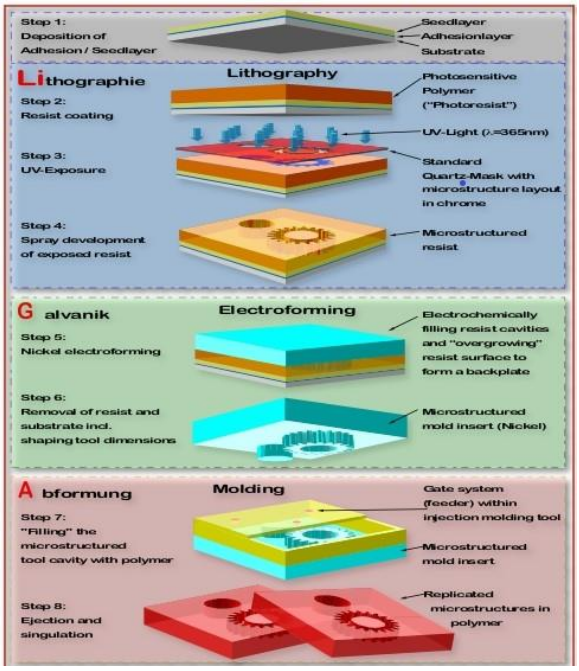

Figure 2.9. Schematic view of the LIGA process; adapted from[39].

2.4.2.2 Electroforming:

It is a process that has great advantages in creating micro-features in inserts for injection molding, such as high dimensional accuracy, precise reproduction of surface details, the production of components with complex shapes and thin walls[40]. Electroforming technology is a metal forming process in which parts are fabricated through electrodeposition on a model. The basic elements of this process are an anode, an electrolyte, a workpiece model for plating and a power supply[41]. In the basic process of electroforming, an electrolytic bath is created inside which the cathode and the anode are immersed: the cathode is the object to be coated while the anode can be made up of the metal to be deposited (an inert metal or graphite).

However, this process has some disadvantages which may hinder its use as a viable manufacturing process from an engineering point of view; they range from long deposition times for significant thicknesses to particularly high costs, as well as having constraints in the choice of materials. The whole process is described in Figure 2.10.

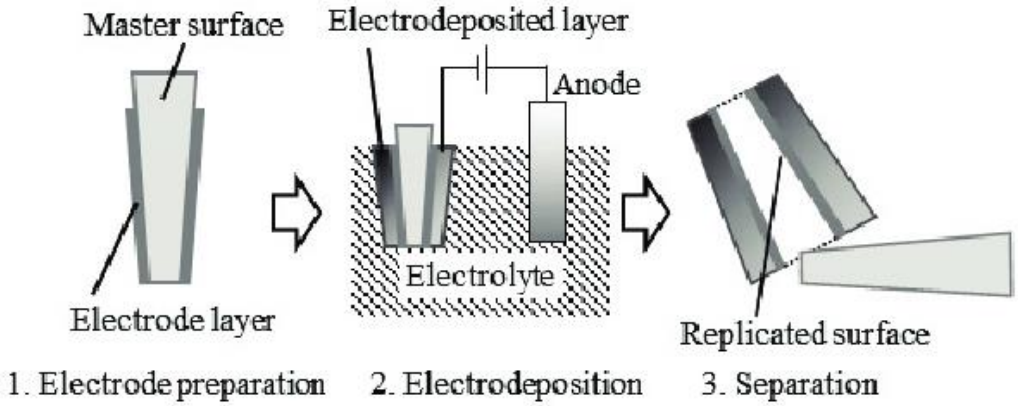

Figure 2.10. Step diagram of the electroforming process; adapted from[40].

2.5 Additive Manufacturing

As seen in the previous paragraph, there are many technologies, both subtractive and additive, that allow the production of metal inserts used in injection molding. Anyway, these techniques are not very fast and are very expensive. For these reasons these are not very attractive for microfluidics, which requires rapid prototyping of devices, keeping costs limited. Often known as 3D printing, Additive Manufacturing (AM) is a process of creating objects from three-dimensional solid model data by joining materials layer by layer[42]. In recent years, Additive Manufacturing has achieved considerable success in the field of injection molding; for example, it is used to produce inserts for metal or plastic injection molds at relatively low cost and with little investment in manufacturing infrastructure[4]. In particular, the advantages of these two technological domains are the following:

- high flexibility due to the fact that the part is produced directly from a CAD model without the need for tools,
- the possibility of creating in a very short time (hours or few days) almost all the geometries that can be designed, using a wide range of materials,
- the lower cost of developing the prototype, compared to other technologies,
- possibility of making economical mold inserts for injection molding of plastic parts that require high levels of customization.

Thus, several AM processes are available to produce injection molding inserts using a wide variety of material types, which have their strengths and weaknesses when it comes to being used for mold inserts. Traditionally, molding with metal inserts is performed with the aim of reducing the cycle time, obtaining molded products with a better aesthetic/dimensional quality and ensuring greater durability of the insert, taking advantage of the thermal and mechanical properties of metals. However, today Additive Manufacturing uses technologies for the production of aluminum and silicone molds, but it is above all the 3D plastic inserts for molds (Figure 2.11) that have revolutionized the production of molds in the plastic processing industry by bringing the AM to the field of microfluidics[4].

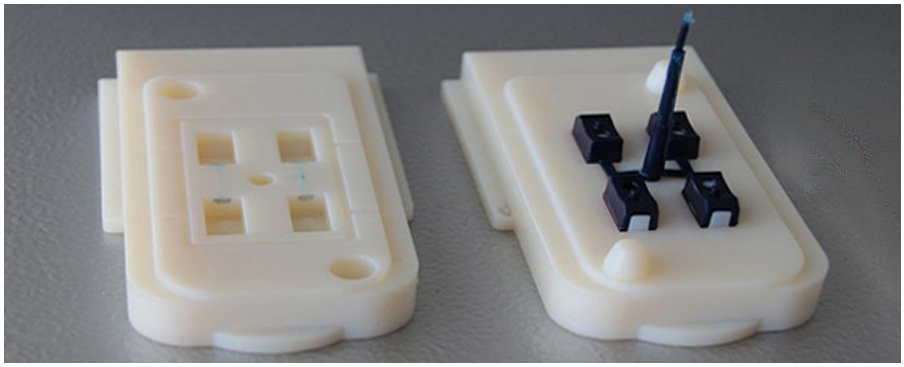

Figure 2.11. Example of 3D plastic mold insert and respective molding part.

Obviously, with the use of plastic resins for manufacturing the inserts, the operating conditions under which the injection molding machine is operated are very different from the case of metal inserts. In fact, the greatest challenge that Additive Manufacturing techniques have to face is precisely aimed at the durability of the plastic insert, today still very low when compared to that of other materials, primarily metal[4]. Injection molding is a process that operates at relatively high melting temperatures and injection pressures of some tens of bars, and these parameters have a negative impact on the lifetime of the mold inserts, reducing their operating cycles. Furthermore, although Additive Manufacturing technologies offer effective methods for the production of complicated microstructures at relatively low costs, not all of them are able to realize these geometries by faithfully following the 3D model, thus making themselves inadequate for some microfluidics applications that require reduced dimensions of the feature.

Chapter 3

Materials and methods

3.1 Design of the microfluidic platform

The microfluidic device was designed with a geometry simple enough to allow for easy reproduction of features through Additive Manufacturing and to allow for the study of the behavior and the interaction between different cell lines on the same platform. The platform will initially operate in static conditions, so that the analyzed cellular behavior will only depend on diffusive fluxes. The design must also offer the possibility of adding perfusion to the device, for example connecting it to a syringe pump. Furthermore, having to carry out biological studies at controlled oxygen partial pressure conditions[43], the design of the platform will include the possibility of placing a cover, made of a material that allows controlling the oxygen permeability, on the top side. The layout was designed to enable different configurations, considering the type of cells to be introduced and acting on the environment in which they are to be studied and analyzed. The basic idea of the chip was to build a central square chamber connected to four identical wells through separate channels; in this way it is possible to seed cells in the four wells, but also in the central chamber, and to study their behavior and possible interactions along the four channels. The first model in 2D of the chip (reported in Figure 3.1) was obtained using AutoCAD® software, a commercial Computer-aided design (CAD) software developed by Autodesk.

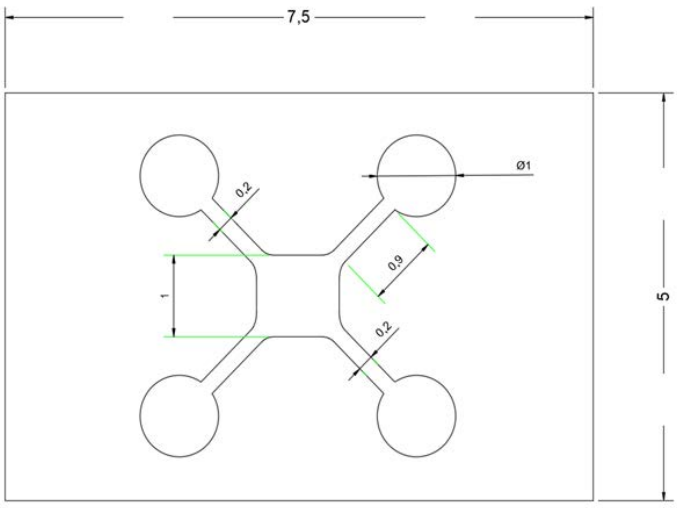

Figure 3.1. 2D device design made using Autodesk AutoCAD®.

From the figure, it is possible to observe that the entire device lies on a rectangular surface equal to 7.5 x 5 cm. The sides of the square central chamber have a length of 1cm, the wells have a diameter of 1 cm, while the channels are 0.9 cm long and have a width of 0.2 cm. Regarding the height of the features relative to the platform base, this was defined later during the design of the insert for the injection molding machine mold. In fact, the 2D model of the chip served as a starting point for a more accurate 3D design of the insert to be made via Additive Manufacturing.

3.2 Design of the insert

The first step for the injection molding process is the production of the inserts; to do so, the Stratasys PolyJet Object350 - Connex3^{TM} printer was used, available at the TE.SI. laboratory in Rovigo. This printer uses PolyJet 3D printing technology, part of the Additive Manufacturing world, and is based on the deposition of liquid layers of curable photopolymers on a tray[4]. These polymers reticulate following exposure to UV light, enabling production of precise parts without the need to further processing before placing the inserts in the mold of the injection machine[4]. The first phase of the 3D printing process requires the design and construction of the insert CAD model[42]. Previous work on this printer showed that excessive scaling down of the features led to faulty pieces in which dimensions were not fully respected; for this reason, it was decided set a nominal height for all elements equal to 600 μm. SolidWorks® software was used for the design of the insert; its 3D model and the final layout are shown in Figure 3.2. In this case, the units of measurement are millimeters and the letters A, B, C, etc identify the most important areas to be addressed in the metrological analysis.

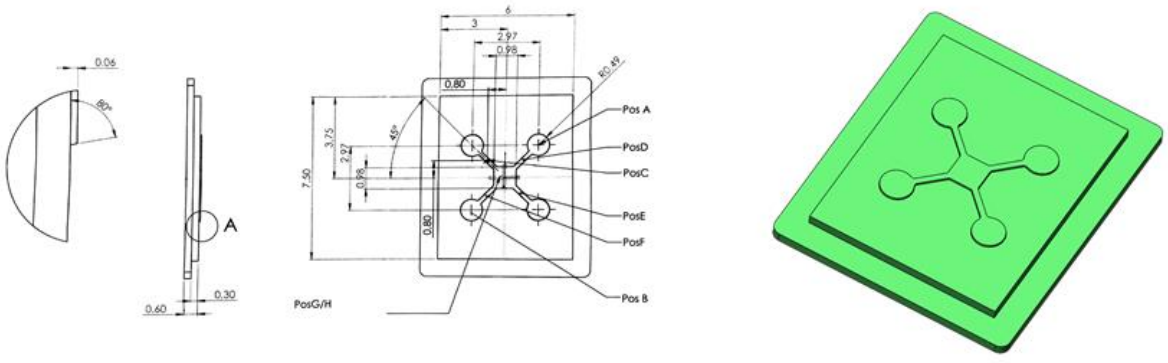

Figure 3.2. 3D Model of the insert designed using SolidWorks® software.

3.2.1 Insert holder plate

In order to use the insert in the injection molding machine, it was necessary to model a mold design and make an aluminum plate to act as an insert holder. In Figure 3.3 it is possible to observe the SolidWorks® model of the movable insert-holder plate that is inserted in the part of the half-mold that opens and closes during the molding process and allows the extraction of the piece by means of the extractors.

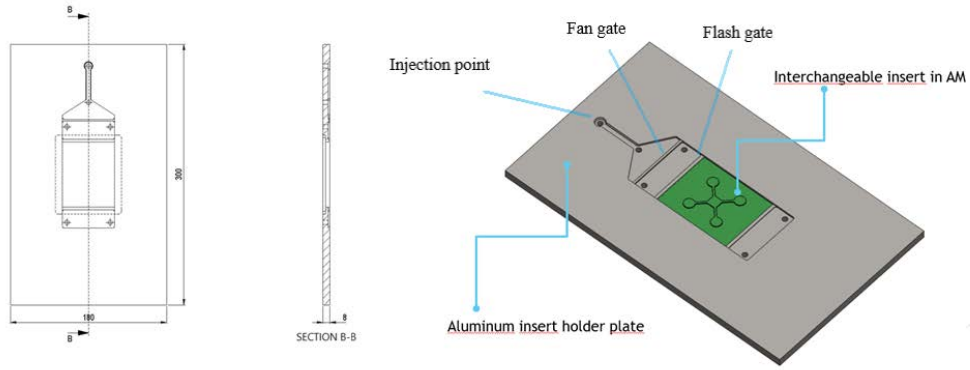

Figure 3.3. Aluminum insert holder plate.

Therefore, the movable insert holder plate was made of aluminum, while the rest of the mold, i.e. the movable and fixed half-mold of the machine, was made of steel. From a geometric point of view, the design of the aluminum plate is characterized by the presence of the fan and the flash gate, the latter sometimes also referred to as the film gate. They are very thin gates compared to the others and are sometimes inserted to make the flow of the material more stable and flatter. In other words, for an initial radial flow front, these gates, and especially the thinner flash gate, try to orient the flow in one direction only so that it is quite uniform when it reaches the insert. The advantage of a uniform flow, in addition to facilitating the filling of the mold cavity with the plastic material, is that of preventing the formation of so-called welding lines (Figure 3.4). Weld lines are defects in the molded part and are related to the evolution of the flow front during the injection phase[44]. In fact, in the collision area between two flow fronts, a junction point is formed which, in addition to being visible and disturbing the aesthetic appearance of the object, represents a point in which the mechanical properties are lower than the other mold regions[45].

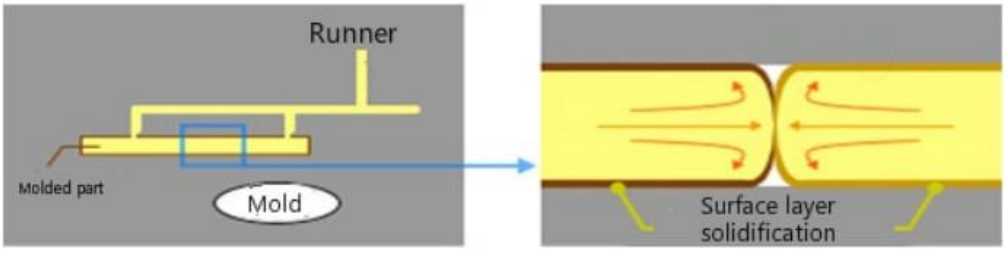

Figure 3.4. Example of welding lines in injection molding; adapted from[45].

3.3 Inserts manufacturing

As reported in the previous paragraph, the Stratasys ObJet350 - Connex3[46] printer was used for the realization of the inserts, the machine is shown in Figure 3.5, while Table 3.1 reports some specifications obtained from the technical data sheet provided directly by Stratasys.

Figure 3.5. Stratasys Objet350 - Connex3; adapted from[46].

Table 3.1. Stratasys Printer Technical Specifications.

Specification	Value
Maximum Build Size (XYZ)	340 x 340 x 200 mm
System Size and Weight	1400 x 1260 x 1100 mm; 430 kg
Resolution (XYZ)	600 dpi - 600 dpi - 1600 dpi
Accuracy	20-85 µm for features below 50 mm, up to 200 µm for full model size
Minimum Layer Thickness	Horizontal build layers as fine as 16 µm
Power Requirements	110-240 VAC 50/60Hz; 1.5 kW single phase
Operating Conditions	18-25°C; relative humidity 30 - 70%

Before printing, the CAD file needs to be converted into a surface tessellation (STL) file that describes the geometry of the surface by discretizing it into triangles. STL is the most common file type for rapid prototyping and 3D printing[42]. Subsequently, the file is transferred to a computerized system and the computer software “slices” the imported ".STL" files, i.e. the digital representation is divided into virtual horizontal layers of varying thicknesses[42]. At this point it is possible to start the actual production process of the insert, but not before having chosen the type of material with which to make the tools. As mentioned, PolyJet technology works using photopolymers, and these are produced and supplied directly by Stratasys; the

photopolymer used is Digital ABS Plus[47], which combines discrete characteristics of resistance to thermal and mechanical stress. This material is sold in sealed cartridges, which have trade names: in the case of Digital ABS Plus, it is made by combining the RGD515 and RGD535 cartridges. The technical data sheet provided by the manufacturer is shown in Figure 3.6.

MECHANICAL PROPERTIES	TEST METHOD	IMPERIAL	IMPERIAL METRIC
Tensile Strength	D-638-03	8,000-8,700 psi	55-60 MPa
Elongation at Break	D-638-05	25-40%	25-40%
Modulus of Elasticity	D-638-04	375,000-435,000 psi	2,600-3,000 MPa
Flexural Strength	D-790-03	9,500-11,000 psi	65-75 MPa
Flexural Modulus	D-790-04	245,000-320,000 psi	1,700-2,200 MPa
HDT, °C @ 0.45MPa	D-648-06	136-154 °F	58-68 °C
HDT, °C @ 0.45MPa after thermal post treatment procedure A	D-648-06	180-194 °F	82-90 °C
HDT, °C @ 0.45MPa after thermal post treatment procedure B	D-648-06	198-203 °F	92-95 °C
HDT, °C @ 1.82MPa	D-648-07	124-131 °F	51-55 °C
Izod Notched Impact	D-256-06	1.69-2.15 ft lb/in	90-115 J/m
Tg	DMA, E»	117-127 °F	47-53 °C
Shore Hardness (D)	Scale D	85-87 Scale D	85-87 Scale D
Rockwell Hardness	Scale M	67-69 Scale M	67-69 Scale M
Polymerized Density	ASTM D792		1.17-1.18 g/cm³

Figure 3.6. Digital ABS Plus data sheet; adapted from[47].

Stratasys describes it as a high temperature resistant material with high toughness and is ideal for rapid prototyping in the production of inserts for injection molding. The machine was thus loaded with cartridges with liquid material and in this case, two cartridges were used to create a single material. The production system then builds each layer individually, with each subsequent layer added to the previous one. The machine is equipped with a head with nozzles from which the photopolymer comes out, and UV lamps that crosslink and harden the material. All this is done on a support material that will act as a base and facilitate removal from the plate. The process steps for manufacturing the inserts are summarized below:

1) Realization of the CAD model of the insert on SolidWorks® and subsequent conversion into an STL file;
2) Importing the model into the control software and virtual positioning of the pieces on the plate. It is also recommended to print in "Glossy" mode to avoid printing support material on the last view layers;
3) Mechanical removal (with a scraper) of the pieces from the support or with a solution that dissolves the latter at the end of the process;
4) Removal of any substrate residues by rinsing with water.

In order to validate the manufacturing process of the inserts, it was decided to mold them at three different inclinations: 0°, 45° and 90° with respect to the axes of 3D printing machine. Since the configuration of the chip has been designed with the four channels inclined at 45° with respect to the plane of the platform, the choice of making the inserts with three different angles has the aim of quantifying, through the three different profiles, the capacity of the machine to recreate the CAD model. To optimize the printing process, it was decided to make all the inserts at the same time, simply by placing their respective angles in the virtual positioning. The whole manufacturing process took about 3 hours.

3.4 Metrological characterization of the inserts

Once the inserts were printed with different angles, they were subjected to metrological characterization to identify which of the three angles best replicated the features created with the CAD model. By metrological characterization, we mean the visual and topographical analysis, and the quantification of the surface roughness of the inserts. This characterization also allows to evaluate the wear of the object following injection molding and to identify any critical areas; therefore, this analysis was also repeated after molding the microfluidic chips. This analysis was performed using the Sensofar S Neox profilometer[48], shown in Figure 3.7 together with its supporting hardware.

Figure 3.7. Sensofar S Neox profilometer; adapted from[48].

This device is a complete microscopy system for non-contact optical profilometry, designed specifically for measurements in the nanometer and micrometric scale, and which uses objectives to perform surface surveys and obtain a detailed topography of a certain area of the workpiece. Moreover, the instrument is quite versatile, as with a single click in the SensoSCAN environment it is possible to switch the system to the best technique for the measurement to be carried out. The three techniques are as follows:

- Ai Focus Variation: scans the sample vertically to obtain a set of continuous images of the surface, ensuring a high acquisition speed;

- Confocal: is a microscopic imaging technique that uses an aperture in the confocal plane of the objective, resulting in the mode with the highest lateral resolution;
- Interferometry: mainly used for the acquisition of data relating to roughness or surface irregularities, it boasts a better vertical resolution.

The machine consists of a head placed on the objectives, and its movement on the plane can be motorized or done by a manual approach. It has three objectives: 2.5x, 20x and 100x; the acquisition of the study area is done through the 2.5x objective, while for the actual measurements only 20x is used. It basically involves performing scans on the XY plane and then increasing in Z and rebuilding the structure in 3D, thus obtaining a single high-resolution image of a more or less large surface. Some machine specifications are shown in Table 3.2.

Table 3.2. Technical characteristics of the S Neox profilometer.

Characteristics	Value
Optical resolution (µm)	0.31
Spatial sampling (µm)	0.34
Working distance WD (mm)	4.5
Field of view FOV (µm)	845 x 707

The steps that were carried out during the data acquisition phase relating to the metrological characterization of the inserts are:

1) Positioning of the sample to be analyzed in the XY plane and manually approaching the piece roughly for quick adjustment along the Z-axis, to re-enter the field of view;
2) Identification of the area to be analyzed with the 2.5x objective and making sure to see the area clearly enough. This is followed by the acquisition of a preview with the 2.5x objective;
3) Switching to the 20x objective to set the Z min and Z max coordinates of the surface involved in the analysis. To impose a top and bottom range in which to perform the measurement, it is advisable to switch to Confocal mode;
4) By imposing a zero as a reference system and using a joystick for movement and rapid control, the upper and lower limits of the Z coordinate are then established for the analysis;
5) To get a more accurate measurement, move to the sketching area, where a preview of the surface to be observed is made. A grid is positioned on the preview, which must cover the entire area to be analyzed;
6) Choice of analysis technique (Confocal, Interferometry or Ai Focus Variation) and 3D mode. it is possible to set some parameters, such as brightness, sensitivity, overlap and

speed factor to improve the acquisition of the measurement and the speed with which it is carried out;

7) Starting the analysis and at the end display of the measurement carried out and possible application of restore functions or filters to improve the topography obtained or remove possible noises.

3.5 Injection Molding

For the molding of microfluidic devices, the machinery used was the Battenfeld HM 110/525H/210S (shown in Figure 3.8).

Figure 3.8. Injection Molding machine.

The machine is composed of a screw that moves inside a cylinder, which is heated in the various sections by electric resistances and by a fully hydraulic locking unit. It also has a parallel integrated locking cylinder with a quick-stroke cylinder, which provides a short design and central power transmission.

Another feature of this machine is to have two different injection units because it can be used for overmolding or LIM (liquid injection molding) for silicones.

In the final part of the hopper, there is also a steel parallelepiped which has the function of cooling the temperature of the pellets entering the cylinder in order to avoid the bridge effect inside and therefore obstruct the passage.

The screw has the function of feeding in the first area, the one near the hopper, of melting in the second and pumping in the last, with decreasing profiles from the hopper to the cylinder head. Furthermore, as mentioned in Chapter 2, once the dosage level has been reached, the screw acts as a punching material and pushes the material into the cavity. Table 3.3 reports the technical characteristics of the two injection units of the press (the clamping unit is the same for both).

Table 3.3. Battenfeld HM 110/525H/210S main specifications.

Unit	Injection unit 525	Injection unit 210
Maximum clamping force (kN)	1100	1100
Screw Diameter (mm)	35	25
L/D ratio of the screw	22:1	22:1
Injection Capacity (cm^3)	193	74
Screw Stroke (mm)	200	150
Specific Injection Pressure (bar)	2743	2940
Heating Capacity (kW)	10.4	6.8

From the table it is possible to observe how an injection unit has a shorter screw stroke; this feature is advisable in the case of molding of small pieces, because this means shorter residence times of the polymer in the cylinder and less degradation.
The control unit of the machine (shown in Figure 3.9) is divided into three parts: the visual unit (man-machine interface) with which it is possible to set the various parameters, the control part of the movements of the various axes of the machine and the on/off unit of the motor and electric resistances.

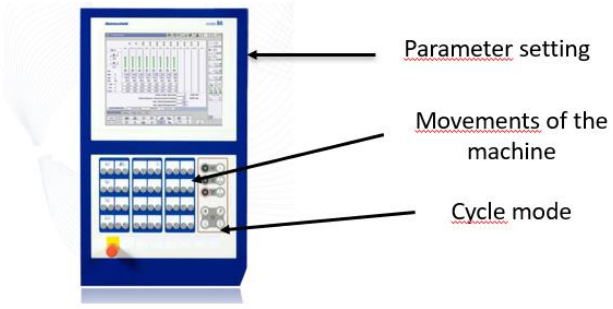

Figure 3.9. Control Unit of Injection Molding machine.

The machine has four cycle modes: movement in tooling, manual movement, cycle and half cycle. In the tooling mode, the machine carries out all the operations it can do with reduced speed and forces, without considering the parameters set, while in the manual mode all the

movements are performed according to the parameters chosen by the operator. The difference between cycle and semi-cycle lies in the fact that in the second case the machine performs all the operations of the cycle, but for a single molded piece.

3.5.1 Choice of material for the microfluidic platform

The microfluidic device will be used to perform biological experiments, which usually involve different cell lines, so the choice must fall on a biocompatible material. In addition, the experiments involve collection of data over a long temporal window (at least 7 days); data collection typically consists on microscope observations of the internal environment created in the platform. Therefore, it is essential to identify a material that is transparent, but at the same time does not give rise to autofluorescence phenomena during the detection phase of the species with fluorescent markers. In summary, the characteristics underlying the choice of material were the following:

1) Good optical transparency is crucial for observation;
2) Biocompatibility;
3) Low oxygen permeability to enable oxygen partial pressure modulation in future experiments;
4) Resistance to chemical products (acid, base, solvent…)
5) Ease of processing and compatibility with the Digital ABS insert;
6) Cost-effectiveness.

As already mentioned in Chapter 1, the popularity of PDMS in the biomedical field is due not only to its cost-effective manufacturing process but also to a number of interesting physical and mechanical properties (e.g. optical transparency, permeability and flexibility) that have proven useful for various applications based on cell culture[49]. However, two properties of PDMS were deemed unsuitable for this study: the leaching of uncured oligomers from the polymer network into microchannel media, and above all the high permeability to gases, especially oxygen[17]. Moreover, the time needed to obtain a final PDMS platform through the replica molding process is higher and more operator-dependent with respect to the injection molding process[25]. The attention has therefore been turned to thermoplastic polymers, lately more and more in vogue in the field of microfluidics being inexpensive materials and having a wide variety of properties to meet the various needs listed above.

Figure 3.10 shows a table that summarizes the main properties of some thermoplastic polymers that are currently used in the field of microfluidics.

Thermoplastics	Thermal expansion coefficient [m/(m K)] 10^{-6}	Young's modulus (GPa)	T_g (°C)	T_m (°C)	Solubility parameter δ $(MPa)^{1/2}$	Water absorption (%)	O_2 permeability ($x10^{-13}$ cm^3. cm cm^{-2} s^{-1} Pa^{-1})	Biocompatibility	Transparency
Cyclo olefin (co) polymer (COC/COP)	60–70	1.7–3.2	70–180	190–320	17.7	0.01	NA	Biocompatible	Transparent
Polymethyl methacrylate (PMMA)	7077	2.4–3.4	105	250–260	20.1	0.1–0.4	0.1	Biocompatible	Transparent
Polyethylene terephthalate (PET)	59.4	2–2.7	70	255	20.5	0.16	0.03	Biocompatible	Transparent
Polyethylene-low density (LDPE)	100–200	0.11–0.45	−125	105–115	17.6	0.005–0.015	2	Biocompatible	Both opaque and transparent
Polyethylene-high density (HDPE)	120	0.8	−80	120–180	18.2	0.005–0.01	0.4	Biocompatible	Both opaque and transparent
Polypropylene (PP)	72–90	1.5–2	−20	160	16.3	0.01–0.1	1.7	Biocompatible	Both opaque and transparent
Polystyrene (PS)	70	3–3.5	95	240	18.7	0.02–0.15	2	Biocompatible	Transparent
Polycarbonate (PC)	65–70	2.6	145	260–270	19.4	0.23	1	Biocompatible	Transparent
Polyvinyl chloride (PVC)	54–110	2.4–4.1	80	100–260	19.4	0.04–0.4	0.04	Biocompatible	Transparent
Polyamide (Nylon)	110	2.5	47–60	190–350	28	1.6–1.9	0.03	Biocompatible	Transparent
Polysulfone(PSU)	55–60	2.48	185	180–190	18.7	0.2–0.8	NA	Biocompatible	Translucent
Polylactic acid (PLA)	740	3.5	60–65	150–160		0.68	NA	Biocompatible (problematic)	Transparent
Polytetrafluoroethylene (PTFE)	112–135	0.4	115	326	12.6	0.005–0.01	3	Biocompatible	Translucent
Polyetheretherketone (PEEK)	26	4–24	143	343	21.9	0.1–0.5	0.1	Biocompatible	Opaque
Acrylonitrile butadiene styrene (ABS)	72–108	1.4–3.1	105	Amorphous	18.8	0.05–1.8	0.5	Not suitable	Both opaque and transparent

Figure 3.10. Properties for thermoplastic polymers, adapted from[50].

In particular, for the purposes of this thesis, it was decided to investigate the possibility of using materials such as Polyethylene Terephthalate (PET), Polymethylmethacrylate (PMMA), Polystyrene (PS) and Polycarbonate (PC)[50]. Although the first two had the lowest oxygen permeability among the four thermoplastic polymers considered, they were both discarded. PET showed difficulties in injection molding due to the differences in thermal conductivity between it and the aluminum plate of the mold, facilitating its crystallization and making it opaque and therefore unsuitable for the intended purposes. PMMA, despite having a chemical inertness to many solutions and solvents, is affected by ethanol, isopropyl alcohol (IPA), acetone and other important solvents used during the process of sterilization[50].

As for PC, nowadays there are many microfluidic devices made with this material thanks to its transparency and its very high glass transition temperature (145°C), which makes it very thermally stable. However, PC has poor resistance to certain organic solvents and its autofluorescence is high, making PC difficult to use when working with fluorescently labelled cells or materials[50].

Polystyrene has a long tradition in molecular and cell biology studies thanks to its biocompatibility and its optical transparency, having long since replaced glass in the production of many objects used in the laboratory, such as Petri dishes, test tubes and microplates[51]. In addition, it has numerous advantages for biological applications including low cost, commercial availability, chemical inertness, chemical stability and stiffness[52]. However, unlike PDMS, being a thermoplastic polymer, in order to make complex devices with this material it is

necessary to resort to injection molding or hot embossing, the costs of which could represent an obstacle to its use[51].

In the end, polystyrene was chosen for the realization of the microfluidic chips used in this thesis, in particular Total PS Crystal 1540 polystyrene was used. This material is as easy-flowing crystalline polystyrene designed for extrusion or injection applications. Moreover, having a high gloss, it is particularly suitable for co-extrusion with a glossy layer. In injection molding with this low viscosity at a high shear rate it has good injectability and combines excellent flowability with a higher softening point (Appendix A.3). Figure 3.11 shows the polymer chain and the structural unit (repeating unit) of polystyrene, while Table 3.4 shows some specifications of Total PS Crystal 1540 polystyrene supplied directly by Total.

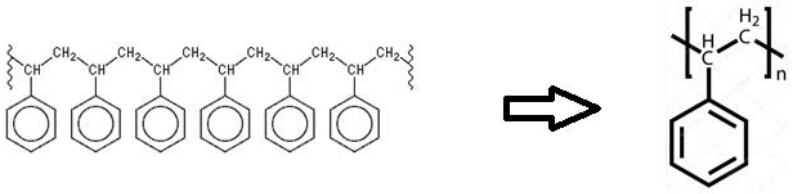

Figure 3.11. Polystyrene chain and structural unit.

Table 3.4. Some mechanical and thermal properties of Total PS Crystal 1540 polystyrene.

Properties	Method	Unit	Value
Melt flow index (200°C-5kg)	ISO 1133 H	g/10mn	12
HDT annealed under 1.8 MPa	ISO 75-2A	°C	83
Tensile strength at break	ISO 527-2	MPa	42
Elongation at break	ISO 527-2	%	2
Tensile modulus	ISO 527-2	MPa	3100
Flexural modulus	ISO 178	MPa	2900
Density	ISO 1183	g/cm³	1.05
Water absorption	ISO 62	%	<0.1

3.5.2 Process parameters

As for the process parameters to be set in the injection molding machine, Total itself provides some recommended parameters for carrying out the molding. However, since we are dealing with a process that uses inserts in Digital ABS produced via Additive Manufacturing, we must also consider the resistance to temperature and pressure of these materials, as they are much more subject to wear than traditional metal inserts. The crucial parameters are the temperatures, from the last part of the screw (the one close to the plasticizing cylinder) to the first part (the

one under the hopper), the cooling and holding time, the injection flow, the holding pressure and the dosing quota. A first series of cycles was carried out to set the optimum parameters using a random test insert also in Digital ABS and injecting Total PS Crystal 1540 polystyrene. These initial operations, although quite long and tedious, are used to prevent new pieces from coming out of the injection molding machine with defects such as short shots, flashes and weld lines. Once optimum parameters have been set and the correct insert has been placed in the mold, the machine has been set up in continuous cycle mode and the first pieces were printed. After a first phase in which the first pieces were discarded, the following ones were collected up to 500. Table 3.5 summarizes the most important parameters that were set in the molding machine.

Table 3.5. Process parameters set for injection molding

Properties	Value
Cylinder temperature close to the mold	240°C
Temperature under the hopper	50°C
Injection flow	10 cm^3/s
Injection pressure	1100 bar
Holding pressure	308 bar
Holding time	30 s
Cooling time	10 s
Clamping force	550 KN
Dosing volume	12 cm^3

3.5.3 Moldflow simulations

Some simulations were carried out in Autodesk Moldflow, a software that simulates high-end plastic injection molding, developed by the Autodesk company and very often used in the engineering field for the optimization of parts, molds, and processes of injection molding. To use Moldflow, it was first necessary to convert the CAD model of the device into a Standard for Product Data Exchange (STEP) file, which is a 3D model file in an ISO standard exchange format that contains three-dimensional data that can be recognized by multiple programs.
At first, the model is oriented in such a way that the XY plane represents the partition plane and the Z-axis is oriented along with the opening of the mold, where the injection point will be. The program allows to work both with 2D mesh when working with constant thickness geometries, and with 3D mesh. In these simulations, Dual Domain (2D) triangular meshes were used, having the advantage of combining a lower computational effort with a more accurate modeling in case of thickness variation. Furthermore, Moldflow contains a library of materials with the respective manufacturer; in general, the choice of material considers the quality indicators of filling, packaging, and deformation of the material. In order to have a simulation closer to reality, it was decided to carry out the simulation with Total's Polystyrene 1541. Although the

program creates the meshes by default, they have been optimized to reduce the difference between the maximum and minimum aspect ratio as much as possible, while still trying to have a very low ratio (the higher the ratio, the worse the mesh). Figure 3.12 shows the device model with the meshes and their characteristics.

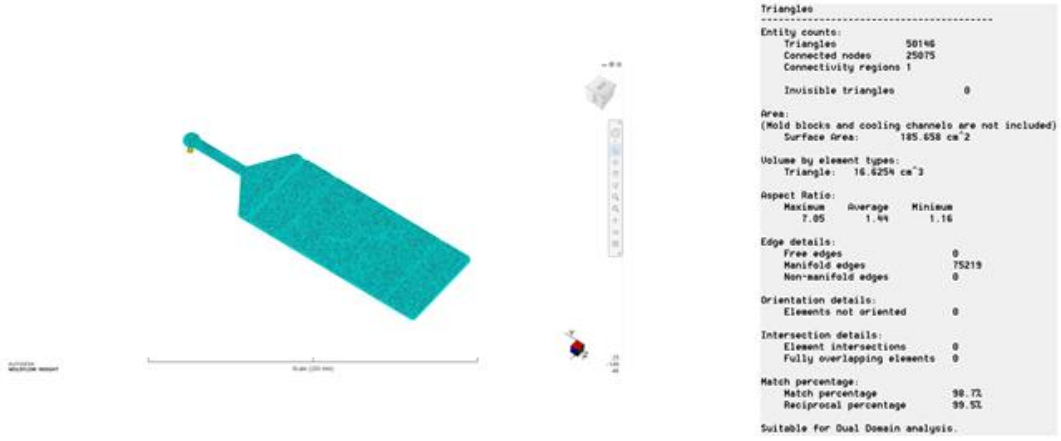

Figura 3.12. Chip model with mesh and mesh information.

The yellow cone on the top left corner represents the position of the injection point, where the polymer enters the mold. As for the information on the mesh, no free and non-manifold edges or not oriented elements must appear, while it is good to have a match percentage greater than 90%, in such a way as to have a high degree of correspondence of the elements on the other side of the part. Once the material to be injected was chosen and the mesh was optimized, the actual simulation of the mold filling phase was performed. Figure 3.13 shows the time taken by the polymer to fill the entire mold, while Figure 3.14 shows in detail how the flow lines vary.

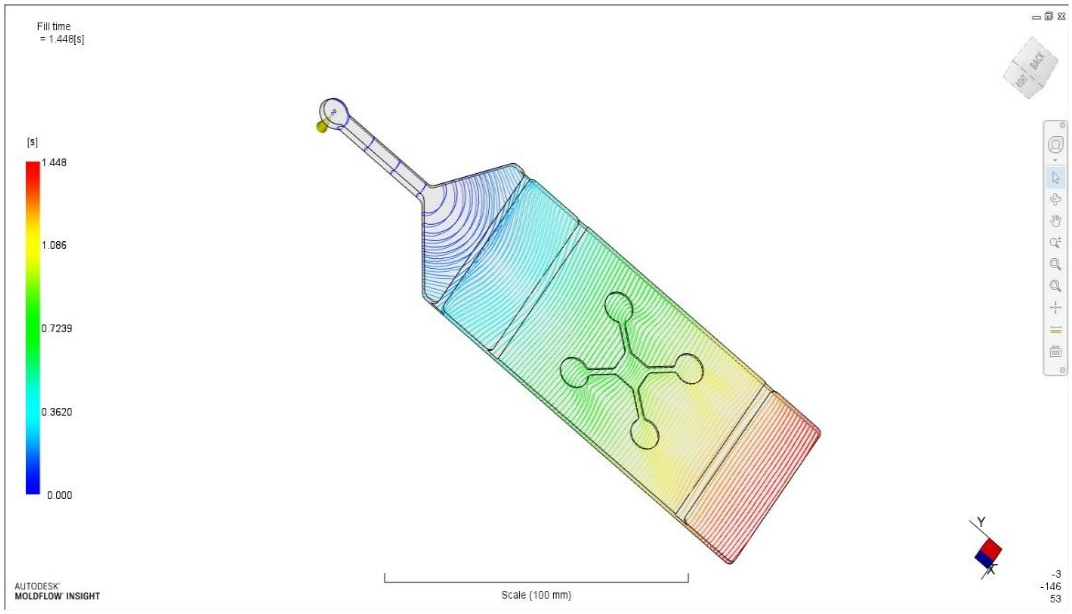

Figure 3.13. Fill time of the mold.

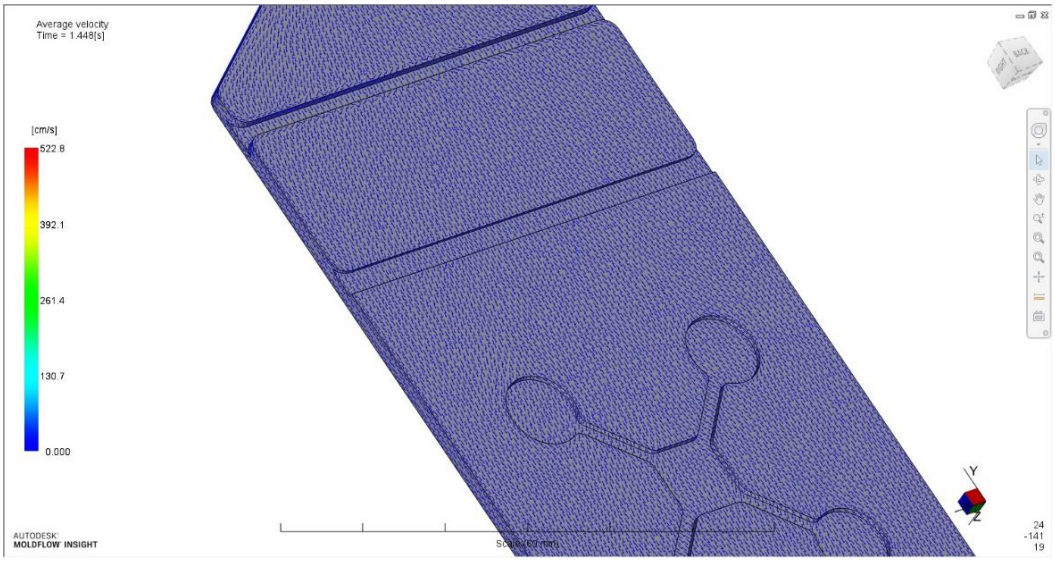

Figure 3.14. Detail of the flow lines.

Keeping in mind that the simulation did not consider either the cooling systems or the type of mold with which the injection molding machine is made, it mainly served to better understand the performance of the flash gate. From Figure 3.13 it is possible to notice the change in direction of the flow injected inside the mold; in fact, if a radial flow is obvious at the beginning, the flash gate allows it to be adjusted in such a way as to have a single flow front. This situation is described even better by Figure 3.14, where the change in orientation of the velocity vectors at the height of the flash gate is evident.

The simulation fully describes the entire injection molding process, from the filling to the holding phase, highlighting the switch-over pressure. Figures 3.15 (a) and 3.15 (b) summarize the entire molding cycle considering the filling time, the percentage of volume filled, the pressure inside the piece and that of switch over, and the polymer flow rate.

The status clearly shows the process switch from flow to pressure control, while from the pressure trend it is possible to see the detail relating to the switching pressure that occurs when the piece is filled to 99%. In fact, the final part of the piece is at zero pressure precisely because that is the last part that is filled with the polymer.

(a)

Filling phase: Status: V = Velocity control
P = Pressure control
V/P= Velocity/pressure switch-over

Time (s)	Volume (%)	Pressure (MPa)	Clamp Force (tonne)	Flow rate (cm^3/s)	Status
0.065	4.24	5.98	0.10	12.06	V
0.130	8.77	7.91	0.18	12.56	V
0.195	13.34	9.18	0.28	12.56	V
0.260	17.90	10.48	0.41	12.65	V
0.325	22.49	11.23	0.53	12.67	V
0.390	27.08	12.06	0.67	12.67	V
0.455	31.65	13.02	0.88	12.63	V
0.520	36.17	13.99	1.12	12.69	V
0.586	40.76	14.93	1.39	12.69	V
0.650	45.27	15.88	1.69	12.69	V
0.715	49.88	16.97	2.08	12.69	V
0.780	54.34	18.11	2.53	12.70	V
0.845	58.84	19.24	3.01	12.72	V
0.911	63.39	20.46	3.56	12.72	V
0.975	67.88	21.71	4.20	12.73	V
1.041	72.41	23.00	4.89	12.74	V
1.105	76.89	24.24	5.58	12.75	V
1.170	81.41	25.50	6.34	12.77	V
1.236	85.91	26.98	7.30	12.78	V
1.301	90.43	28.34	8.22	12.79	V
1.365	94.89	29.69	9.18	12.79	V
1.425	99.01	30.93	10.11	12.77	V/P
1.430	99.34	27.65	9.26	7.53	P
1.435	99.57	24.75	8.30	5.28	P
1.447	99.93	24.75	8.19	5.69	P
1.448	100.00	24.75	8.23	5.69	Filled

Filling phase results summary :

Maximum injection pressure (at 1.4248 s) = 30.93A6 MPa

(b)

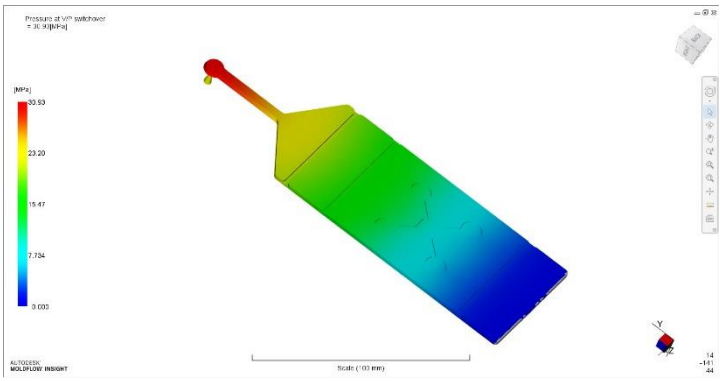

Figure 3.15. (a) Description of the molding cycle and (b) switch-over pressure.

3.6 Metrological characterization of the device and post molding insert

The metrological characterization of both the microfluidic chips and the insert after the molding of the chips followed the same procedure already discussed in paragraph 3.4 for the choice of the best insert to use. The only exception concerns the device which, unlike the inserts, has a geometry carved into the upper surface, due to the presence of the different features. To validate the entire production process, it was decided to mold to 500 pieces and see how the insert measured until the end of the molding. As for the polystyrene chips, of the 500 printed pieces, one chip every 50 pieces was analyzed. The areas analyzed are the same for both the insert and the chips and, in both cases, the areas selection covered all the features that were considered of particular interest. The results of the measurements can be visualized through an image that represents the 3D topography, or by extracting two coordinates (X and Z) with the possibility of obtaining a graph that describes the real trend. The software allows to extract the numerical profile through a file in DAT format formed by a list of pairs of the two coordinates; these DAT files can then be converted into Excel files to obtain graphs with the measures of the features and compare them with the nominal profiles.

3.7 Biological validation tests

In order to evaluate the goodness of the platform from a biological point of view, some validation tests were performed at the BIAMET laboratory of the Department of Industrial Engineering of the University of Padua. The tests mainly involved assessing the biocompatibility of the chips, the adhesion and survival of the cells inside the device by performing microscopic analyses, and finally designing a cover to obtain a clamping unit for the microfluidic device. Regarding this last point, since in the literature there are many examples of bonding between polystyrene and PDMS, it was decided to use polydimethylsiloxane as a membrane placed between the chip and the relative cover. The PDMS used in the BIAMET laboratory is provided by Dow Corning's Sylgard 184, one of the most popular polydimethylsiloxanes in the biomedical field. In the literature, it is defined as an elastomeric kit supplied in two components: a silicone base and a curing agent (Figure 3.16), which cross-links with the polymeric matrix.

Figure 3.16. Dow Corning's Sylgard 184: silicone elastomer base (on the left) and curing agent (on the right).

It is usually cross-linked at a temperature above 100°C, but can also cross-link at room temperature, obviously after a longer time. However, some properties of the polymer such as final tensile strength, hardness and Young's modulus increase leading to a higher hardening temperature. After polymerization, the polymer does not require further treatments, while it may be useful to subject the mixture to degassing in a vacuum chamber, before pouring it into the mold, to ensure the absence of air bubbles. Table 3.6 lists some properties of the polymer supplied by the manufacturer.

Table 3.6. Typical properties for Dow Corning's Sylgard 184.

Properties	Unit	Result
Viscosity (Mixed)	Pa·s	3.5
Thermal Conductivity	W/m °K	0.27
Useful temperature range	°C	-45 to 200°C
Cure Time at 25°C	hours	48
Heat Cure Time at 100°C	minutes	35
Heat Cure Time at 125°C	minutes	20
Heat Cure Time at 150°C	minutes	10
Tensile Strength	MPa	6.7

3.7.1 2D cellular cultures of neuroblastoma cells

Cellular tests were performed using two cell species: SK-N-DZ cells and SK-N-AS cells, both bone marrow metastatic neuroblastoma cell lines. Cell culture is performed in the BIAMET laboratory and follows a strict protocol for the correct maintenance and proliferation of cells. Cells grow inside the so-called flasks, conventional 2D cell cultures equipped with vented caps and of different sizes depending on the cell culture area required. In general, the T-25, T-75, or T-150 flakes are used which differ according to the area available for cell culture, respectively of 25 cm^2, 75 cm^2, 150 cm^2. Figure 3.17 shows the three types of flakes and some details on their correct use[53].

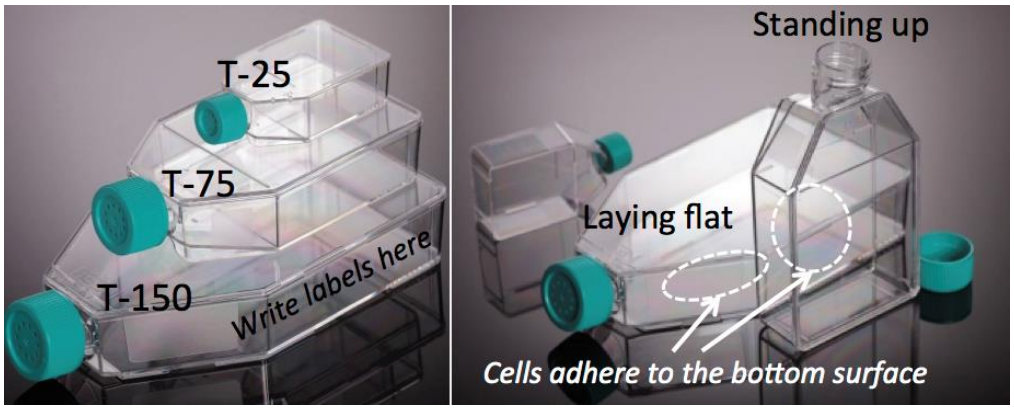

Figure 3.17. The T-25, T-75 and T-150 flakes; adapted from[53].

A flask must allow the cells to adhere and grow to the bottom within the surface, so they must be kept in a controlled atmosphere (20% of O_2, 5% CO_2) at a physiological temperature of 37°C. All this is done inside a CO_2 incubator, guaranteeing conditions of temperature, humidity and CO_2 content as faithful as possible to those required by cell cultures. Figure 3.18 shows the incubator in use in the BIAMET laboratory.

Figure 3.18. Heracell vios 160i CO_2 Incubator.

Inside, the samples are arranged on floors placed at different heights completely isolated from the external environment; moreover, in addition to the normal door, the incubator is equipped with a glass door that further protects against contamination when opened for inspection. As for the culture of SK-N cells used in the experiments, they were stored in 75 cm^2 flasks bathed in culture media made of 87% v/v Dulbecco's Modified Eagle Medium (DMEM), 10% v/v Fetal Bovine Serum (FBS), 1% v/v Penicillin-Streptomycin (an antibiotic to prevent contamination and 1% v/v of Mineral Essential Medium (MEM). Periodically, these flasks undergo a splitting procedure to avoid crowding of the cells on their bottom surface and to a replacement of the medium of culture. These operations of splitting the cells, as well as their seeding in microfluidic devices, take place under laminar flow cabinets that allow operating in sterile conditions through air filtration protecting cell cultures from external contamination.

3.7.2 Protocols for cell splitting and counting

As soon as the cell density is high inside the flask or experiments in microdevices must be conducted, it is necessary to provide for a splitting of the cells. To do this, a particular enzyme is used, Trypsin, which has the task of detaching the cultured cells that grow adhering to the lower surface of the flask. However, first of all, the residual culture medium which contains trypsin inhibitors must be removed; furthermore, since its optimum working temperature is 37°C, the Trypsin/EDTA solution is heated in a water bath up to that temperature. All the operations described in this protocol are carried out under the biosecurity hood, the splitting process for a single flask (75 cm^2) consists of the following steps:

- Aspirate the culture medium using a serological pipette and store approximately 4 mL of this in a 15 mL Falcon tube;
- The addition to the flask of about 7 mL of PBS, an aqueous saline solution widely used in dilutions to bring cell cultures to volume and kept at room temperature, to remove all traces of the old culture medium, including dead cells;
- Aspiration and discharge of the solution with PBS and addition of 2 mL of Trypsin previously heated to 37°C. Subsequently, the flask is placed in the incubator for 3 min;
- After that, the flask is observed through a microscope to see if Trypsin has acted and its inhibition is proceeded by adding the 4 mL of old medium to the flask;
- By means of a pipette, the cells are aspirated from the bottom of the flask and placed in the 15 ml Falcon tube. Before putting the solution into the centrifuge, it is recommended to take a small volume (how much depends on the experiment) of the total for cell counting;
- Centrifugation of the Falcon tube at 1100 rpm for 3 min with soft deceleration mode activated. In this way, the sedimentation of the cells is induced, obtaining a dense pellet to the bottom of the flask, while the residues remain in the supernatant (the upper liquid phase);
- The liquid is aspirated, while a suitable aliquot of cells after the count is placed in the new 75 cm^2 flask with the addition of 8-9 mL of fresh culture medium, also previously heated to 37°C;

This type of action is performed in the laboratory typically every 3-4 days. In general, the color of the culture medium is used to consider the health of the cells and their growth; in fact, this also includes phenol red ($C_{19}H_{14}O_5S$), whose color is sensitive to pH. If the color in the flask changes from red to brown/yellow, then the attack of carbohydrates by microorganisms may be considered possible, with consequent inspection of the sample and eventual replacement of medium. As for the cell count, this operation can be done simultaneously with the centrifugation of the Falcon tube, using 1mL of solution taken from the total one contained therein. This

operation is extremely important especially during cell seeding in microfluidic devices in order to provide an adequate density of cells in the places predisposed to them. In this case, a stain is used, Gibco™ Trypan blue (Figure 3.19), which is able to quantify live cells by labelling only dead cells.

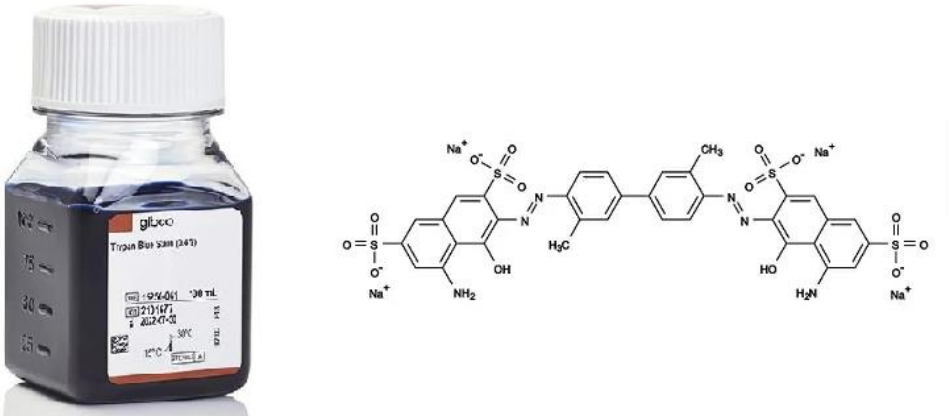

Figure 3.19. Gibco™ Trypan blue and its chemical structure.

In fact, this dye is able to selectively stain cells because it cannot penetrate the cell membrane of living cells, while it can do so for dead cells, since it is porous. Since the dye enters and colors the cytoplasm of cells in blue, a device capable of carrying out their count under the microscope is required: this instrument is called Burker's Chamber. It is a chamber consisting of a rectangular slide with an area of 7.5x3.5 cm and a thickness of 4 mm capable of determining the average number of live cells per unit volume of the resulting solution of Trypan blue and of the analyzed sample. In particular, in the central part the device has 2 smaller rooms of 3x3 mm, 0.1 mm deep, each divided into 9 squares of 1 mm delimited by three parallel lines. In turn, each square is divided into 16 squares of 0.2x0.2 mm. Figure 3.20 shows an example of a Burker chamber and the geometric structure of each room.

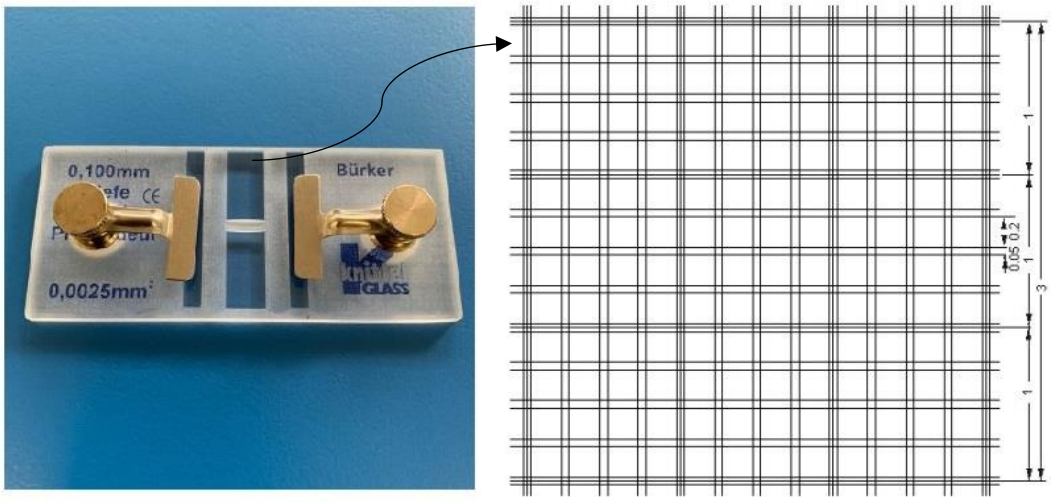

Figure 3.20. Burker's chamber and its room in detail.

Therefore, to perform the cell count of a 1 mL of solution, follow these steps:

- Dilution of the sample with fresh culture medium and gently pipetted to avoid sedimentation and cell clustering;
- Collection of 10 µl of this solution with a micropipette and placement of this in one of the rooms of the Burker chamber. The same amount (10 µl) of Trypan blue is added to the solution;
- Microscope observation with a 10x magnification of 10 µl of the solution consisting of the sample plus the stain and cell count of at least 5 squares;
- The total number of cells is statistically calculated with the following equation:

$$N_{cells} = N_{average} \cdot d_f \cdot V \cdot 10^4 \quad (3.1)$$

Where $N_{average}$ indicates the number of cells counted in relation to the number of quadrants considered (usually 5), d_f represents the dilution factor which takes into account the presence of the Trypan blue and V is the original volume of the solution (1 mL).

3.7.3 Seeding in PS microdevices

Before cell seeding, the devices must be sterilized by washing with ethanol and double rinsing with sterilized water using laboratory pipettes, and subsequent UV treatment for about 20 min. As mentioned in the previous paragraphs, since one of the final objectives of this thesis is to study the behavior and growth of cancer cell species in different conditions, it was decided to conduct these experiments with SK-N-DZ and SK-N-AS cells. Obviously, the cell seeding procedure in the PS devices had to follow all the protocols described in the previous paragraph, that is, those of splitting and counting, but the different areas involved had to be considered. It was decided to seed the cells in the 4 wells at the corners of the chip, while the central square chamber was left empty; in particular, 2 wells were occupied by one cell species, the remaining 2 by the other. The surface of each well was calculated with the formula of the area of a circle (πr^2), while a cell density equal to 500 cells/mm^2 was fixed. In turn, each well was filled with the correct number of cells diluted in 120 µL of medium, thus with a total volume for four wells of 600 µL. The number of cells for each well and the total one of the entire device were calculated as follows:

$$N_{cell}^{well} = S^{well} \cdot \rho \quad (3.2)$$

$$N_{cell}^{tot} = N_{cell}^{well} \cdot 4 \quad (3.3)$$

where with S^{well} the surface of the single well has been indicated, while ρ represents the cell density, fixed at 500 cells/mm^2. Table 3.7 summarizes all the quantities referred to the seeding

of a single PS chip, while Figure 3.21 shows two PS devices with the cellular seeding just described.

Table 3.7. Quantities for cell seeding in a single chip.

Quantities	Values
Surface of single well	78.5 mm^2
Cell density	500 cells/mm^2
Number of cells for each well	40.000 cells
Total number of cells in the chip	160.000 cells
Volume of medium in a well	120 µL
Total volume of medium in the chip	600 µL

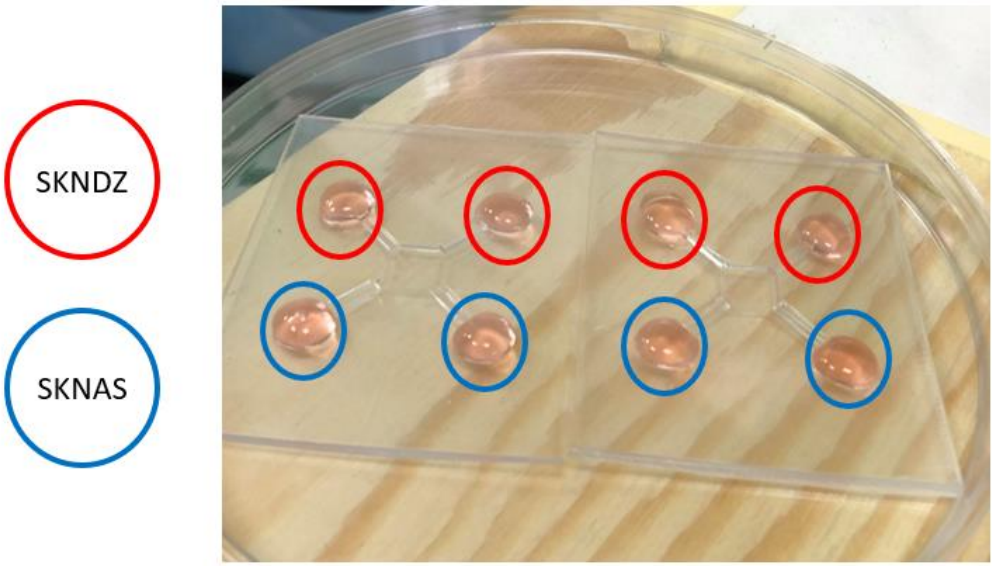

Figure 3.21. Cell seeding of SK-N-DZ and SK-N-AS cells in PS devices.

During the seeding phase, the cells were allowed to adhere to the surface of the device without the use of additional protein coating. In fact, fibronectin, a glycoprotein stored at -18°C, is usually used to promote cell adhesion to the extracellular matrix. The cells were then kept in culture for several days and the culture medium was changed every 24 hours as follows: the exhausted medium was vacuum aspirated and replaced with about 150 µL of new medium.

3.7.4 Cell viability test

Before carrying out the medium change after 24 hours, the viability of the cells was suitably verified under the microscope. This operation was routinely performed in the following days to have a visual inspection-based validation of the experiments carried out. To observe the state of the cells within the 4 wells, two types of fluorescent dyes, Hoechst 33258 (Figure 3.22) and Calcein-AM (Figure 3.23), were used exploiting a fluorescence microscope.

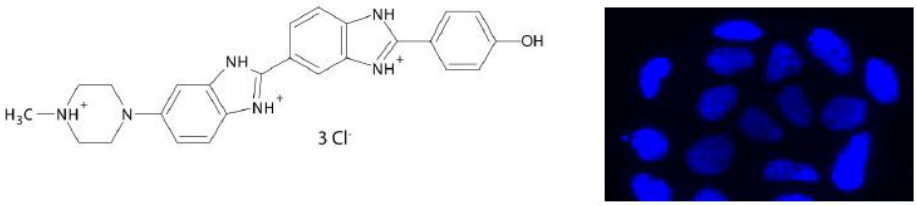

Figure 3.22. Hoechst 33258: its chemical structure and blue fluorescence; adapted from[54].

Hoechst 33258 stain is part of the family of dyes that highlight DNA under a fluorescence microscope. Therefore it is used to visualize nuclei, without distinguishing between dead or living cells. It is a blue fluorescent stain with an emission wavelength of 461 nm and an excitation wavelength of 361 nm[54].

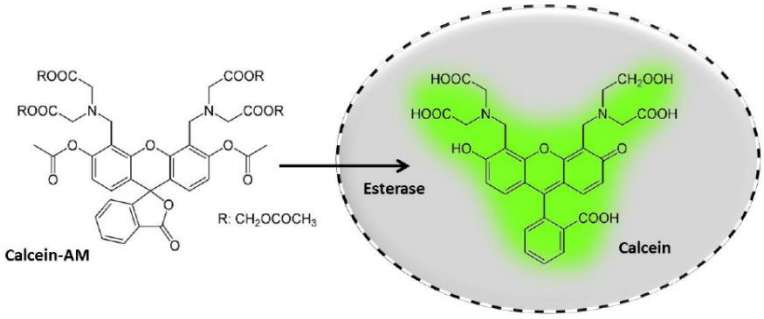

Figure 3.23. Chemical structure of Calcein-AM and its change to fluorescent Calcein; adapted from[55].

Calcein-AM is a fluorescent dye with an excitation of 495 nm and emission wavelengths of 515 nm[55]. Since it is a compound that can easily permeate the cell membrane, it does not fluorescence outside of them. Furthermore, only if it penetrates inside the cell and its hydrolysis takes place, then Calcein is produced, which is a strongly fluorescent hydrophilic compound. In this way, the obtained fluorescence signal is proportional to the number of live cells present in the cell suspension.

Both of the two dyes are non-toxic and soluble in water and organic solvents. In fact, the staining solution is prepared with the following composition: in a total volume of 1 mL, 1 µL is made up of Calcein-AM, 4 µL of Hoechst 33258 dye, the rest is the base medium DMEM without FBS. Once the solution is prepared, it is injected into the device in which the cells are

seeded, which is then placed inside the incubator for about half an hour to allow the solution to permeate inside the structure. immediately after exiting the incubator, the PS microfluidic platform was analyzed using a fluorescence microscope, the EVOS FLoid Cell Imaging Station (Figure 3.24) available in the BIAMET laboratory. The microscope is equipped with a fluorescent lamp that allows to excite the fluorescent dyes and to capture the light emitted through different filters (one for each stain, since they have different emission wavelengths).

Figure 3.24. EVOS FLoid Cell Imaging Station.

3.7.5 Clamping the microfluidic device

Once the biocompatibility assessments were carried out and the cell growth was analyzed over several days under the microscope, it was decided to complete the initial configuration of the chip by adding a clamping unit to the microfluidic platform. First, the PS chip was finished by hand with the use of a power tool, then a PET clamping unit and a PDMS membrane were made. The membrane acts as an intermediate layer between the microdevice and the top clamp. As already mentioned at the beginning of this paragraph, there is a long tradition in the field of microfluidics concerning the bonding between PS and PDMS. There are several examples in the literature that describe different techniques developed in recent years to seal thermoplastic microdevices with PDMS, given that there are still two materials with quite different surface characteristics. However, in this case it was preferred to simply proceed by using the same clamping unit to create a sandwich-shaped structure held together by screws and bolts. Consequently, the top and bottom layers of the rectangular-shaped PET clamping unit were perforated at the four corners to ensure this seal.

This configuration (Figure 3.25) was taken as a starting point in the literature and subsequently adapted to the PS chips considered in this thesis[56].

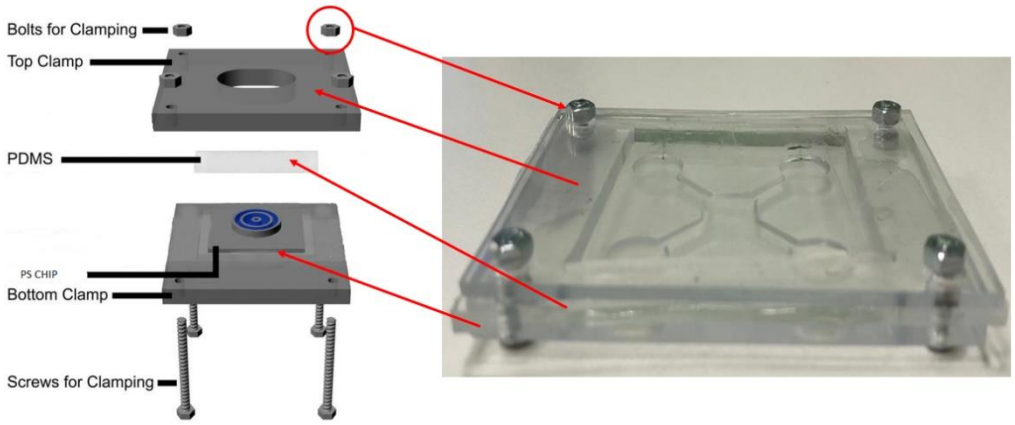

Figure 3.25. Clamping the microfluidic device: final configuration.

So, starting from the bottom up, the final configuration is as follows:

- Layer 1: bottom clamp in PET with height equal to 2 mm.
- Layer 2: device in PS with height equal to 2mm.
- Layer 3: layer in PDMS with height equal to 3 mm.
- Layer 4: top clamp in PET with height equal to 2 mm.

The PDMS layer has been inserted because, operating with two materials with poor oxygen permeability such as PS and PET, the elastomer guarantees cell survival inside the device, being very permeable compared to the other two compounds. This is because the experiments carried out so far have served to simply evaluate the viability of the cells and not to test them in hypoxic conditions. To make the membrane in PDMS the following protocol was followed:

- Preparation of the PDMS mixture mixing the silicone base and the curing agent in a ratio of 10:1;
- Degassing the solution prepared in a dryer using a vacuum pump;
- Pouring the mixture into a rectangular Petri dish in order to obtain a layer with a height equal to 3 mm;
- Curing in the oven at 65°C for 75 min;
- Removal of the cross-linked polymer from the mold;
- Cut of the membrane and its finishing in such a way as to adapt it to the PS chip. The holes for the screws are done using a biopsy punch with a diameter of 4 mm.

As for the material used for the clamping unit, PET was chosen for its excellent optical transparency. In fact, since an additional layer has been added anyway, this property of PET is very useful when the sample is inspected under a microscope.

3.7.5.1 Biological validation with clamp unit

The cell seeding procedure was the same that was followed for seeding without the presence of the clamping unit. The number of seeded cells as well as the division of the two-cell species in the 4 wells was also the same. The only difference is that in this case, during the sterilization

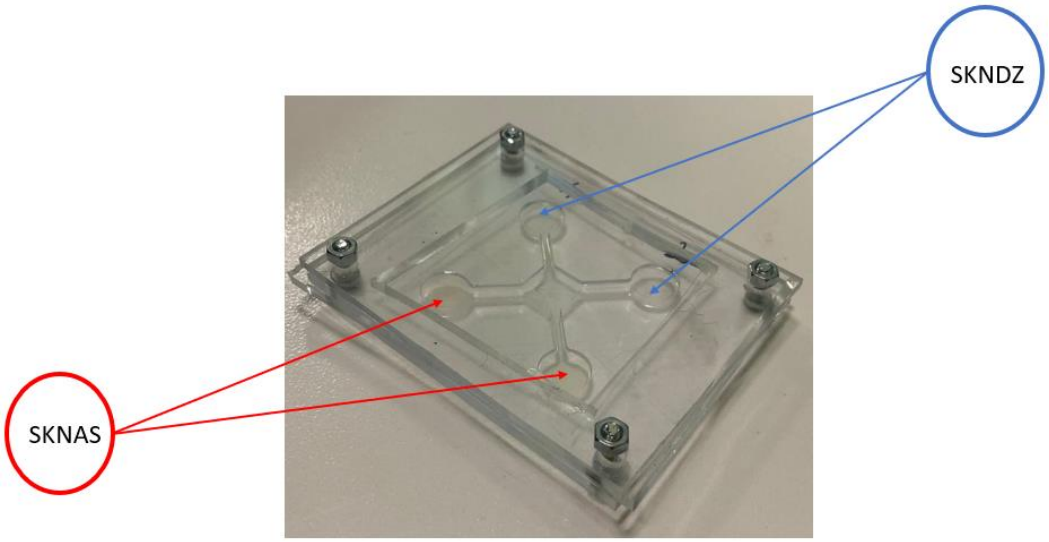

Figure 3.26. Example of cell seeding in the PS chip with clamping unit.

phase of the device, every part of the platform must be sterilized: clamping unit and screws under UV rays while the PDMS layer is autoclaved at 121°C. The cells were seeded inside each well and then closed with the cover of the device. Once closed, the device is placed directly in the incubator without the use of additional supports. Figure 3.26 shows the experimental setup of the final chip configuration.

3.7.6 3D cellular cultures of neuroblastoma cells

Much of the biological experiments carried out in the laboratory involved cell seeding in a 2D environment. However, although this type of seeding has numerous advantages ranging from highly controlled culture condition to the easy observation under the microscope, it does not ensure a realistic representation of what happens in human tissues. Three-dimensional cell cultures are certainly more expensive and are more complicated to be realized in microfluidic devices than two dimensional ones, anyway these certainly ensure a better simulation of the in vivo microenvironment of the human body. Actually, in this case, cells are placed in a 3D space, and can therefore migrate in the three directions X, Y and Z; furthermore, the cell-cell and cell-environment contacts are no longer limited by the surface of the microfluidic platform[57]. Figure 3.27 illustrates in a simplified way the main differences that exist between a cell cultivation in 2D and one in 3D.

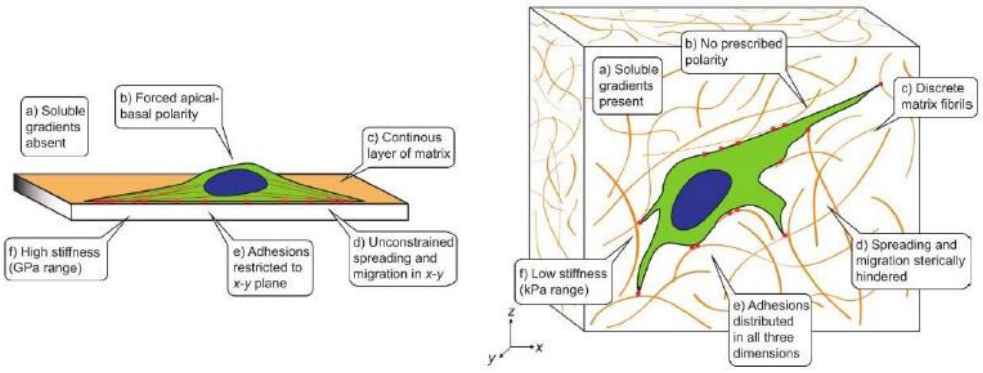

Figure 3.27. Simplified illustration of 2D and 3D cell culture; adapted from[57].

Accordingly, it was decided to use the PS chip as a base for three-dimensional structures with encapsulated neuroblastoma cells, in order to replicate in 3D the same experiments described above in 2D. The materials that are extensively discussed in literature and quite suitable to realize these 3D structures are hydrogels, in particular Gelatin Methacrylate (GelMA) hydrogels. Recent studies carried out in the BIAMET laboratory[58] led to the construction of three-dimensional structures with the use of these materials, optimized in shape and size such as to allow an accurate study of cell migration in the presence of exosomes. In this regard, the structure of the PS chip made it possible to realize in each well of the microfluidic platform four hydrogel cylinders of the same size. This guarantees a certain repeatability of the experiments.

3.7.6.1 GelMA hydrogel preparation and experimental tests

Always referring to previous studies[58], the GelMA used for these experiments was produced with a degree of functionalization (DoF) of 70±10%. By functionalization we mean the methacrylation of the amino groups of the macromolecules of porcine gelatin to obtain a photoreactive product known as methacrylate gelatin. Since the degree of functionalization is a measurable value through proton nuclear magnetic resonance (H NMR), the 10% uncertainty is justified by possible errors in the measurements. Once GelMA was obtained and characterized, the methacrylate gelatin based hydrogel was prepared at 8% (w/v) of GelMA in a 1x PBS solution (pH ≃ 7.4). Irgacure 2959 was used as photoinitiator, in the concentration of 0.5% (w/v) in order to initiate the cross-linking of the functional groups of GelMA through a mechanism of radical polymerization. A 365 nm UV LED lamp was used to perform the curing, with an exposure time of 60 seconds to limit cellular damages. Using these materials concentrations, the internal structure of the hydrogel is such as to guarantee stability to the hydrogel itself, and at the same time to ensure high cell viability and migration. However, GelMA hydrogels are characterized by low viscosity and therefore by printability using micro-extrusion-based 3D printing techniques. It was therefore decided to add 0.7% Agarose (w/v), a gelatinous substance that allows to increase the viscosity of the hydrogel, improving its

printability, keeping constant the GelMA concentration. Agarose addition also allowed to increase the biocompatibility of the formulated hydrogel, obtaining higher cell viability.
Regarding the work done in this thesis, 3D disks were directly realized into the four wells of the PS chip. The hydrogel solution was prepared with an amount of medium and cells in such a way as to have a cell concentration of 5 million cells per mL of hydrogel and with a volumetric hydrogel/medium ratio below 1:25. Once the hydrogel solution was produced, cells were added with the medium before subjecting it to UV exposure. Then 100 microliters of the new mixture were taken with a micropipette and the wells of the chip were filled to subject them to the UV lamp realizing three-dimensional structures with encapsulated cells. Figure 3.28 shows an example of cell seeding in the PS chip with the addition of the hydrogel structures.

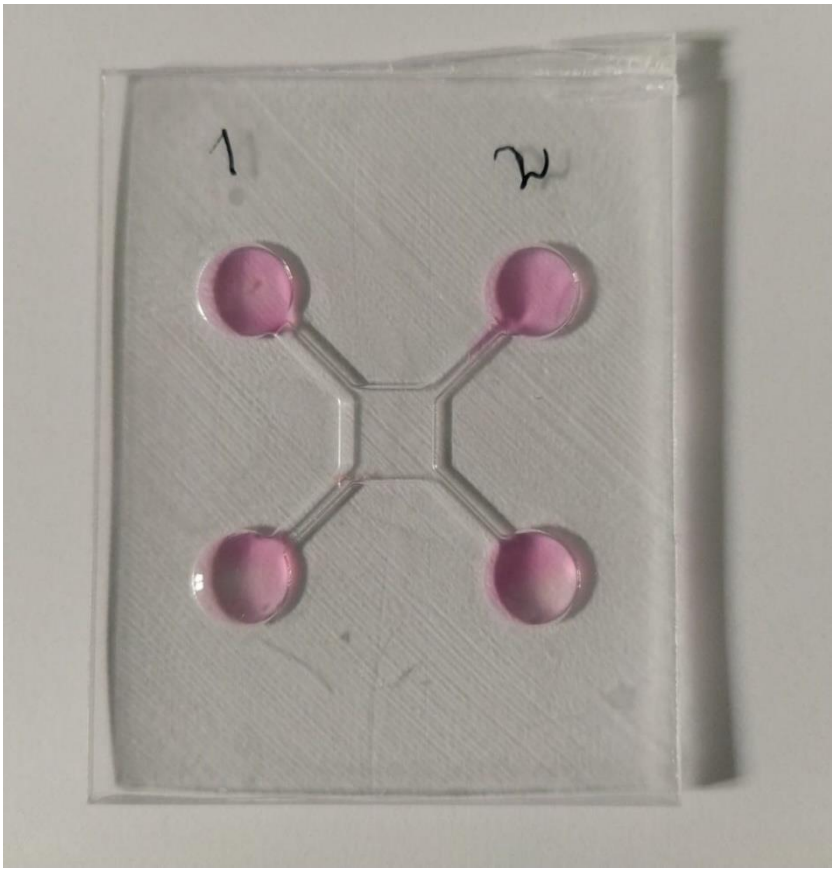

Figure 3.28. An example of 3D cell cultures in the PS device with the SK-N-AS species in wells 1 and 2.

Chapter 4

Results and discussions

This chapter will analyze and discuss the results obtained from the procedures described in chapter 3. First, the realization of the inserts and the result of the metrological characterization on the profilometer will be described, establishing which of the three angles is closest to the CAD model. Next, the results of the chip and insert characterization after injection molding will be evaluated. The final section will focus on the results obtained from the biological validation experiments carried out at the BIAMET laboratory.

4.1 Realization of the inserts

The Digital ABS inserts have been produced using the ObJet350 - Connex3 printer exploiting PolyJet technology and by combining the two cartridges RGD515 and RGD535, as already extensively discussed in paragraph 3.3. Before printing, the machine deposited a support layer (SUPPORT - FULLCURE 705) which, at the end of the production operations of the inserts, lasting about 3 hours, was separated from the latter with the use of a special scraper. Following separation from the support, the 3 inserts did not require any further treatment, except for a rinsing with water to eliminate any support residues. Figure 4.1 shows the three inserts produced simultaneously by the printer with three different angles with respect to the axis of the 3D printing machine.

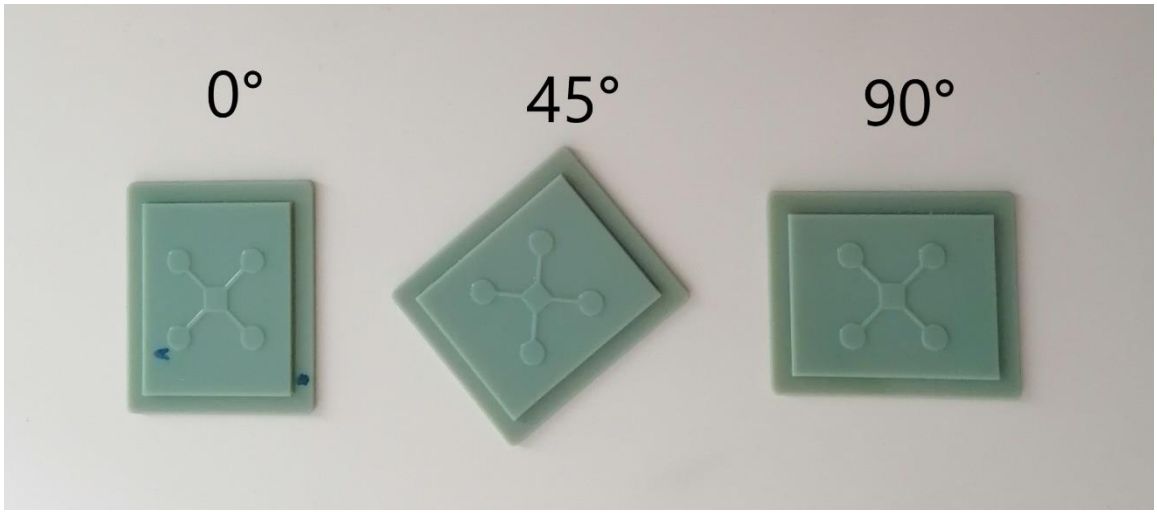

Figure 4.1. Inserts made with PolyJet technology: 0° (left), 45° (center) and 90° (right) insert.

Macroscopic observation does not allow to appreciate the difference between inserts according to their respective angles. However, since the deposition of the layers takes place along the Z direction, orthogonal to the printer plane, once the piece is finished, it is possible to observe lines representing the passes made by the nozzles head. These lines are oriented according to the angle set at the beginning with the virtual positioning of the pieces in the work plane.

4.2 Metrological characterization of the inserts

Profilometric analyses were carried out to first establish which of the three inserts shown in Figure 4.1 best conformed to the measurements of the CAD model. Subsequently, the profilometer was used to evaluate the wear level of the chosen insert after injection molding.
First of all, given the presence of symmetry in the plane of the insert, it was necessary to distinguish for the purposes of the measurements an upper and a lower part of the insert, as well as a left and a right side. Consequently, for convenience, the top left well in all three inserts was denoted by the letter A. In order to reduce the time required to scan the piece, only some key features were analyzed with the profilometer. In particular, as shown in Figure 4.2, the areas analyzed on the profilometer concerned the wells at the top left (A) and the one at the bottom right, the central chamber and the four channels that connect the central chamber to the respective wells. In addition, the roughness of the piece was calculated by examining an area of the central chamber.

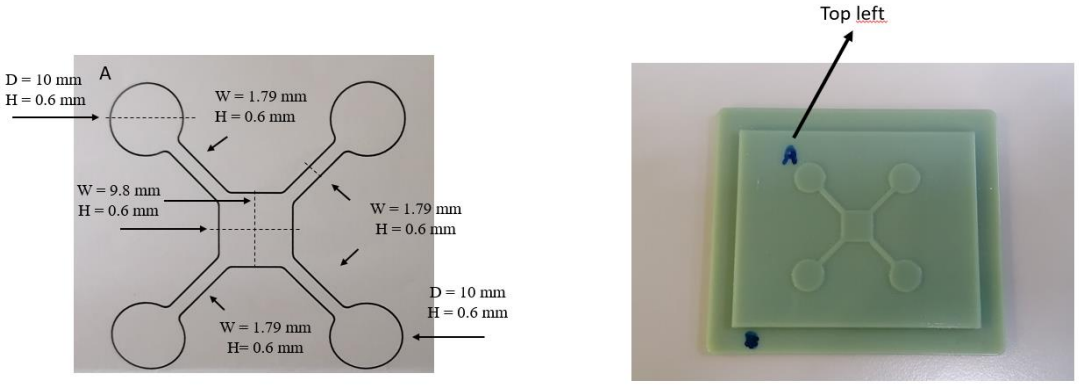

Figure 4.2. 2D model of the insert and an example of its printing in Digital ABS.

The analysis of the inserts carried out on the profilometer specifically concerned the following features:

- Diameter and height of the top left and bottom right wells.
- Width and height of the four channels.
- Width, height and length of the central chamber.
- Surface roughness

The profilometer analyses showed good repeatability of the printed objects; all three inserts in fact have quite similar profiles. The instrument detects the upper and lower surfaces very well but fails to follow the connecting walls between them. The *"restore"* function of the instrument can be implemented to reconstruct the side profile on the basis of that small number of points found. To evaluate the difference between a measurement with and without the *"restore"* application, the well at the top left of the 45° insert was used as an example (Figures 4.3 and 4.4). The Sensofar program allows exporting in graphic form both the display of the topography of the analyzed area and the corresponding profile with the measurements made.

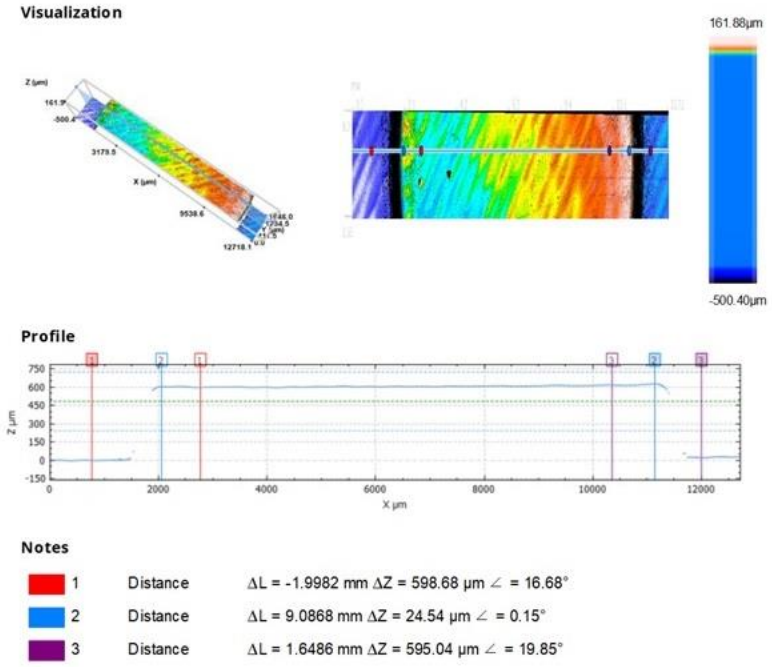

Figure 4.3. Top left well profile without restore application.

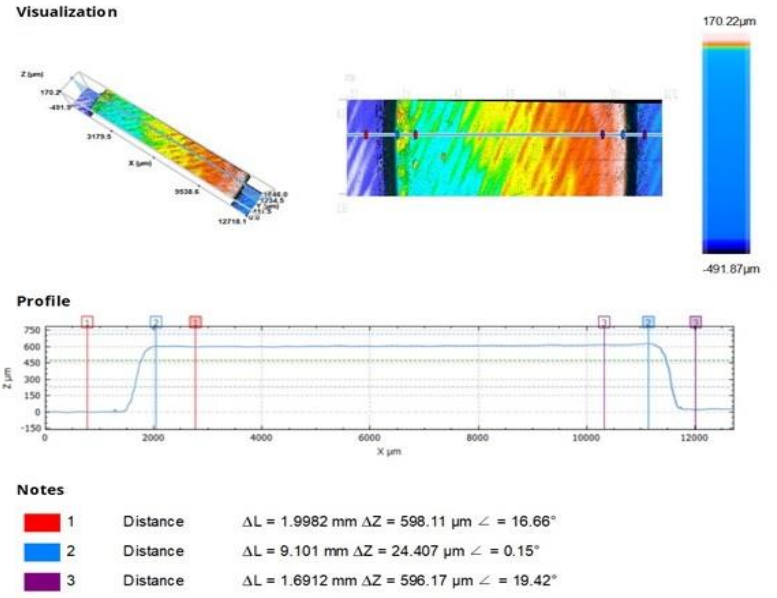

Figure 4.4. Top left well profile with restore application.

From the profiles it can be seen that the reconstruction carried out by the program for the insert does not significantly change the result of the measurements; therefore, for greater clarity in the graphs, it was decided to continue with the acquisition using the "*restore*" application. Although the side profiles are not exactly vertical, the heights are comparable to the nominal ones (600 µm). The shape of the side profiles could depend on partial dripping before crosslinking during the deposition phase of the photopolymer by the print head. As already mentioned in chapter 3, the program allows the profiles obtained to be exported in pairs of X and Z coordinates with the possibility of converting them into graphs in Excel. Figure 4.5 shows the diagram produced by Excel relating to the profile of the well mentioned above which has been compared with the nominal profile.

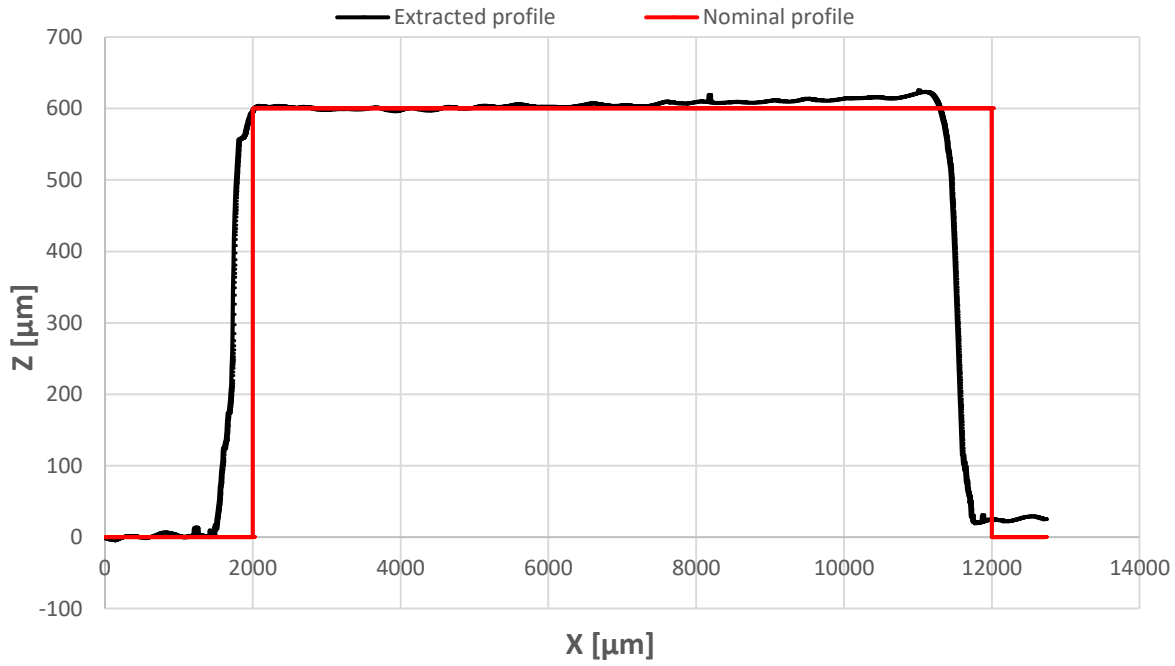

Figure 4.5. Extracted top left well profile (black), compared to the nominal one (red).

In addition to the fact that the side profiles are not completely vertical, the figure also shows the presence of rounded edges and this is always linked to the dripping at the border during printing. The same diameter appears a little shorter than the nominal one.

In Figure 4.6 the three profiles of the wells at the bottom right of the three inserts at 0°, 45° and 90° are compared with the nominal one.

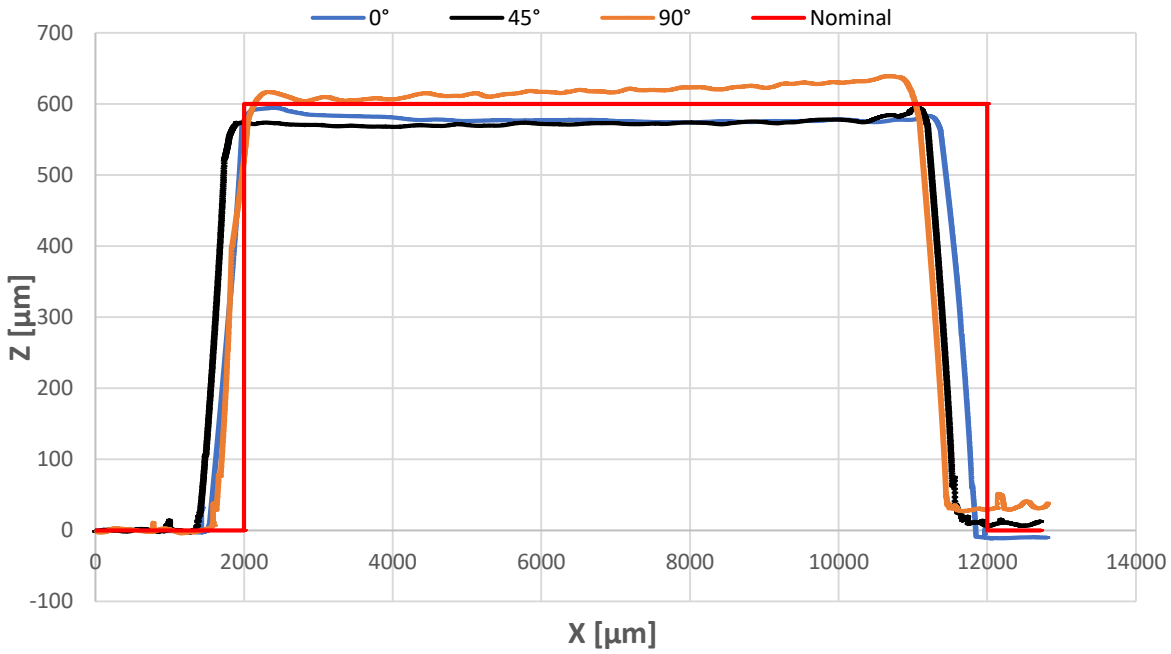

Figure 4.6. Bottom right well profiles: comparison between the three inserts and nominal profile.

In all three profiles it is possible to observe the presence of rounded edges, as well as the imperfect replication of the diameter of the well. However, it should be noted that rounded features do not negatively affect the performance of microfluidic platforms. Furthermore, the height of the well is a much more important measure than its diameter for the purpose of cell seeding. Figures 4.7 and 4.8 show two other examples for the comparison between features: the width of the central chamber and of the channel at the top left between the well and the central chamber.

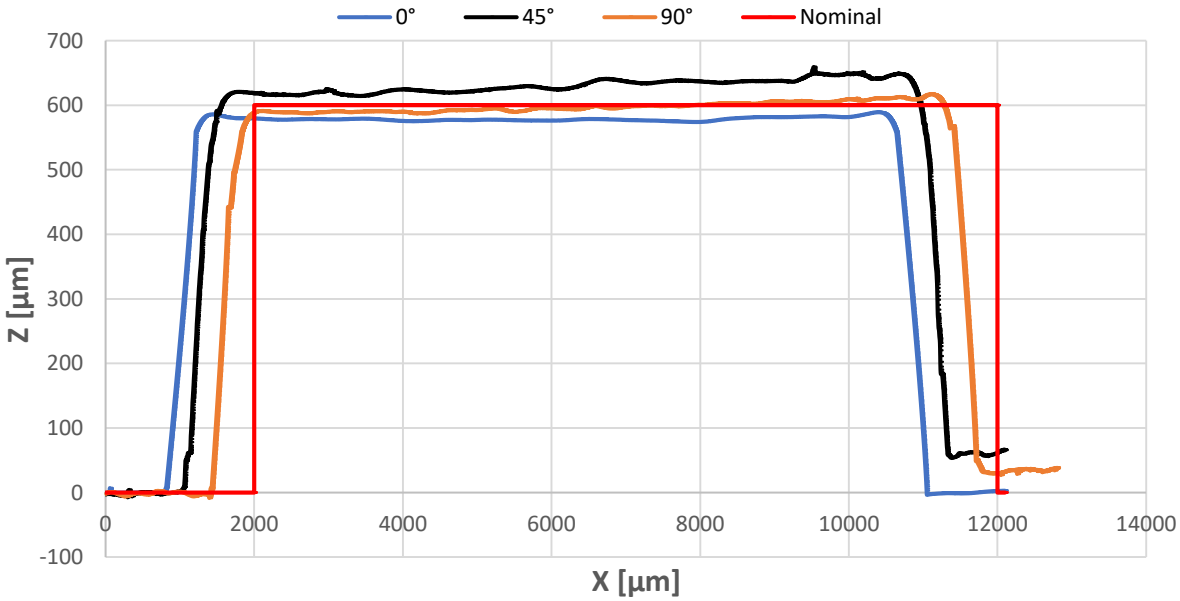

Figure 4.7. Central chamber profiles: comparison between the three inserts and nominal profile.

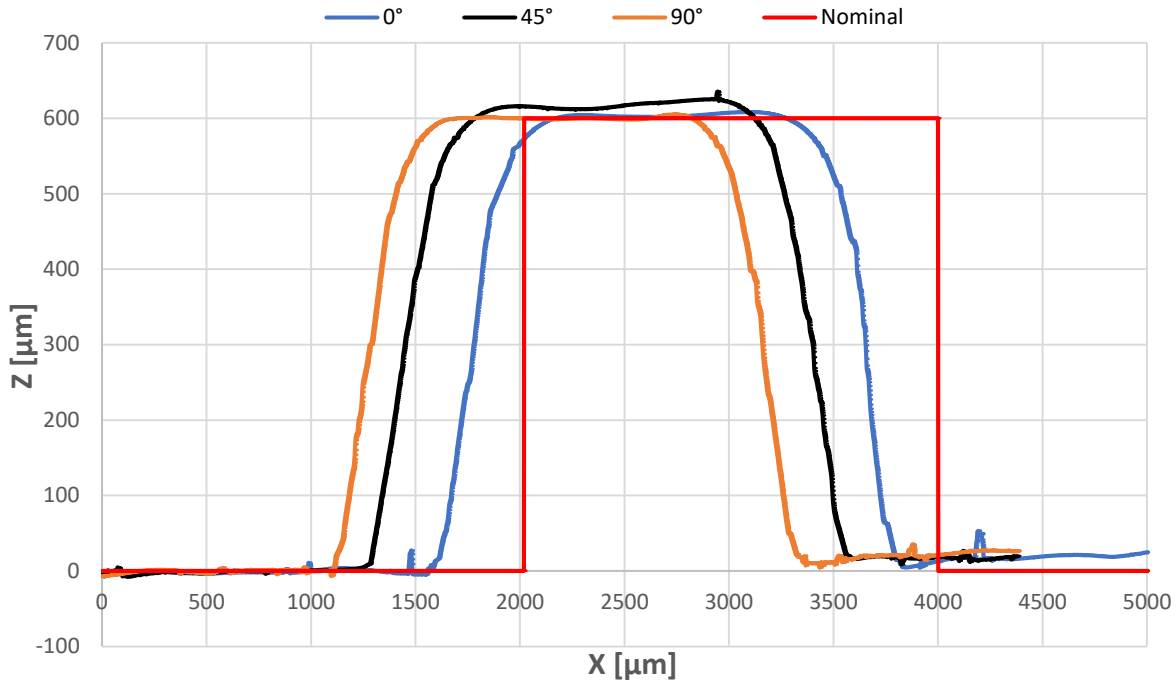

Figure 4.8. Top left channel profiles: comparison between the three inserts and nominal profile.

Although there is no perfect replication of the nominal profile in the two graphs, the trends in the three inserts are quite similar. This makes it clear that, if on one hand there are some problems related to the crosslinking process, on the other hand the machine is still able to guarantee a good degree of replication of the CAD model. In addition, from the graphs, it is appreciated how the height represents the feature most similar to that of the CAD model; this can be linked to the fact that the printer works by reconstructing the figure layer by layer (along the Z direction). Tables 4.1 and 4.2 summarize and compare the most important measurements made on the profilometer on the three inserts.

Table 4.1. Widths of the features in the three inserts.

Degrees	Units	Diameter (top left)	Diameter (bottom right)	Central chamber width	Central chamber length	Channel width (top left)	Channel width (bottom left)	Channel width (top right)	Channel width (bottom right)
0°	mm	9,287	9,382	9,382	9,251	1,393	1,371	1,345	1,383
45°	mm	9,222	9,369	9,298	9,311	1,403	1,423	1,397	1,423
90°	mm	9,311	9,266	9,339	9,341	1,376	1,347	1,397	1,397

Table 4.2. Heights of the channels in the three inserts.

Degrees	Units	Channel heights (top left)		Channel heights (bottom left)		Channel heights (top right)		Channel heights (bottom right)	
0°	µm	602,9	595,4	603,9	591,7	601,5	588,4	594,9	595,3
45°	µm	618,4	605,9	627,2	600,4	606,7	597	615,9	606,7
90°	µm	601,4	588	604,6	595,1	593,9	581,5	590,8	587,4

From the tables, it is clear that most of the measures of the features are quite comparable, even in their differing from the nominal ones. As for the channels, having designed them with a width of about 2 mm and a height of 0.6 mm, thus having an aspect ratio of 3.33, has allowed the machine to replicate these measures quite well. Since for purposes related to the fluid dynamics of the microfluidic platform it is very important to have the widest channels possible, it was decided to use the 45° insert for the injection molding machine. In fact, the widths of the channels between the central chamber and the wells are those closest to the nominal ones. This can be explained by the fact that the 45° insert is arranged in the work surface of the 3D printer inclined at this angle with respect to the head with the nozzles. When the head constructs the layers, the channels are oriented at 0° and 90° concerning it and this allows greater precision in their realization.

4.2.1 Insert at 45°: characterization post-molding

The 45° insert was analyzed on a profilometer following the molding cycle of 500 PS pieces in order to assess the degree of wear. In figure 4.9 it is possible to see the two inserts at 45° compared: on the left the insert before injection molding, on the right after molding.

Figure 4.9. 45° insert before and after injection molding.

Although the outermost part shows some signs of wear and has partially yielded in the lower right corner during the extraction phase of the piece from the plate, this is irrelevant for the purposes of making the device. Visually, the insert appears to have retained a regular geometry, unaffected by the repeated molding cycles. One negative aspect is that, having been subjected to high temperatures, the insert features are now more polished, thus making the profilometer detection more difficult. The features examined in the post-molding insert are the same as before, and graphs were built in Excel to compare the profiles of the 45° insert before and after

injection molding. The following graphs show some profiles chosen for the comparison between the starting insert (black) and the same after molding (amaranth).

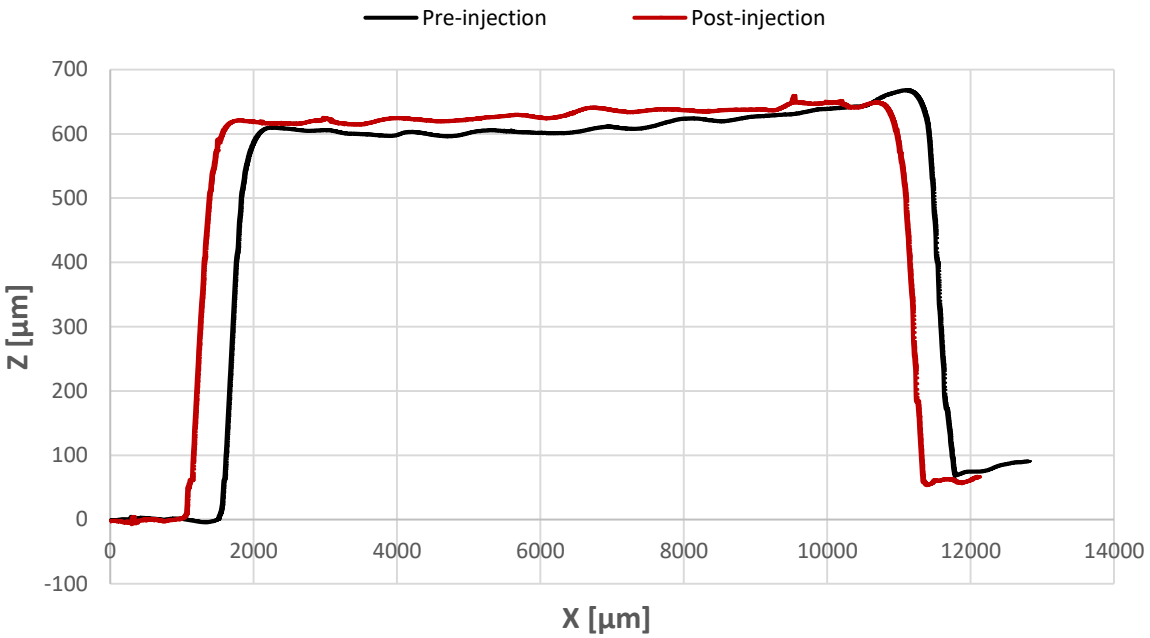

Figure 4.10. Top left well: pre-injection (black) and post-injection (amaranth) profiles.

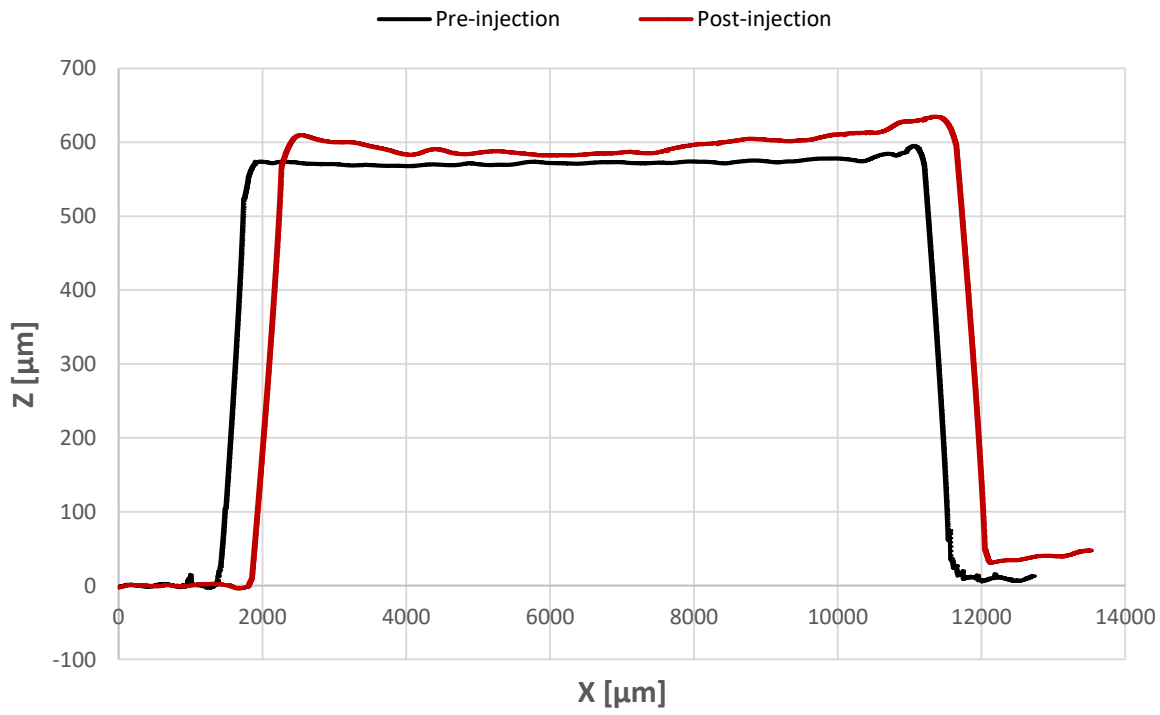

Figure 4.11. Bottom right well: pre-injection (black) and post-injection (amaranth) profiles.

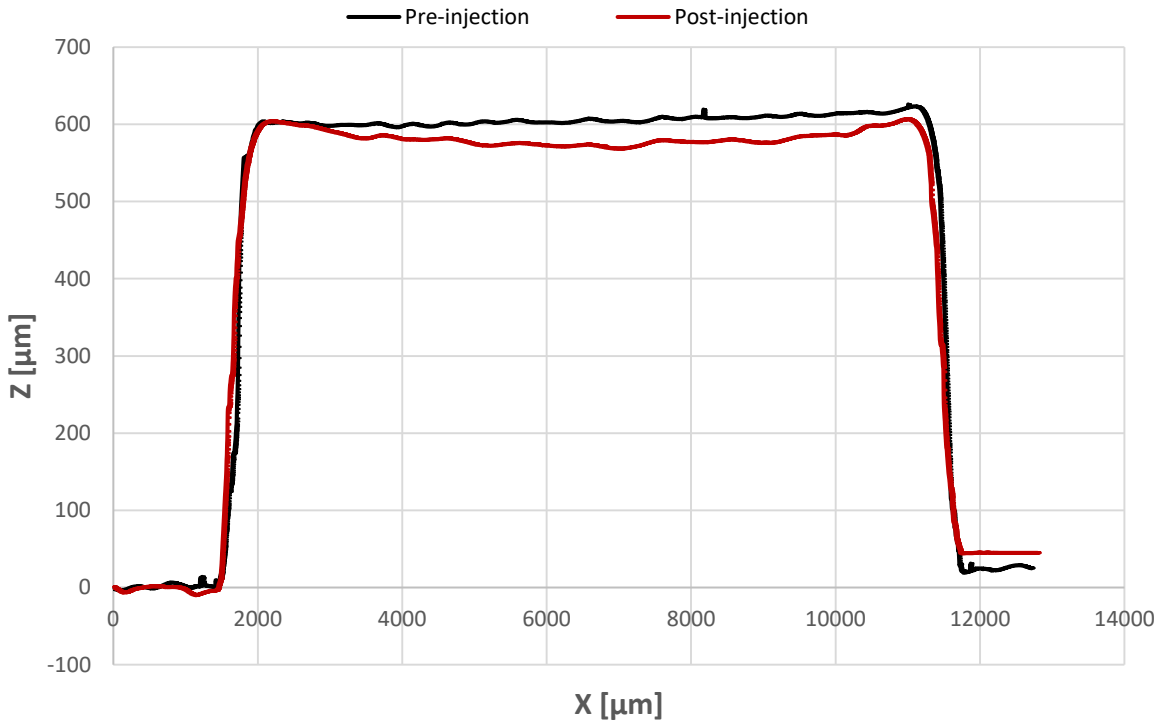

Figure 4.12. Central chamber: pre-injection (black) and post-injection (amaranth) profiles.

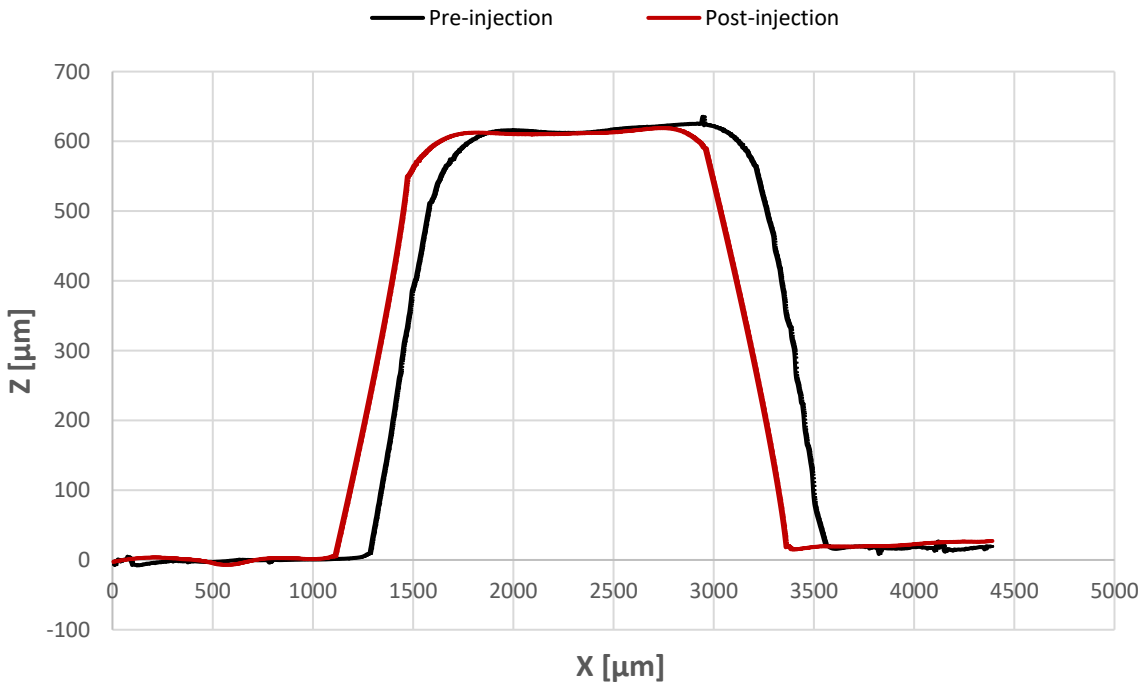

Figure 4.13. Top left channel: pre-injection (black) and post-injection (amaranth) profiles.

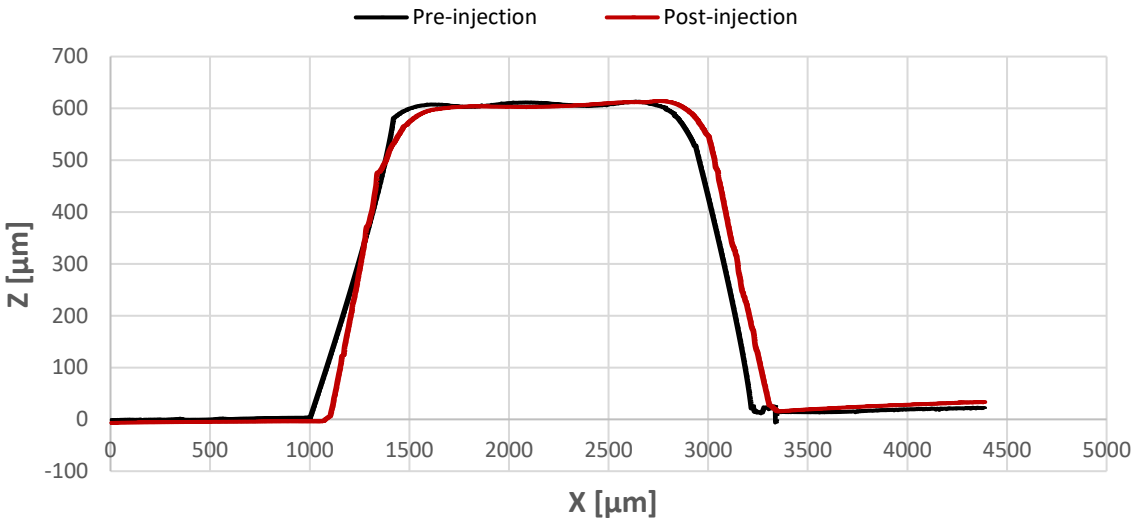

Figure 4.14. Top right channel: pre-injection (black) and post-injection (amaranth) profiles.

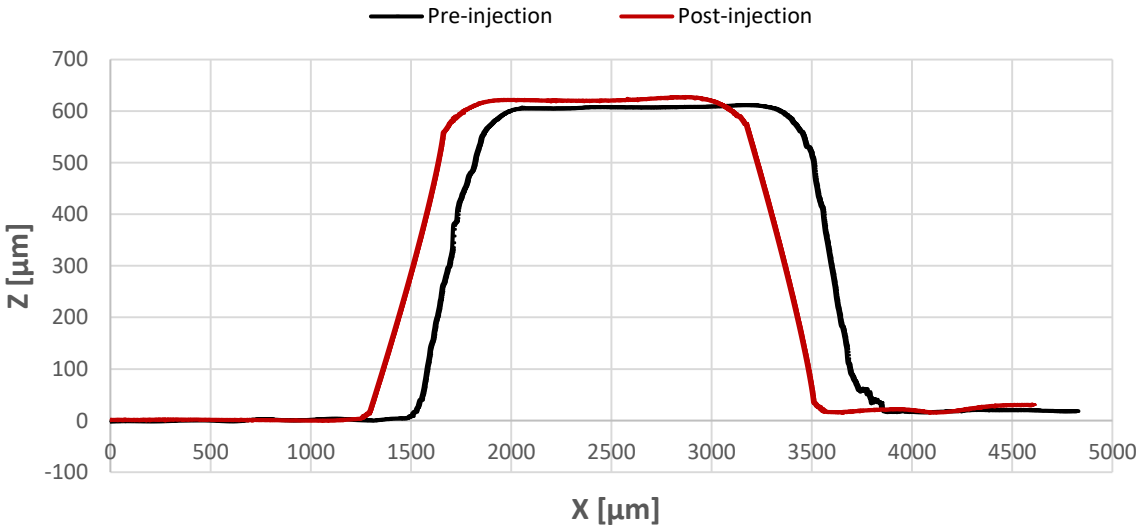

Figure 4.15. Bottom left channel: pre-injection (black) and post-injection (amaranth) profiles.

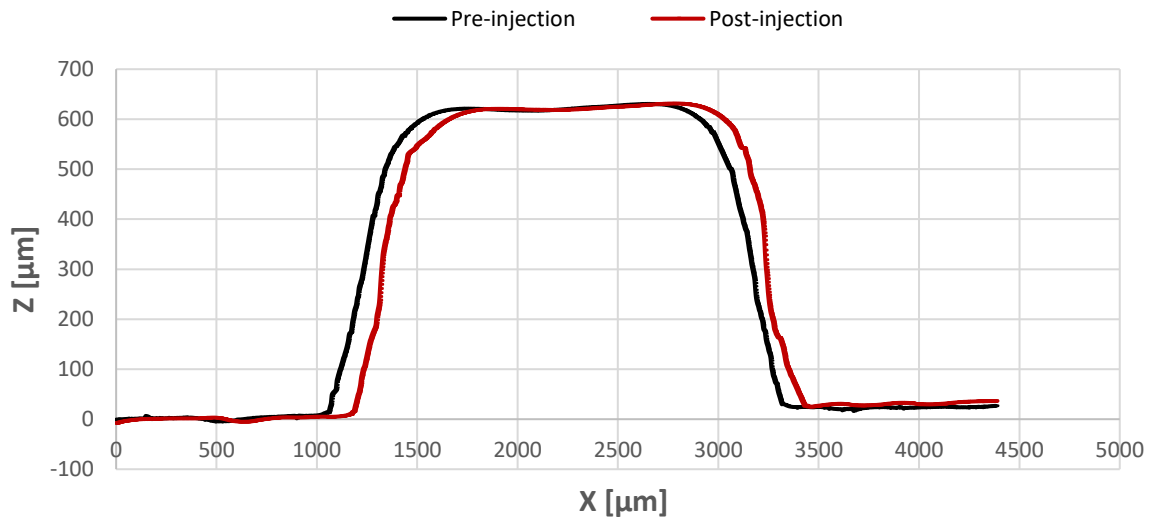

Figure 4.16. Bottom right channel: pre-injection (black) and post-injection (amaranth) profiles.

As can be seen from the graphs, the profiles are quite similar to each other, indicating that the insert did not wear significantly during injection molding. To have a better evaluation of the state of wear of the features of the channels, these were measured in three different points along the channel; then an average was calculated and compared with the pre-molding insert value and with the nominal one. Figure 4.17 shows the photo of the insert taken with the profilometer, highlighting the different points along the channels where the measurements were taken, while Table 4.3 compares these values.

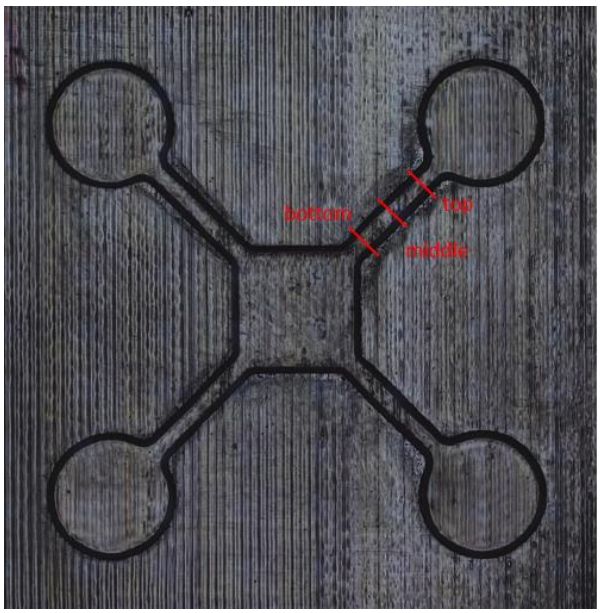

Figure 4.17. Image of the insert using the profilometer.

Table 4.3. Profile comparison of channel heights and widths for the 45° insert.

Feature	Insert pre-molding		Insert post-molding (average value)		Nominal value
Channel width (top left)	1,403 mm		1,378 mm		1,79 mm
Channel width (bottom left)	1,423 mm		1,338 mm		1,79 mm
Channel width (top right)	1,397 mm		1,345 mm		1,79 mm
Channel width (bottom right)	1,423 mm		1,409 mm		1,79 mm
Channel heights (top left)	618,4 µm	605,9 µm	608,4 µm	603,5 µm	600 µm
Channel heights (bottom left)	627,2 µm	600,4 µm	610,6 µm	599 µm	600 µm
Channel heights (top right)	606,7 µm	597 µm	601,6 µm	586 µm	600 µm
Channel heights (bottom right)	615,9 µm	606,7 µm	610 µm	601,7 µm	600 µm

From the data in the table, it can be deduced how all the features of the four channels have undergone variations compared to the before-molding measurements. However, there are no significant variations in shape and height either with the pre-molded insert, or with nominal values.

4.3 Production and metrological characterization of the PS device

The molding of the 500 polystyrene chips through injection molding took place by means of the Battenfeld HM 110/525H/210S of Rovigo, widely discussed in Chapter 3. Figure 4.18 shows on the left the aluminum plate with the 45° insert used in the mold inside, while on the right an example of a printed PS chip.

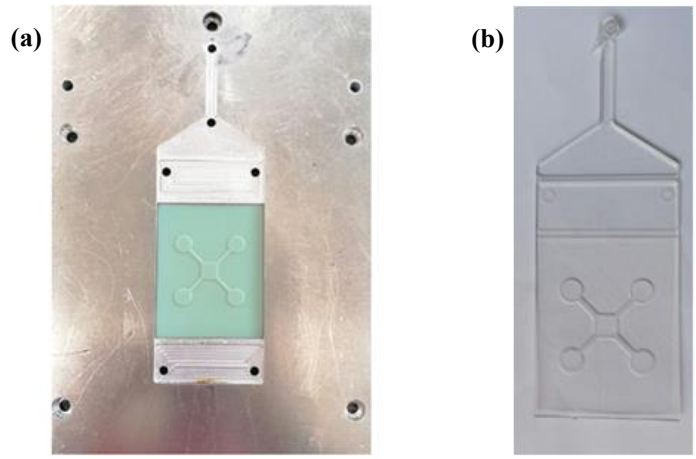

Figure 4.18. (a) Insert holder plate and (b) an example of PS chip.

The injection molding process ended as scheduled with the molding of 500 pieces without any particular problems being encountered. The microfluidic platform was transparent in appearance, with a slight curvature due to internal tensions during the solidification phase due to the high temperatures of the mold. Furthermore, from the figure it is possible to appreciate the 45° lines in the chip due to the use of the corresponding insert. The very fact that these lines are present could suggest that there has been a good degree of replication between the insert and the chip itself.

Regarding its characterization on the profilometer (Figure 4.19), it is important to underline that, unlike the inserts, the features in the chips are hollowed inwards with respect to the surface of the platform. Therefore, all the measurements will have negative values for the Z coordinate.

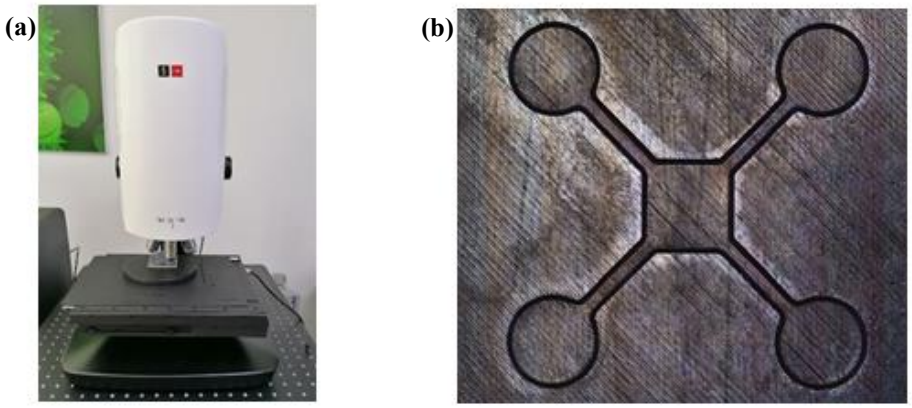

Figure 4.19. (a) Device positioned under the profilometer and (b) a brightfield images of the features device.

The profiles of the various devices examined with the Sensofar program were extracted and reconstructed on Excel obtaining the following graphs that compare the devices at different molding cycles.

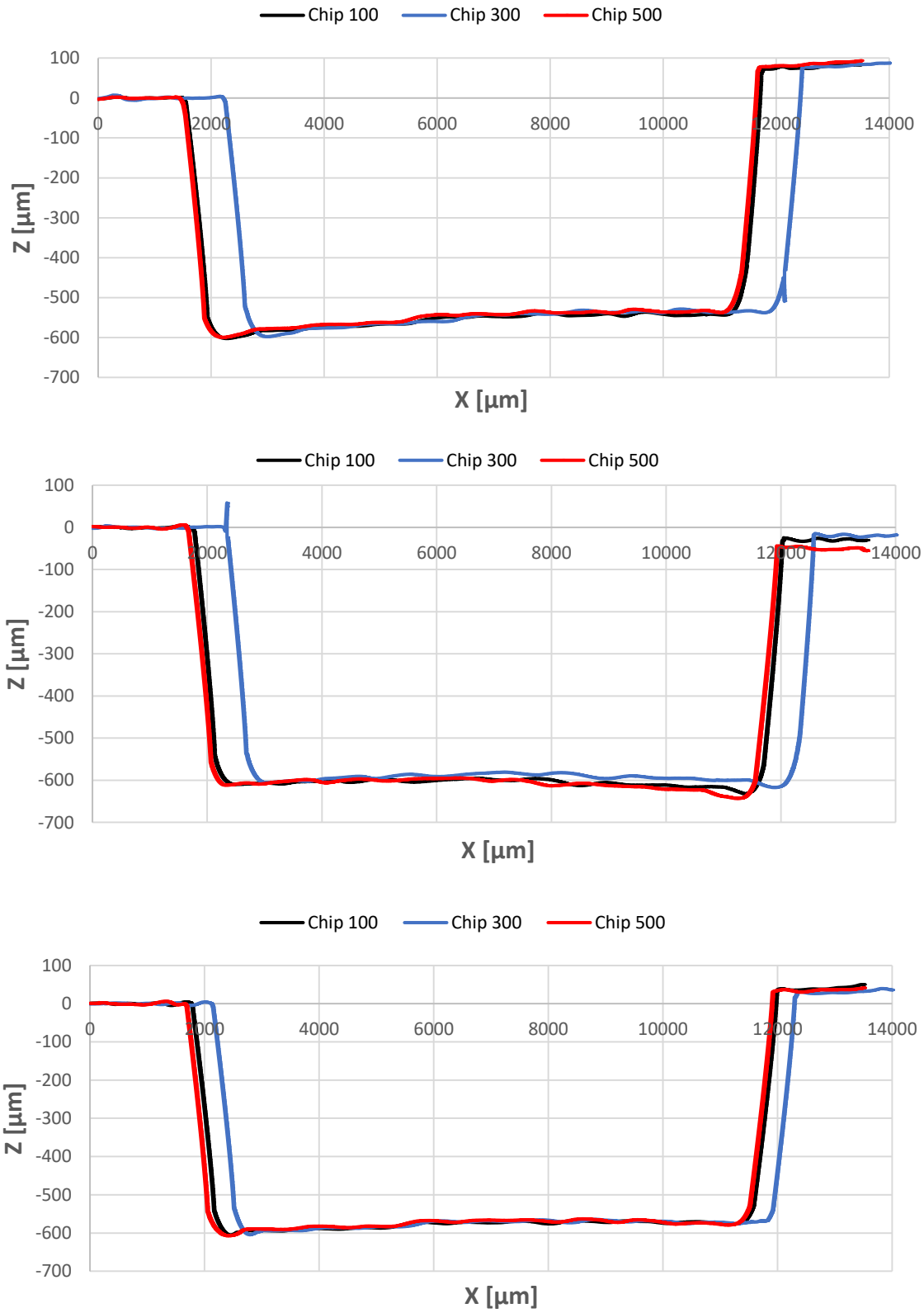

Figure 4.20. Comparison between Chips 100, 300 and 500: bottom right well, central chamber and top left well.

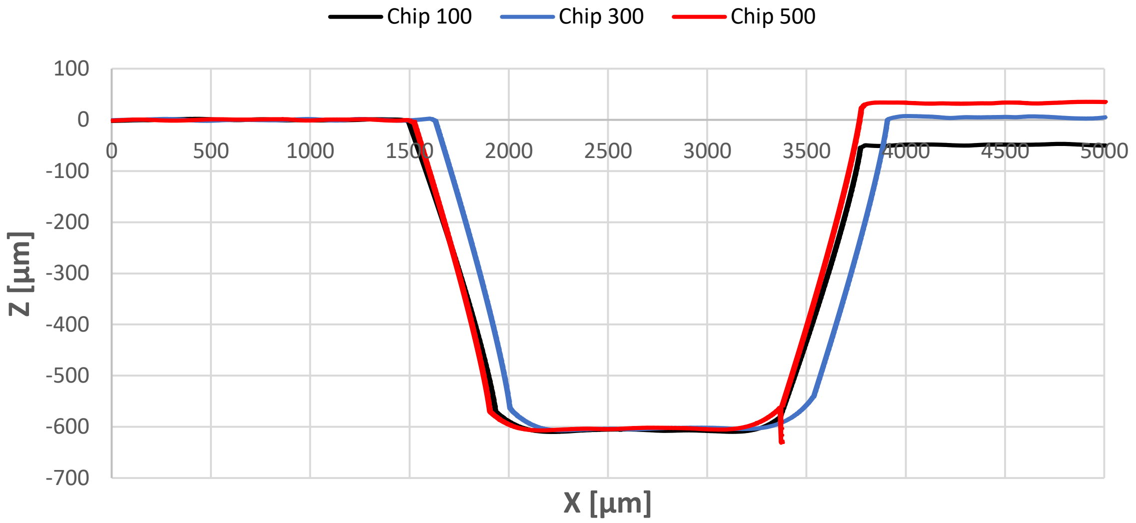
Chip 100
Chip 300
Chip 500
100
0
-100
-200
-300
-400
-500
-600
-700
0
500
1000
1500
2000
2500
3000
3500
4000
4500
5000
Z [µm]
X [µm]

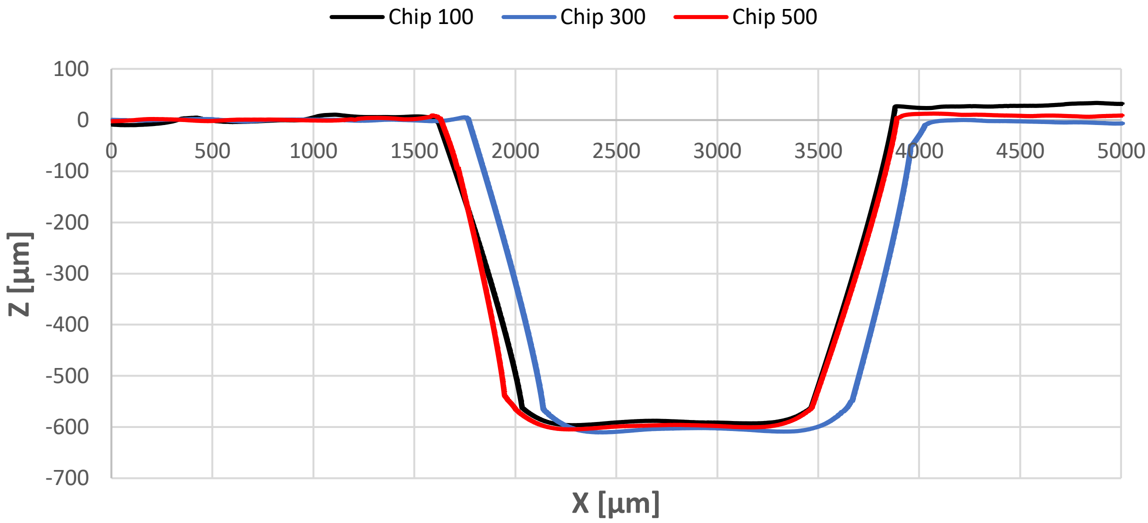
Chip 100
Chip 300
Chip 500
100
0
-100
-200
-300
-400
-500
-600
-700
0
500
1000
1500
2000
2500
3000
3500
4000
4500
5000
Z [µm]
X [µm]

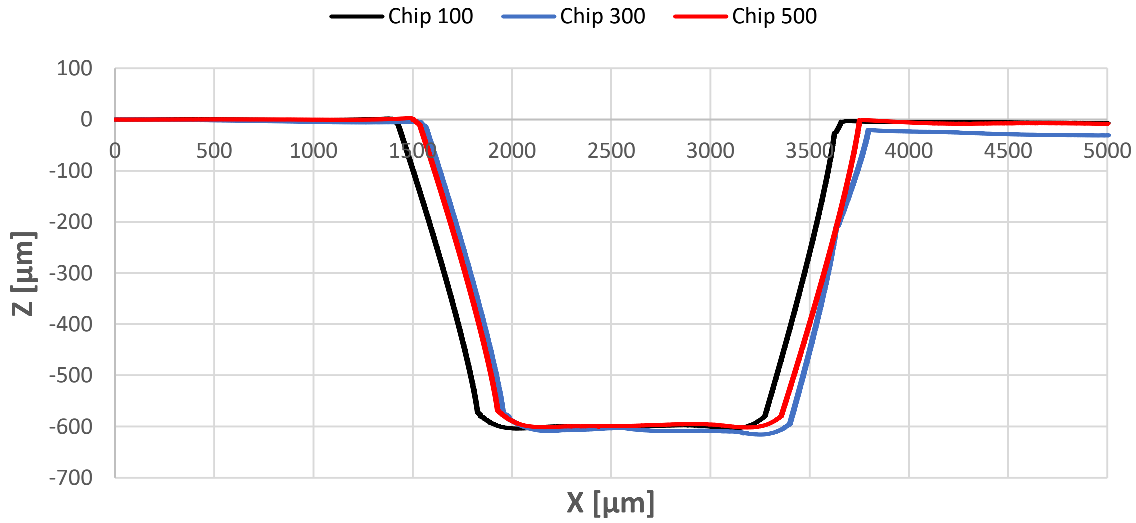
Chip 100
Chip 300
Chip 500
100
0
-100
-200
-300
-400
-500
-600
-700
0
500
1000
1500
2000
2500
3000
3500
4000
4500
5000
Z [µm]
X [µm]

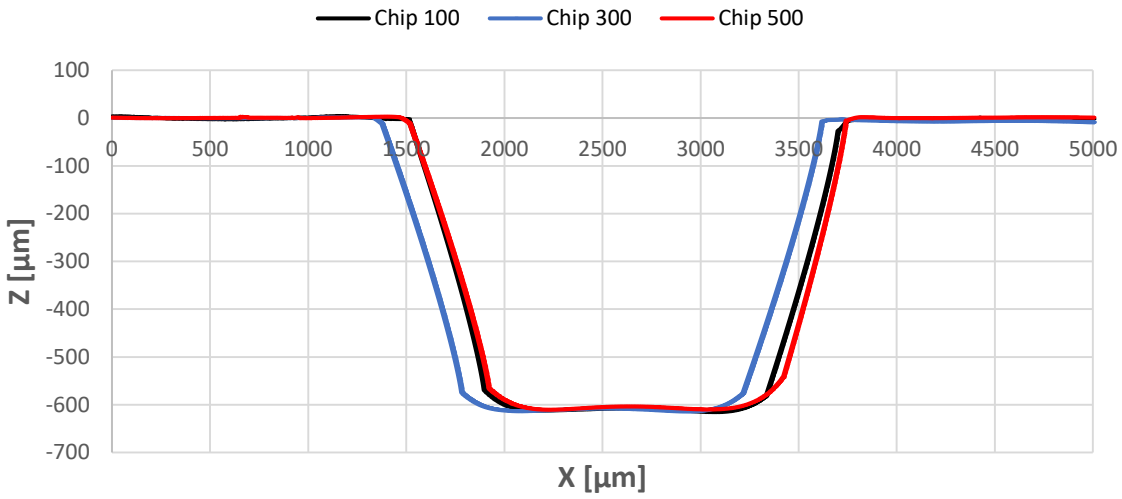

Figure 4.21. Comparison between Chips 100, 300 and 500: top left, top right, bottom left and bottom right channels.

Starting from considering that the features of the three chips are very similar to each other, it is possible to notice the slightly inclined profiles from the graphs relating to the two wells. The diameters are the features that are most affected by the slight curvature of the chip leaving the injection molding machine; anyway, excluding the latter, the other features have a height similar to the nominal one. Table 4.4 compares some features of the 100, 300 and 500 chips with the 45° insert and the nominal ones (those of the channels are taken as averages).

Table 4.4. Comparison between 100, 300 and 500 chip profiles with 45° insert and nominal ones.

Features	Units	Chip 100		Chip 300		Chip 500		Insert 45°		Nominal
Diameter (top left)	mm	9,106		9,123		9,167		9,222		10
Diameter (bottom right)	mm	9,105		9,172		9,12		9,369		10
Central chamber width	mm	9,12		9,368		9,306		9,298		10
Channel width (top left)	mm	1,356		1,401		1,354		1,403		1,79
Channel width (bottom left)	mm	1,342		1,379		1,335		1,423		1,79
Channel width (top right)	mm	1,366		1,391		1,352		1,397		1,79
Channel width (bottom right)	mm	1,366		1,432		1,393		1,423		1,79
Channel heights (top left)	µm	607	571,3	604,3	607,9	607,7	626,4	618,4	605,9	600
Channel heights (top right)	µm	598,9	595,7	598,9	589,9	598,8	589,2	606,7	597	600
Channel heights (bottom left)	µm	612,5	608,8	605,8	605	608,9	589	627,2	600,4	600
Channel heights (bottom right)	µm	603,4	600,9	608,4	607,1	606,8	608,6	615,9	606,7	600

From Table 4.4 it is possible to obtain the following information:

- The features of the devices are obviously affected by how the insert is able to replicate those of the CAD model during its realization with the 3D printer;
- The heights in the various profiles are the features that come closest to the nominal ones;
- The measurements of the chips are affected by some factors that impact on their determination on the profilometer, among them the slight curvature on the surface that is different on each platform and consequently the restore application that reconstructs the profiles. This can be understood well from the channel graphs where the program has assumed a rather linear trend for the lateral profiles.

4.4 Biological validation: results

The biological tests carried out at the BIAMET laboratory of the University of Padua allowed to complete the validation of the entire production process of the PS microfluidic platforms developed in this thesis. These were carried out following the protocols described in Chapter 3 and led to encouraging results both for the biocompatibility of the material and for cells growth and viability.

4.4.1 Biocompatibility and viability tests

First of all, the PS chip (Figure 4.22) that came out of the injection molding machine was suitably finished to be subjected to various biological tests in the laboratory, eliminating the parts added only for the molding process.

Figure 4.22. An example of a PS chip used in the BIAMET laboratory.

The microfluidic platform was then subjected to various sterilization treatments and made suitable for cell seeding. To carry out the biocompatibility tests, it was decided to seed the cells on the four external wells of the microdevice. To avoid possible loss of medium along the channels towards the central chamber, PDMS prints of the same size as the channels were made in order to have a better seal and allow the cells to correctly adhere to the surface of the well.

Seeding took place in such a way as to have two cell species for every two wells and a cell density of 500 cells/mm^2 per well.

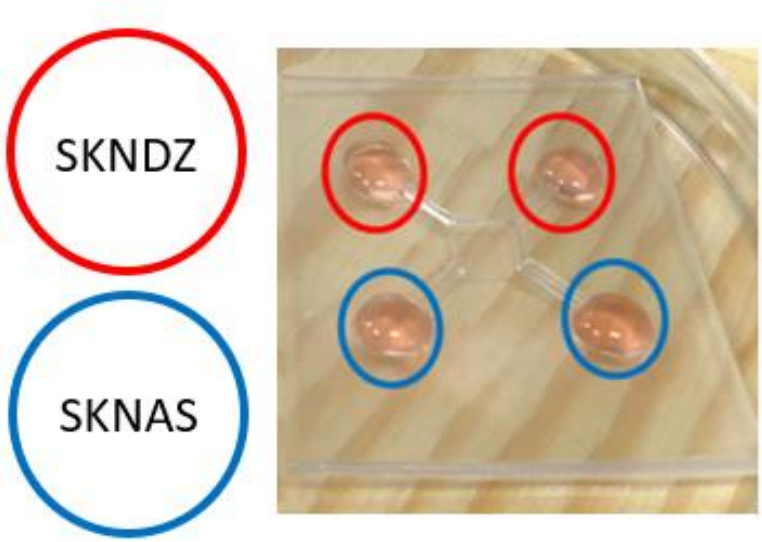

Figure 4.23. Ps device after the seeding of two neuroblastoma cell lines.

The fluorescence tests to verify the viability of the platform were carried out using the Hoechst 33258 and Calcein AM markers after 24 hours after seeding. Figure 4.24 and Figure 4.25 report representative results for both cellular species obtained under the microscope with the two markers used in the experiment for the microfluidic device. SK-N-DZ cells, much more delicate as cell species than AS, need longer replication times and tend to require the use of 20x magnification in some experiments to have better focus.

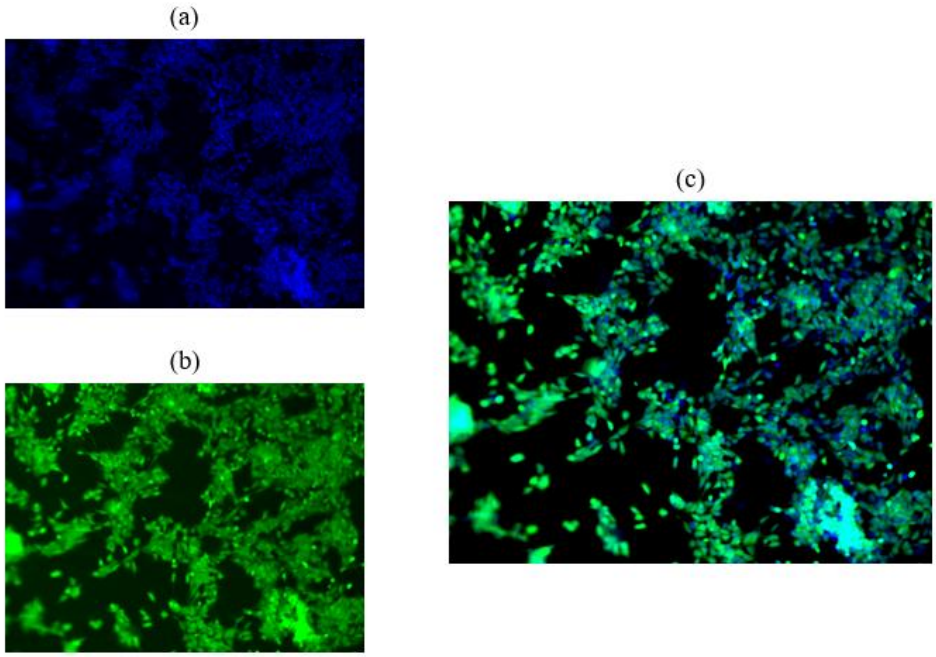

Figure 4.24. Cells staining of SK-N-AS after 24 hours from seeding: a) Cell nuclei marked in blue with HOECHST; (b) Cell cytoplasm marked in green with Calcein; (c) Overlay; 10x magnification.

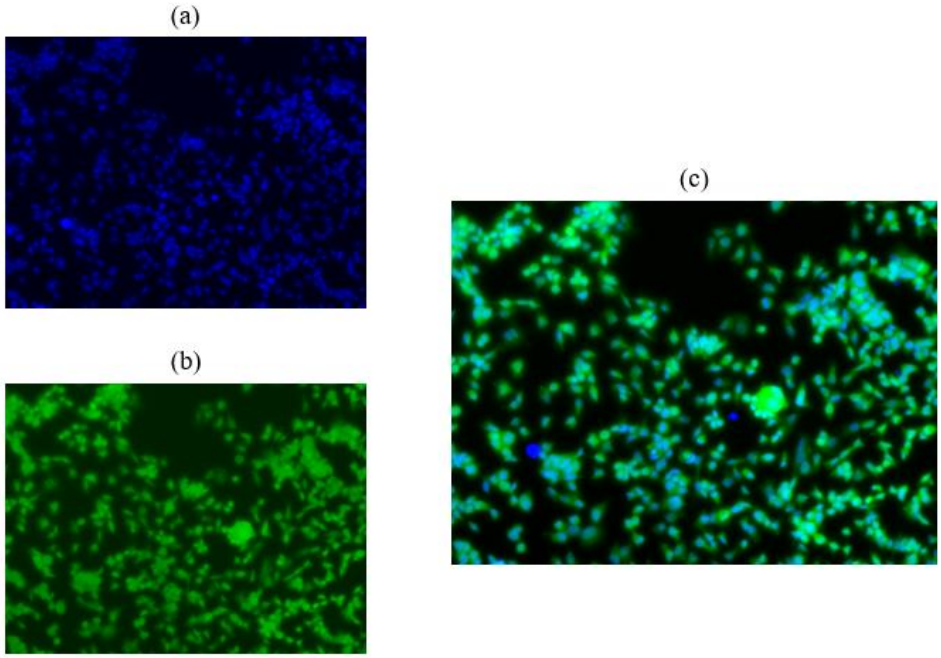

Figure 4.25. Cells staining of SK-N-DZ after 24 hours from seeding: a) Cell nuclei marked in blue with HOECHST; (b) Cell cytoplasm marked in green with Calcein; (c) Overlay; 20x magnification.

After 24 hours from seeding the test showed good cell viability for both cell species. As regards the microfluidic platform, it showed neither sealing problems nor autofluorescence under the microscope. The cell visualization procedure was repeated for several wells and at different areas of the microdevice to assess cell viability. The results observed inside one well after 24 hours were reconstructed from individual images collected under the microscope with a 4x magnification and are reported in Figure 4.26.

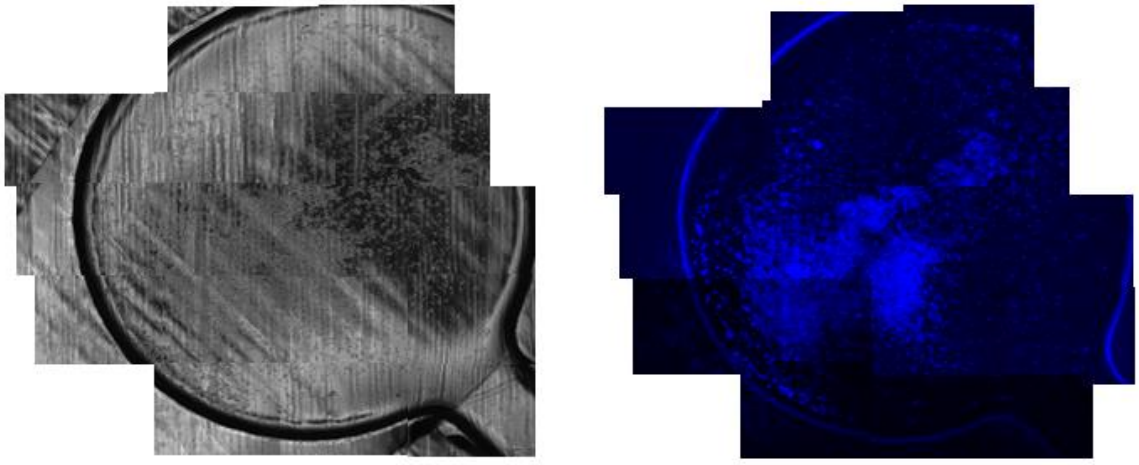

Figure 4.26. Brightfield view (on the left) and Cell nuclei marked in blue (on the right) of a seeding well.

Subsequently, the chips were placed back inside the incubator and then analyzed on the microscope with the same procedure 5 days after seeding, highlighting an excellent state of growth and cell viability (Figure 4.27 and Figure 4.28).

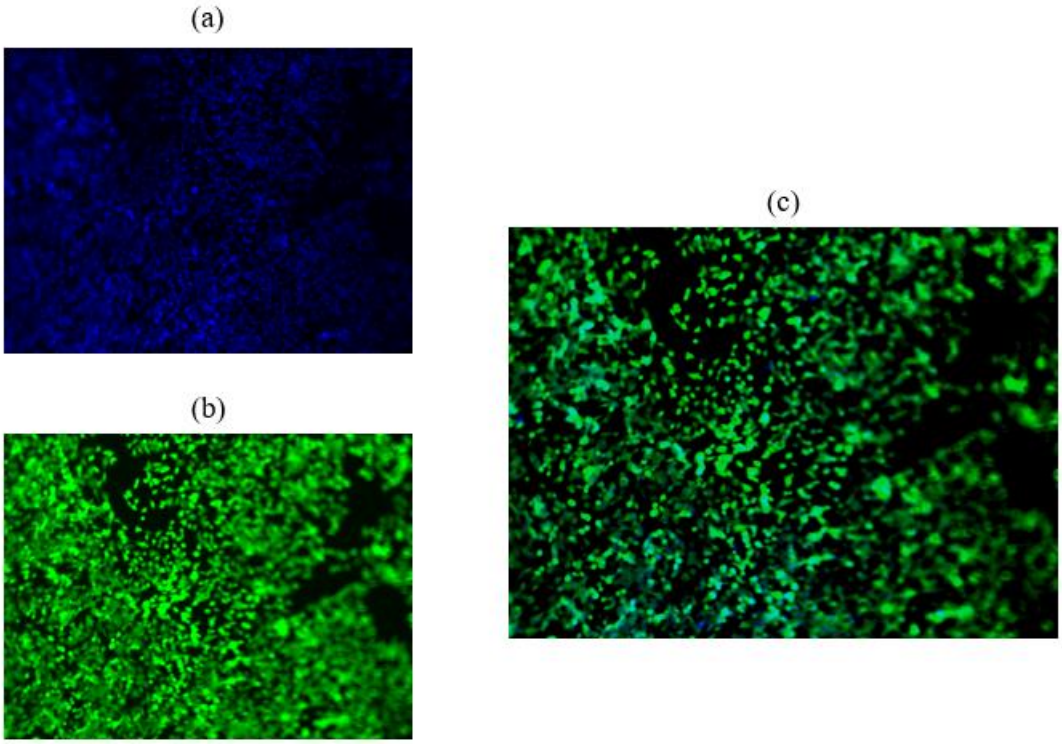

Figure 4.27. Cells staining of SK-N-AS after 5 days from seeding: a) Cell nuclei marked in blue with HOECHST; (b) Cell cytoplasm marked in green with Calcein; (c) Overlay; 10X magnification.

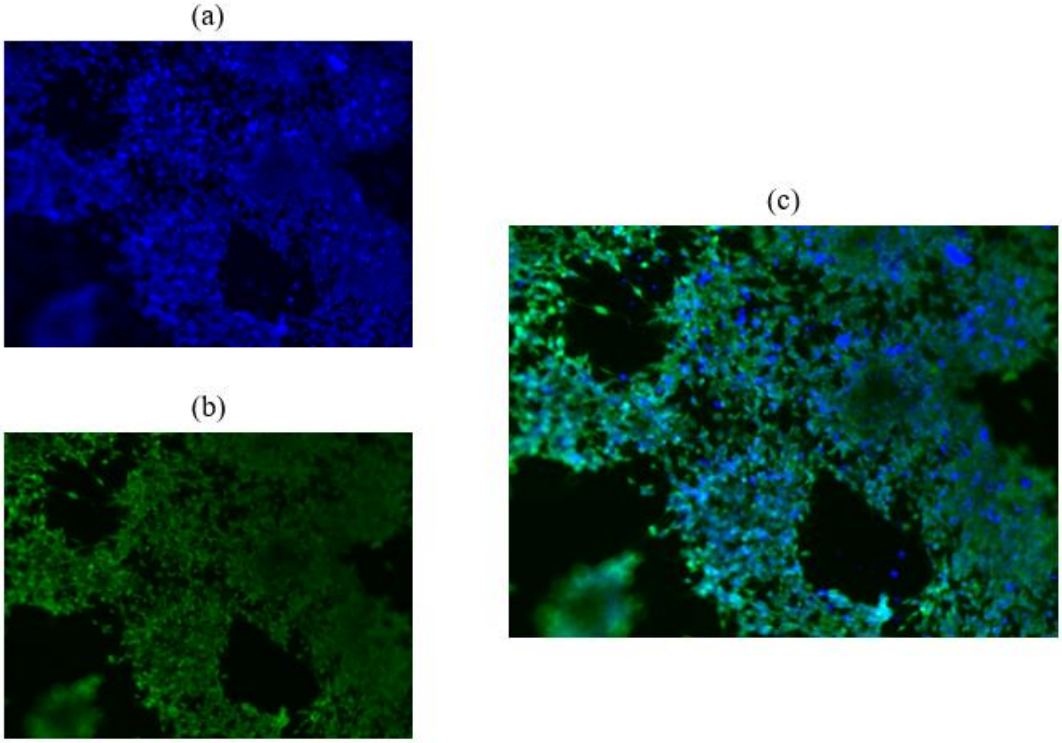

Figure 4.28. Cells staining of SK-N-DZ after 5 days from seeding: a) Cell nuclei marked in blue with HOECHST; (b) Cell cytoplasm marked in green with Calcein; (c) Overlay; 10X magnification.

4.4.2 Biocompatibility and viability tests with clamping unit

The final configuration with the clamping unit allowed to avoid the use of the Petri dish when incubating the microfluidic platform. Furthermore, when tightening by means of screws and bolts was added, the hydraulic seal was improved and the use of PDMS molds in the channels was not necessary. The seeding and incubation procedure, as well as the microscopic analysis, were identical to those for the platform without cover. The following figures show the results of the viability tests using Hoechst 33258 and Calcein AM as cell markers 1 and 5 days after cell seeding. The images were taken at 10x and 20x magnifications.

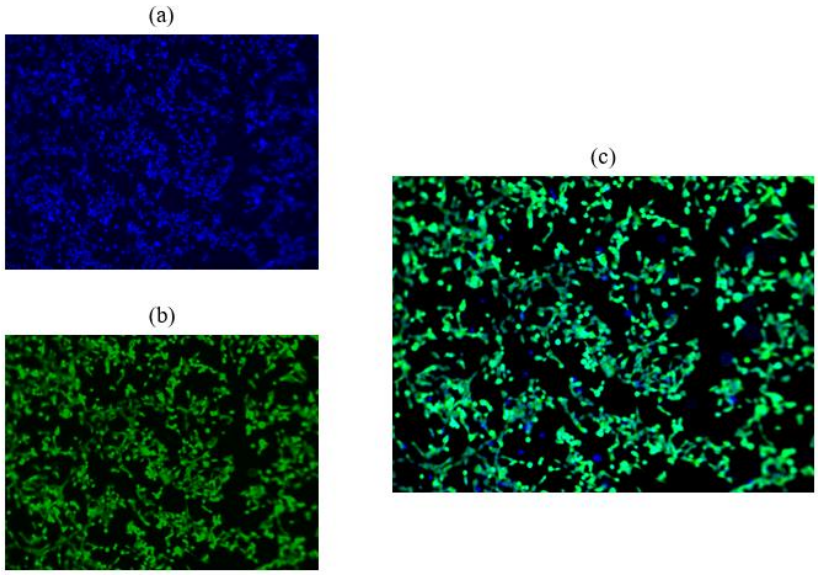

Figure 4.29. Cells staining of SK-N-AS after 1 day from seeding with clamping unit: a) Cell nuclei marked in blue with HOECHST; (b) Cell cytoplasm marked in green with Calcein; (c) Overlay; 10x magnification.

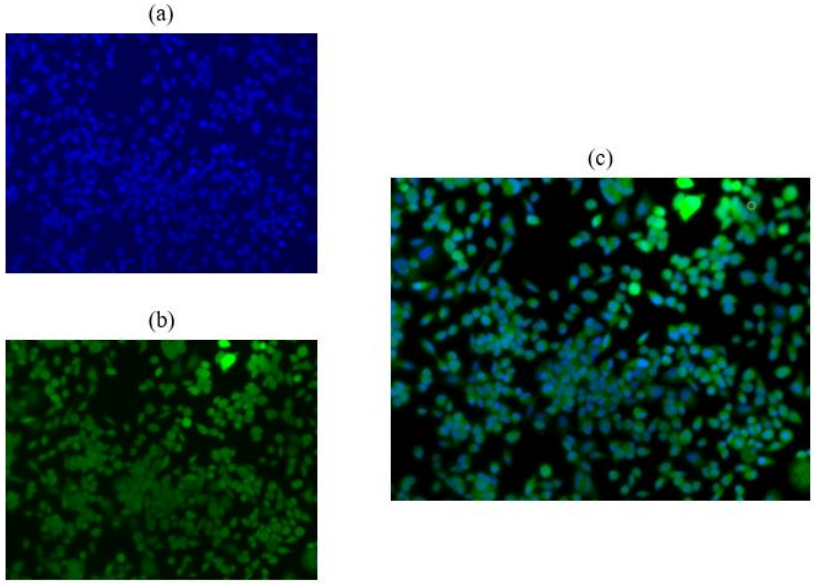

Figure 4.30. Cells staining of SK-N-DZ after 1 day from seeding with clamping unit: a) Cell nuclei marked in blue with HOECHST; (b) Cell cytoplasm marked in green with Calcein; (c) Overlay; 20x magnification.

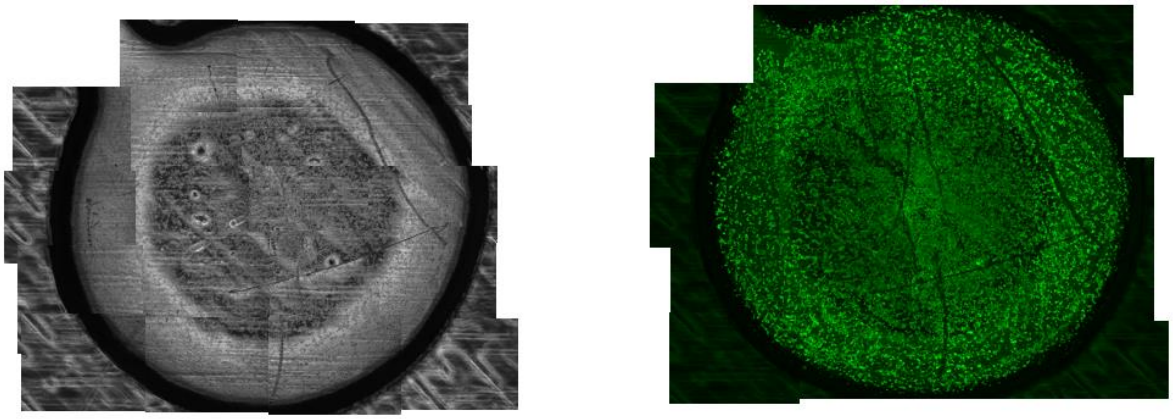

Figure 4.31. Brightfield view (on the left) and Cell cytoplasm marked in green (on the right) of the well.

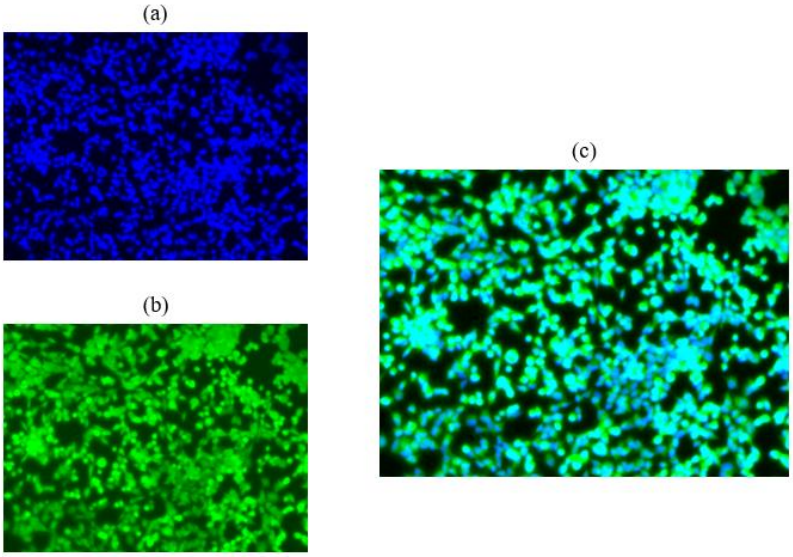

Figure 4.32. Cells staining of SK-N-AS after 5 days from seeding with clamping unit: a) Cell nuclei marked in blue with HOECHST; (b) Cell cytoplasm marked in green with Calcein; (c) Overlay; 10x magnification.

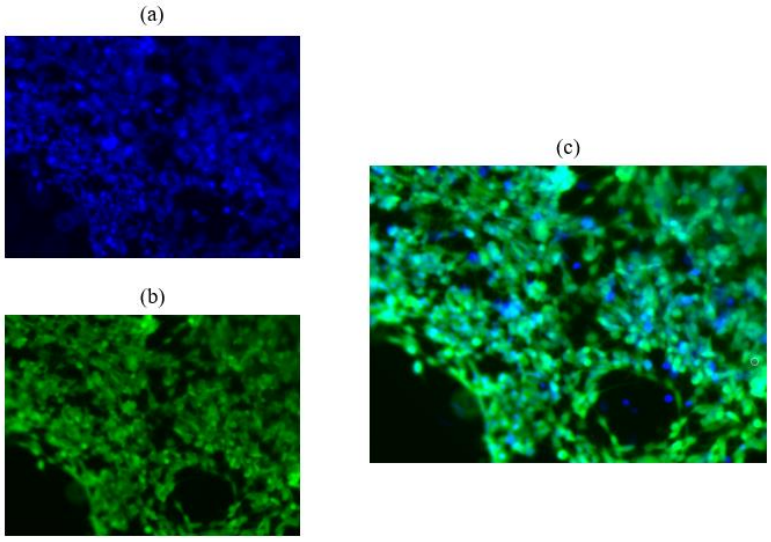

Figure 4.33. Cells staining of SK-N-DZ after 5 days from seeding with clamping unit: a) Cell nuclei marked in blue with HOECHST; (b) Cell cytoplasm marked in green with Calcein; (c) Overlay; 10x magnification.

Therefore, from a biological point of view, regardless of the cell species tested, a high cell viability was verified even 5 days after cell seeding in each sample. In addition, there were no phenomena of fragmentation of the nucleus and cytoplasm in the cells, typical of the processes of apoptosis. As was evident from Figures 4.24 and 4.25, the adhesion of cells to the PS microfluidic platform also occurred even after one day of incubation: cells nuclei and cytoplasm appeared clearly distinct, and this suggests the presence of an environment conducive to their survival. Obviously, to have greater completeness on the goodness of the experiments and to be able to draw more complete conclusions it would be necessary to increase the days of incubation of the cells, also using different cell densities.

4.4.3 Biocompatibility and viability tests with GelMA

As mentioned in Chapter 3, the PS chip was used to build three-dimensional structures for cellular experiments.

Tests with neuroblastoma cells were performed using GelMA hydrogels prepared as described in the protocol reported in paragraph 3.7, especially the macromolecules used were characterized by a degree of functionalization (DoF) of 70 ± 10%. The viability results obtained by using the two markers Hoechst 33258 and Calcein AM appeared very promising after the first day of incubation. However, images taken 5 days after incubation showed very weak signals of cell viability within the 3D structure. Figures 4.34 and 4.35 show the images of cells in 3D after one day of incubation for the two cell species of neuroblastoma.

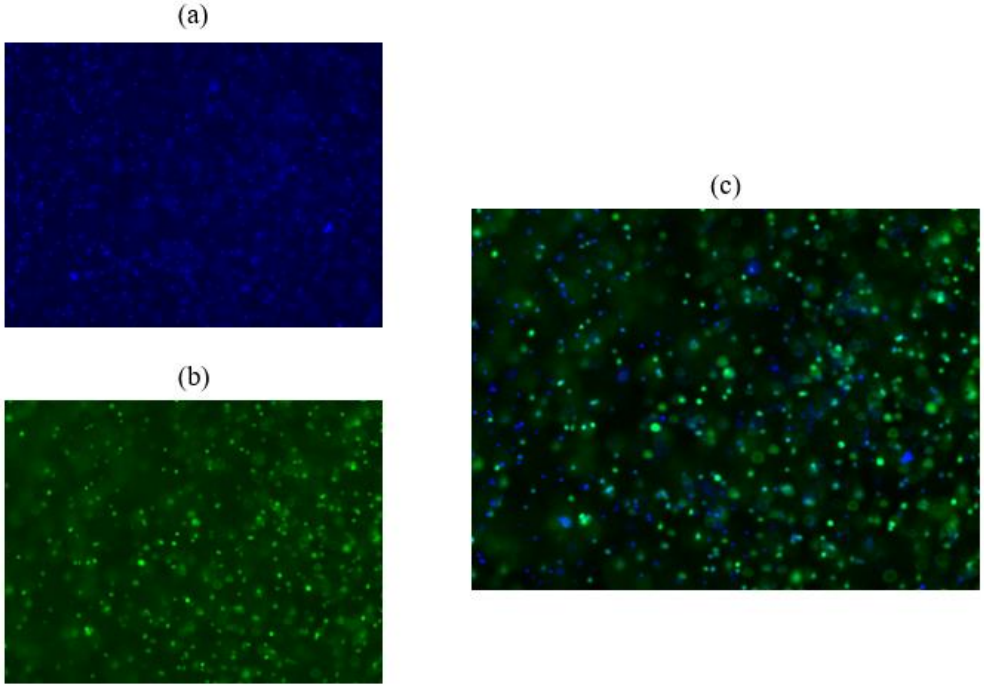

Figure 4.34. Cells staining of SK-N-AS after 1 day from seeding with GelMA: a) Cell nuclei marked in blue with HOECHST; (b) Cell cytoplasm marked in green with Calcein; (c) Overlay; 10x magnification.

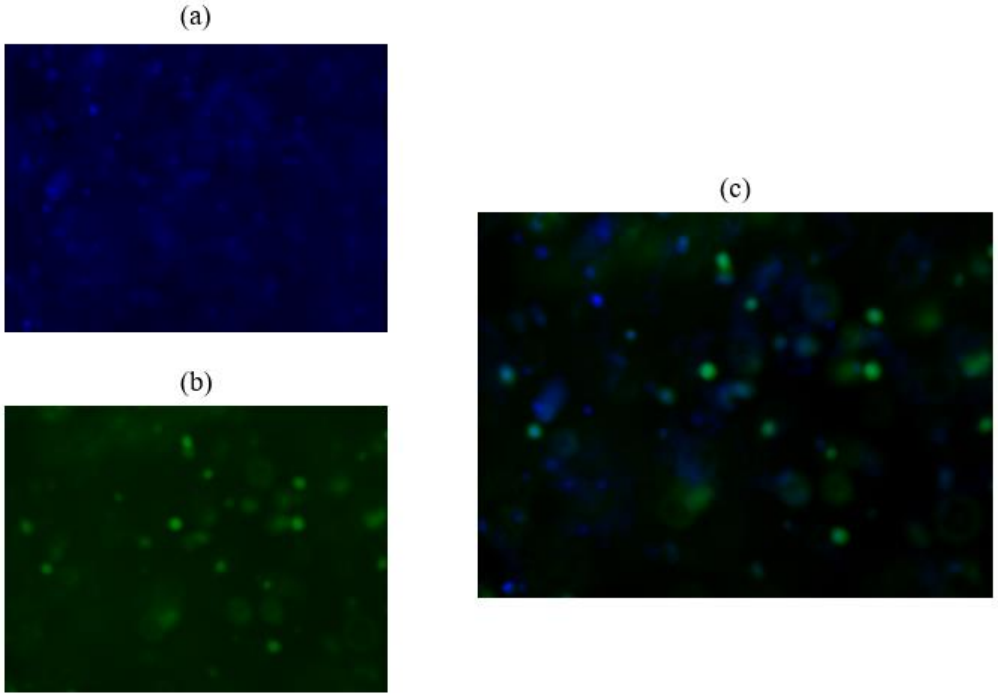

Figure 4.35. Cells staining of SK-N-DZ after 1 day from seeding with GelMA: a) Cell nuclei marked in blue with HOECHST; (b) Cell cytoplasm marked in green with Calcein; (c) Overlay; 20x magnification.

As already explained, in the following experiments it was decided to add a certain percentage of Agarose to the GelMA-based hydrogels in order to increase the biocompatibility of the material. Cell viability results within these structures are not yet available because contamination problems have been found in the laboratory.

Conclusion

The work carried out in this thesis was aimed at the realization of a microfluidic platform in PS for studies on neuroblastoma cancer cells by Injection Molding. In particular, Additive Manufacturing technology was used for the production of inserts in Digital ABS material for the machine mold. The validation of the entire production process of making the microfluidic platform consisted of the metrological characterization of the insert before and after Injection Molding to evaluate possible wear phenomena of the tool following the molding of the devices. The latter were also analyzed performing measurements using a profilometer to verify the actual replication of the CAD model; subsequently, they were tested in the laboratory to validate them for their biological validation.

The results obtained for the characterization of the insert both before and after molding and of the PS chips are the following:

- the insert realized with the 3D printer showed a high degree of replication of the CAD model;
- the insert revealed no signs of wear after molding 500 PS pieces, ensuring good resistance to high injection and mold temperatures;
- the chips produced using Injection Molding are characterized by a good degree of replication, with a geometry of the channels and wells very similar to that of the insert.

From the mechanical point of view, the device was produced with good optical transparency, with a slight inward curvature which was anyway irrelevant for the purposes of cellular experiments. As for biological evaluations, the device provided a good performance with excellent adhesion of cells to the microfluidic platform and significant cell growth, even after a couple of days from seeding. Only two neuroblastoma cell species were used for the experiments described in this thesis; anyway, the chip configuration makes it very versatile for cellular experiments. For example, another interesting application could be that of studying the effect of the introduction of exosomes in the central chamber, analyzing the fluid dynamic behavior of all the components inside the microdevice, with and without the clamping unit.

In conclusion, the use of polymeric materials in Microfluidics represents an excellent alternative to glassy materials and PDMS, both for their cost-effectiveness and for optical and mechanical properties, very interesting from the biomedical point of view. Furthermore, the possibility of apply Additive Manufacturing for the production of tools for Injection Molding (the most used technique for the production of plastic materials) in a very short time and with a high level of customization, has allowed creating solid basis for the use of these materials in Microfluidics.

Appendix

A.1 Objet350 Connex3 data sheet

Objet350 and Objet500 Connex3

Driven by powerful PolyJet™ technology

Proven PolyJet 3D Printing is famous for smooth surfaces, fine precision and diverse material properties. It works a bit like inkjet document printing, but instead of jetting drops of ink onto paper, the print head jets microscopic layers of liquid photopolymer onto a build tray and instantly cures them with UV light. The fine layers build up to create a prototype or production part.

Along with the selected model material, the 3D printer features two support material options: SUP705, which is easily removed with a WaterJet; and SUP706, which is soluble for automated post-processing and increased geometric freedom to print complex and delicate features and small cavities.

With its astonishingly realistic aesthetics and ability to deliver special properties such as transparency, flexibility and even bio-compatibility, PolyJet 3D Printing offers a competitive edge in consumer products prototyping, precision tooling and specialized production parts.

System Specifications	
Model Materials	Rigid Opaque: VeroWhitePlus™, VeroBlackPlus™, VeroGray™, VeroBlue™, VeroCyan™, VeroMagenta™, VeroYellow™ Rubber-like: TangoPlus™, TangoBlackPlus™, TangoBlack™, TangoGray™ Transparent: VeroClear™ and RGD720 Simulated Polypropylene: Rigur™ and Durus™ High Temperature Bio-compatible
Digital Materials	Digital ABS™ and Digital ABS2™ in ivory and green Hundreds of vibrant, repeatable colors in opaque and translucent Rubber-like blends in a range of Shore A values and color Polypropylene materials with improved heat resistance
Material Options	Over 1,000
Maximum Materials per Part	82
Support Material	SUP705 (WaterJet removable)
	SUP706 (soluble)
Maximum Build Size (XYZ)	Objet350: 340 x 340 x 200 mm (13.4 x 13.4 x 7.9 in.) Objet500: 490 x 390 x 200 mm (19.3 x 15.4 x 7.9 in
System Size and Weight	1400 x 1260 x 1100 mm (55.1 x 49.6 x 43.4 in.); 430 kg (948 lbs.) *Material Cabinet:* 330 x 1170 x 640 mm (13 x 46.1 x 26.2 in.); 76 kg (168 lbs.)
Resolution	X-axis: 600 dpi; Y-axis: 600 dpi; Z-axis: 1600 dpi
Accuracy	20-85 microns for features below 50 mm; up to 200 microns for full model size
Minimum Layer Thickness	Horizontal build layers as fine as 16 microns (.0006 in.)
Build Modes	Digital Material: 30-micron (.001 in.) resolution High Quality: 16-micron (.0006 in.) resolution High Speed: 30-micron (.001 in.) resolution
Software	Objet Studio™ intuitive 3D printing software
Workstation Compatibility	Windows 7/ Windows 8
Network Connectivity	LAN - TCP/IP
Operating Conditions	Temperature 18-25°C (64-77°F); relative humidity 30-70% (non-condensing)
Power Requirements	110-240 VAC 50/60Hz; 1.5 kW single phase
Regulatory Compliance	CE, FCC

stratasys

E info@stratasys.com / STRATASYS.COM
ISO 9001:2008 Certified

OVERMACH

Via Giuseppe Righi, 12 - Moletolo - 43122
Parma Tel.: 0521-771071 - Fax: 0521-771291
Web: www.overmach.it

E-mail: prototipazione@overmach.it

A.2 Digital ABS Plus data sheet

Digital ABS Plus

POLYJET SIMULATED ABS PLASTIC

At the core:
PolyJet Technology

PolyJet technology creates precise prototypes that set the standard for finished-product realism. Its fine resolution makes complex shapes, intricate details and smooth surfaces possible. PolyJet 3D Printing works by jetting layers of liquid photopolymer onto a build tray and instantly curing them with UV light. The fine layers build up to create a precise 3D model or prototype. Models are ready to handle right out of the 3D printer, with no post curing needed.

Keep valuable resources in-house

You'll be amazed when you see how easy it is to produce realistic models in-house. PolyJet 3D Printers offer not only unparalleled speed, they make it easy for you to print with the widest range of material properties.

No special facilities needed

You can install PolyJet 3D Printers just about anywhere. No special venting is required because PolyJet 3D Printers don't produce noxious fumes, chemicals or waste.

Good ideas sell easier

PolyJet 3D Printers improve communication and collaboration because they produce amazingly accurate representations of your ideas that you can share with your team and your clients for a faster, more confident buy-in.

MECHANICAL PROPERTIES	TEST METHOD	IMPERIAL	IMPERIAL METRIC
Tensile Strength	D-638-03	8,000-8,700 psi	55-60 MPa
Elongation at Break	D-638-05	25-40%	25-40%
Modulus of Elasticity	D-638-04	375,000-435,000 psi	2,600-3,000 MPa
Flexural Strength	D-790-03	9,500-11,000 psi	65-75 MPa
Flexural Modulus	D-790-04	245,000-320,000 psi	1,700-2,200 MPa
HDT, °C @ 0.45MPa	D-648-06	136-154 °F	58-68 °C
HDT, °C @ 0.45MPa after thermal post treatment procedure A	D-648-06	180-194 °F	82-90 °C
HDT, °C @ 0.45MPa after thermal post treatment procedure B	D-648-06	198-203 °F	92-95 °C
HDT, °C @ 1.82MPa	D-648-07	124-131 °F	51-55 °C
Izod Notched Impact	D-256-06	1.69-2.15 ft lb/in	90-115 J/m
Tg	DMA, E»	117-127 °F	47-53 °C
Shore Hardness (D)	Scale D	85-87 Scale D	85-87 Scale D
Rockwell Hardness	Scale M	67-69 Scale M	67-69 Scale M
Polymerized Density	ASTM D792		1.17-1.18 g/cm³

SYSTEM AVAILABILITY	LAYER THICKNESS CAPABILITY	SUPPORT STRUCTURE	AVAILABLE COLORS
Objet260/350/500 Connex3™	**Digital Material 2/3 mode:** 30 microns (0.0012 in.)	SUP705 (WaterJet removable) SUP706* (soluble) Objet1000 uses only SUP705	Green (RGD515 Plus and RGD535) Ivory (RGD515 Plus and RGD531)
Stratasys J735™ Stratasys J750™	**High Mix or High Speed mode:** 27 microns (0.0011 in.) **High Quality mode:** 14 microns (0.00055 in.)		
Objet1000 Plus™	**Digital Material 2 mode:** 36 microns (0.0014 in.)		

** Not compatible with or HQ mode for Stratasys J750.*

stratasys

STRATASYS.COM
ISO 9001:2008 Certified

HEADQUARTERS
7665 Commerce Way,
Eden Prairie, MN 55344
+1 800 801 6491 (US Toll Free)
+1 952 937 3000 (Intl)
+1 952 937 0070 (Fax)

1 Holtzman St., Science Park,
PO Box 2496
Rehovot 76124, Israel
+972 74 745 4000
+972 74 745 5000 (Fax)

A.3 Polystyrene Crystal 1540 data sheet

TOTAL

Refining & Chemicals
Polymers

POLYSTYRENE CRYSTAL 1540

Technical Data Sheet
Easy Flow crystal Polystyrene
Manufactured in Europe

Description

POLYSTYRENE CRYSTAL 1540 is an easy flowing crystal polystyrene designed for extrusion or injection applications. In extrusion, it allows to increase extruder output and thermoforming cycle times when mixed with a high impact polystyrene such as POLYSTYRENE IMPACT 7240. Having high gloss, it is particularly suitable for glossy-layer co-extrusion. In injection moulding, POLYSTYRENE CRYSTAL 1540 with this low viscosity at high shear rate has a good injectability and combines an excellent fluidity with a higher softening point.

Applications

Dairy sheet, cups (dilution with impact polystyrene)

Injection: Boxes, office equipment - e.g. filing trays, CD boxes, pen bodies, internal fridge parts, toys, cups.

Properties

Rheological	**Method**	**Unit**	**Value**
Melt flow index (200°C-5kg)	ISO 1133 H	g/10mn	12
Thermal			
Vicat softening point 10N (T° increase = 50°C/h)	ISO 306A50	°C	91
Vicat softening point 50N (T° increase = 50°C/h)	ISO 306B50	°C	86
HDT unannealed under 1.8 MPa	ISO 75-2A	°C	73
HDT annealed under 1.8 MPa	ISO 75-2A	°C	83
Coefficient of linear thermal expansion		mm/°C	7.10 E-5
Mechanical			
Unnotched Charpy impact strength	ISO 179/1eA	KJ/m²	8
Tensile strength at break	ISO 527-2	MPa	42
Elongation at break	ISO 527-2	%	2
Tensile modulus	ISO 527-2	MPa	3100
Flexural modulus	ISO 178	MPa	2900
Rockwell hardness	ISO 2039-2		L 70
Electrical			
Dielectric strength		kV/mm	135
Surface resistivity	ISO IEC 93	Ohms	>10 E+14
Miscellaneous			
Density	ISO 1183	g/cm³	1.05
Moulding shrinkage		%	0.4-0.7
Water absorption	ISO 62	%	<0.1

General Information

- Standard properties: All tests carried out at 23°C unless otherwise stated. Mechanical properties are measured on injection moulded tests specimens.
- Bulk density: bulk density is approximately 0.6 g/cm3.
- Please refer to the Safety Data Sheet for further information.
- Please refer to the safety data sheet (SDS) for handling and storage information. It is advisable to convert the product within six months after delivery provided storage conditions are used as given in the SDS of our product. SDS may be obtained from the website: www.totalrefiningchemicals.com

TOTAL RESEARCH & TECHNOLOGY FELUY
Zone Industrielle C
B-7181 Feluy
Belgium

July 2013

website : www.totalrefiningchemicals.com

Bibliography

1. Yeo, L. Y., Chang, H. C., Chan, P. P. Y. & Friend, J. R. Microfluidic devices for bioapplications. *Small* **7**, 12–48 (2011).
2. Lee, U. N. *et al.* Fundamentals of rapid injection molding for microfluidic cell-based assays. *Lab Chip* **18**, 496–504 (2018).
3. Fiorini, G. S. & Chiu, D. T. Disposable microfluidic devices: Fabrication, function, and application. *Biotechniques* **38**, 429–446 (2005).
4. Mitterlehner, T., Beisteiner, C., Rieger, H., Dunzendorfer, P. & Steinbichler, G. Back injection molding with additive manufactured mold inserts using all-inkjet printed substrates. *Annu. Tech. Conf. - ANTEC, Conf. Proc.* **2017-May**, 7–12 (2017).
5. Ashraf, M. W., Tayyaba, S. & Afzulpurkar, N. Micro Electromechanical Systems (MEMS) based microfluidic devices for biomedical applications. *Int. J. Mol. Sci.* **12**, 3648–3704 (2011).
6. Gupta, S., Ramesh, K., Ahmed, S. & Kakkar, V. Lab-on-chip technology: A review on design trends and future scope in biomedical applications. *Int. J. Bio-Science Bio-Technology* **8**, 311–322 (2016).
7. Chow, A. W. Lab-on-a-chip: Opportunities for chemical engineering. *AIChE J.* **48**, 1590–1595 (2002).
8. Squires, T. M. & Quake, S. R. Microfluidics: Fluid physics at the nanoliter scale. *Rev. Mod. Phys.* **77**, 977–1026 (2005).
9. Breslauer, D. N., Lee, P. J. & Lee, L. P. Microfluidics-based systems biology. *Mol. Biosyst.* **2**, 97–112 (2006).
10. Daxesoft Ltd. Laminar Flow and Turbulent Flow of Fluids. Available at:

    https://withdebasishsir.wixsite.com/learnphysics/single-post/2017/09/09/Laminar-Flow-and-Turbulent-Flow-of-fluid
11. How to Choose a Microfluidic Tubing ? *Elveflow* (2018). Available at:

    https://www.fluigent.com/microfluidic-expertise/what-is-microfluidic/how-to-choose-a-microfluidic-chip/
12. Ren, K., Zhou, J. & Wu, H. Materials for microfluidic chip fabrication. *Acc. Chem. Res.* **46**, 2396–2406 (2013).
13. Nge, P. N., Rogers, C. I. & Woolley, A. T. Advances in microfluidic materials, functions, integration, and applications. *Chem. Rev.* **113**, 2550–2583 (2013).
14. Materials for microfluidic chips fabrication _ a review 2017 - Elveflow. Available at:

    https://www.elveflow.com/microfluidic-reviews/general-microfluidics/materials-for-microfluidic-chips-fabrication-a-review-2017/
15. Becker, H. & Gärtner, C. Polymer microfabrication technologies for microfluidic systems. *Anal. Bioanal. Chem.* **390**, 89–111 (2008).
16. Introduction to poly-di-methyl-siloxane (PDMS) - Elveflow. Available at:

    https://www.elveflow.com/microfluidic-reviews/general-microfluidics/the-poly-di-methyl-siloxane-pdms-and-microfluidics-2

17. Regehr, K. J. *et al.* Biological implications of polydimethylsiloxane-based microfluidic cell culture. *Lab Chip* **9**, 2132–2139 (2009).

18. Tsao, C. W. & DeVoe, D. L. Bonding of thermoplastic polymer microfluidics. *Microfluid. Nanofluidics* **6**, 1–16 (2009).

19. Tsao, C. W. Polymer microfluidics: Simple, low-cost fabrication process bridging academic lab research to commercialized production. *Micromachines* **7**, (2016).

20. Arias, P. A. Planning Models for Distribution Grid: A Brief Review Piedy. *U. Prto J. Eng.* **4**, 42–55 (2017).

21. Overview, P. *et al.* Historical Note: Lithography's Origins. 3–87 (1808).

22. Microfluidics for point-of-care diagnostic devices_ a review - Elveflow. Available at:

https://www.elveflow.com/microfluidic-reviews/general-microfluidics/microfluidics-for-point-of-care-diagnostic-devices-a-review/

23. Whitesides, G. M., Ostuni, E., Jiang, X. & Ingber, D. E. S Oft L Ithography in B Iology. *Annu. Rev. Biomed. Eng.* **3**, 335–73 (2001).

24. Weibel, D. B., DiLuzio, W. R. & Whitesides, G. M. Microfabrication meets microbiology. *Nat. Rev. Microbiol.* **5**, 209–218 (2007).

25. McDonald, J. C. & Whitesides, G. M. Poly(dimethylsiloxane) as a material for fabricating microfluidic devices. *Acc. Chem. Res.* **35**, 491–499 (2002).

26. Peng, L., Deng, Y., Yi, P. & Lai, X. Micro hot embossing of thermoplastic polymers: A review. *J. Micromechanics Microengineering* **24**, (2014).

27. Attia, U. M., Marson, S. & Alcock, J. R. Micro-injection moulding of polymer microfluidic devices. *Microfluid. Nanofluidics* **7**, 1–28 (2009).

28. The Future and Popularity of Mass Production_ How Injection Molding Interprets Industrial Design Ideas _ Design Swan. Available at:

https://www.designswan.com/archives/the-future-and-popularity-of-mass-production-how-injection-molding-interprets-industrial-design-ideas.html

29. Plastic Injection Molding Process Simulation. Available at:

https://www.ecomolding.com/plastic-injection-molding/

30. Dimla, D. E., Camilotto, M. & Miani, F. Design and optimisation of conformal cooling channels in injection moulding tools. *J. Mater. Process. Technol.* **164**–**165**, 1294–1300 (2005).

31. why use hot runner for thin wall moulds - Micon Plastic Mould Factory. Available at:

https://www.miconmould.com/china-mold-maker/why-use-hot-runner-for-thin-wall-moulds-62.html

32. Bissacco, G., Hansen, H. N., Tang, P. T. & Fugl, J. Precision manufacturing methods of inserts for injection molding of microfluidic systems. *Proc. - ASPE Spring Top. Meet. Precis. Micro/Nano Scale Polym. Based Compon. Device Fabr. ASPE 2005* 57–63 (2005).

33. Additive vs. Subtractive Manufacturing. Available at:

https://formlabs.com/blog/additive-manufacturing-vs-subtractive-manufacturing/#:~:text=Additive%20manufacturing%20processes%20build%20objects,removes%20material%20to%20create%20parts.

34. Popov, K. B. *et al.* Micromilling: Material microstructure effects. *Proc. Inst. Mech. Eng. Part B J. Eng. Manuf.* **220**, 1807–1813 (2006).

35. Guckenberger, D. J., De Groot, T. E., Wan, A. M. D., Beebe, D. J. & Young, E. W. K. Micromilling: A method for ultra-rapid prototyping of plastic microfluidic devices. *Lab Chip* **15**, 2364–2378 (2015).

36. Mahendran, S., Devarajan, R., Nagarajan, T. & Majdi, A. A Review of Micro-EDM. **II**, (2010).

37. Minhat, A. E., Hj Khamis, N. H., Yahya, A., Andromeda, T. & Nugroho, K. Model of pulsed electrical discharge machining (EDM) using RL circuit. *Int. J. Power Electron. Drive Syst.* **5**, 252–260 (2014).

38. Gale, B. K. Outline Introduction to the LIGA Microfabrication Process What is LIGA ? The LIGA Process High Aspect Ratio Patterning X-ray Lithography Critical Parameters in DXRL Exposures Key Features of DXRL Microstructures.

39. APPLIED MICROSWISS - Replication tools in Nickel,Silicon and PDMS,Nickel-components,Services,LiGA-technique,microtechnology,nanotechology,replication. Available at:

    https://www.applied-microswiss.ch/Manufacturing_Basics_EN_24-03-2020.html

40. Kume, T., Egawa, S., Yamaguchi, G. & Mimura, H. Influence of Residual Stress of Electrodeposited Layer on Shape Replication Accuracy in Ni Electroforming. *Procedia CIRP* **42**, 783–787 (2016).

41. Hernández, P. *et al.* Electroforming Applied to Manufacturing of Microcomponents. *Procedia Eng.* **132**, 655–662 (2015).

42. Yazdi, A. A. *et al.* 3D printing: an emerging tool for novel microfluidics and lab-on-a-chip applications. *Microfluid. Nanofluidics* **20**, 1–18 (2016).

43. Funamoto, K. *et al.* A novel microfluidic platform for high-resolution imaging of a three-dimensional cell culture under a controlled hypoxic environment. *Lab Chip* **12**, 4855–4863 (2012).

44. Nguyen-Chung, T. Flow analysis of the weld line formation during injection mold filling of thermoplastics. *Rheol. Acta* **43**, 240–245 (2004).

45. Weld lines,plastic injection molding defects-ecomolding. Available at:

    https://www.injectionmould.org/2019/06/01/weld-lines/

46. Stratasys Ltd. Objet350 and Objet500 Connex3 Spec Sheet. (2017).

47. Stratasys Systems. Digital ABS Plus. 2 (2018).

48. S neox - 3D optical profilometer. Available at:

    https://www.sensofar.com/metrology/products/sneox/

49. Halldorsson, S., Lucumi, E., Gómez-Sjöberg, R. & Fleming, R. M. T. Advantages and challenges of microfluidic cell culture in polydimethylsiloxane devices. *Biosens. Bioelectron.* **63**, 218–231 (2015).

50. Gencturk, E., Mutlu, S. & Ulgen, K. O. Advances in microfluidic devices made from thermoplastics used in cell biology and analyses. *Biomicrofluidics* **11**, (2017).

51. Berthier, E., Young, E. W. K. & Beebe, D. Engineers are from PDMS-land, biologists are from polystyrenia. *Lab Chip* **12**, 1224–1237 (2012).

52. Wang, Y. *et al.* Benchtop micromolding of polystyrene by soft lithography. *Lab Chip*

11, 3089–3097 (2011).

53. Haynes_SplittingCells - OpenWetWare. Available at: https://openwetware.org/wiki/Haynes:SplittingCells

54. Hoechst 33258, nuclear counterstain,cell cycle _ Genecopoeia. Available at: https://www.genecopoeia.com/product/hoechst-33258/

55. Cloning, S. C., Cloning, S. C., Ld, T. & Cloning, S. C. Testing the Toxicity of Calcein-AM under Single Cell Cloning Conditions.

56. Wu, K. T. *et al.* Transition from turbulent to coherent flows in confined three-dimensional active fluids. *Science (80-.).* **355**, (2017).

57. Chen, Q. & Wang, Y. The application of three-dimensional cell culture in clinical medicine. *Biotechnol. Lett.* **42**, 2071–2082 (2020).

58. Santi Gaia (2020). Production of gelatin methacrylate printable bioniks for cancer cells studies. *Master Thesis*, University of Padova

Web sites

https://withdebasishsir.wixsite.com/learnphysics/single-post/2017/09/09/Laminar-Flow-and-Turbulent-Flow-of-fluid (Last Access 28/09/2020)

https://www.fluigent.com/microfluidic-expertise/what-is-microfluidic/how-to-choose-a-microfluidic-chip/ (Last Access 28/09/2020)

https://www.elveflow.com/microfluidic-reviews/general-microfluidics/materials-for-microfluidic-chips-fabrication-a-review-2017/ (Last Access 28/09/2020)

https://www.elveflow.com/microfluidic-reviews/general-microfluidics/the-poly-di-methyl-siloxane-pdms-and-microfluidics-2 (Last Access 28/09/2020)

https://www.elveflow.com/microfluidic-reviews/general-microfluidics/microfluidics-for-point-of-care-diagnostic-devices-a-review/ (Last Access 27/09/2020)

https://www.ecomolding.com/plastic-injection-molding/ (Last Access 29/09/2020)

https://www.miconmould.com/china-mold-maker/why-use-hot-runner-for-thin-wall-moulds-62.html (Last Access 29/09/2020)

https://formlabs.com/blog/additive-manufacturing-vs-subtractive-manufacturing/#:~:text=Additive%20manufacturing%20processes%20build%20objects,removes%20material%20to%20create%20parts. (Last Access 30/09/2020)

https://www.injectionmould.org/2019/06/01/weld-lines/ (Last Access 28/09/2020)

https://www.sensofar.com/metrology/products/sneox/ (Last Access 29/09/2020)

https://openwetware.org/wiki/Haynes:SplittingCells (Last Access 28/09/2020)

Ringraziamenti

In primo luogo vorrei ringraziare la professoressa Elisa Cimetta per avermi permesso di concludere il mio percorso di studi universitari con un'attività di laboratorio e di ricerca.

Ringrazio di cuore tutti i miei compagni di laboratorio per le bellissime giornate trascorse assieme ed in particolare Sara Micheli per avermi costantemente seguito e consigliato durante tutti questi mesi di attività di tesi. Vi voglio bene.

Ringrazio tutto lo staff del laboratorio TE.SI. di Rovigo, in particolare l'Ing. Marco Sorgato e Riccardo Manzetto, per avermi dato la possibilità di utilizzare i loro macchinari.

Ringrazio i miei genitori, Giuseppe e Maria Ausilia, perché senza il loro sostegno emotivo, morale ed economico non avrei potuto fare tutto ciò; non li ringrazierò mai abbastanza.

Ringrazio mio fratello per l'aiuto concessomi durante questi mesi e perché è sempre presente in ogni momento.

Ringrazio i miei due, ormai ex, coinquilini, Francesco e Daniele, con cui ho trascorso anni davvero splendidi a Padova.

Ed infine vorrei ringraziare simbolicamente proprio la città che mi ha accolto, Padova, che mi ha permesso di conoscere persone nuove e di instaurare bellissimi rapporti di amicizia.